

Using NDII patterns to constrain semi-distributed rainfall-runoff models in tropical nested catchments

Nutchanart Sriwongsitanon^{1,2}, Wasana Jandang^{1,2}, [James Williams²](#), Thienchart Suwawong^{1,2}, [Ekkarin Maekan^{1,2}](#), and Hubert H.G. Savenije³

¹ Department of Water Resources Engineering, Faculty of Engineering, Kasetsart University, Bangkok, Thailand

² Remote Sensing Research Centre for Water Resources Management (SENSWAT), Faculty of Engineering, Kasetsart University, Bangkok, Thailand

³ Delft University of Technology, Stevinweg 1, 2600 GA Delft, The Netherlands

Correspondence to: Nutchanart Sriwongsitanon (fengnns@ku.ac.th)

Abstract. A parsimonious semi-distributed rainfall-runoff model has been developed for flow prediction. In distribution, attention is paid to both timing of runoff and heterogeneity of moisture storage capacities within sub-catchments. This model is based on the lumped FLEXL model structure, which has proven its value in a wide range of catchments. To test the value of distribution, the gauged Upper Ping catchment in Thailand has been divided into 32 sub-catchments, which can be grouped into 5 gauged sub-catchments where internal performance is evaluated. To test the effect of timing, firstly excess rainfall was calculated for each sub-catchment, using the model structure of FLEXL. The excess rainfall was then routed to its outlet using the lag time from storm to peak flow (T_{lagF}) and the lag time of recharge from the root zone to the groundwater (T_{lagS}), as a function of catchment size. Subsequently, the Muskingum equation was used to route sub-catchment runoff to the downstream sub-catchment, with the delay time parameter of the Muskingum equation being a function of channel length. Other model parameters of this semi-distributed FLEX-SD model were kept the same as in the calibrated FLEXL model of the entire Upper Ping river basin (UPRB), controlled by station P.1 located at the centre of Chiang Mai Province. The outcome of FLEX-SD was compared to: 1) observations at the internal stations; 2) the calibrated FLEXL model; and 3) the semi-distributed URBS model - another established semi-distributed rainfall-runoff model. FLEX-SD showed better or similar performance both during calibration and especially in validation. Subsequently, we tried to distribute the moisture storage capacity by constraining FLEX-SD on patterns of the NDII (Normalized Difference Infrared Index). The readily available NDII appears to be a good proxy for moisture stress in the root zone during dry periods. The maximum moisture holding capacity in the root zone is assumed to be a function of the maximum seasonal range of NDII values, and the annual average NDII values to construct 2 alternative models: FLEX-SD-NDII_{Max-MinMaxMin} and FLEX-SD-NDII_{Avg}, respectively. The additional constraint on the moisture holding capacity ($Sumax$) by the NDII, particularly in FLEX-SD-NDII_{Avg}, improved both model performance and the realism of its distribution across the UPRB, which corresponds linearly to the percentage of evergreen forests ($R^2 = 0.69$). improved both model performance and the realism of the distribution. Distribution of $Sumax$ using annual average NDII values was found to be well correlated with the percentage of evergreen forest in 31 sub-catchments. Spatial average NDII values were proved to be highly corresponded with the root zone soil moisture of the river basin, not only in the

Formatted: Font: Italic, Complex Script Font: Italic

Formatted: Subscript

Formatted: Superscript

~~dry season but also in the water-limited ecosystem.~~ To check how well the models represents simulated root zone soil moisture (St_z), the performance of the FLEX-SD-NDII models were compared to time series of the Soil Wetness Index (SWI). The correlation between the St_z root zone storage and the daily SWI appeared to be very good, even better than the correlation with the NDII, which does not provide good estimates during wet periods, because NDII does not provide good estimates
5 during wet periods. The SWI, which is partly-model-based, was not used for calibration, but appeared to be an appropriate index for validation.

1 Introduction

Runoff is one of the most important components of the hydrological cycle and can be monitored by the installation of a gauging station. Unfortunately, there are only a limited number of high-quality gauging stations available due to topographic, financial,
10 and human resources limitations. A wide variety of rainfall-runoff models has been developed in gauged and ungauged catchments in different parts of the globe. Most rainfall-runoff models are categorised as lumped models, which can provide runoff estimates only at the site of calibration. These models include FLEXL, FLEX-Topo (Euser et al., 2015; Gao et al., 2014), NAM (Bao et al., 2011; Tingsanchali and Gautam, 2000; Vaitiekuniene, 2005; Yew Gan et al., 1997), SCS (Hawkins, 1990; Lewis et al., 2000; Mishra et al., 2005; Suresh Babu and Mishra, 2011; Yahya et al., 2010), and many others. Among
15 the wide range of existing lumped rainfall-runoff models, FLEXL has proven to be an adequate model for runoff estimation in a wide range of catchments (Fenicia et al., 2011; Fenicia et al., 2008; Gao et al., 2014; Kavetski and Fenicia, 2011; Tekleab et al., 2015). This model was further developed by Gharari et al. (2011) and Gao et al. (2016) to account for the spatial variability of landscape characteristics (FLEX-TOPO), useful for prediction in ungauged basins (Savenije, 2010).

~~To alleviate the limitation of lumped rainfall-runoff models, URBS was developed as a semi-distributed nonlinear rainfall runoff routing model, which can account for the spatial and temporal variation in rainfall by separating a catchment into a series of sub-catchments (Mapiam and Sriwongsitanon, 2009). Therefore, URBS claims to provide runoff estimates not only~~
25 ~~at a gauging station but also at any required upstream location (Carroll, 2004; Malone, 1999). URBS has been applied successfully for real time flood forecasting in a range of catchments from small to very large basins in Australia and in many countries worldwide (Malone, 2006; Malone et al., 2003; Mapiam and Sriwongsitanon, 2009; Mapiam et al., 2014; Rodriguez et al., 2005; Sriwongsitanon, 2010). However, this model only addresses the distribution of travel times and does not address the effect of distributed storage capacities that affect the partitioning of moisture and hence the water balance.~~

30 However, the generation of runoff exhibits spatial and temporal variability in nature, which is not effectively accounted for by the conceptualisation of lumped models. Hence, the distribution of key routing and storage parameters are implemented in semi-distributed frameworks to better understand their effects on the partitioning of moisture and water balance. URBS

Formatted: Font: Italic, Complex Script Font: Italic

Formatted: Font: Italic, Complex Script Font: Italic, Subscript

Formatted: Font: Italic, Complex Script Font: Italic

Formatted: Font: Italic, Complex Script Font: Italic, Subscript

Formatted: Complex Script Font: 10 pt

accounts for the spatiotemporal variability of rainfall by separating the catchment of interest into a series of sub-catchments (Mapiam and Sriwongsitanon, 2009). This framework allows runoff to be estimated at any required upstream location (Carroll, 2004; Malone, 1999), providing useful application for real time flood forecasting in a variety of catchments in Australia and globally (Malone, 2006; Malone et al., 2003; Mapiam and Sriwongsitanon, 2009; Mapiam et al., 2014; Rodriguez et al., 2005; Sriwongsitanon, 2010). But accounting for distributed routing and storage parameters alone does not address the variability of moisture storage capacities of sub-catchments, which are key parameters for runoff generation. The fact that remote sensing (RS) proxies for moisture storage are available in ungauged basins makes RS an essential additional data source for distributed modelling, even though such proxies themselves have intrinsic model-based uncertainties. Remotely sensing observation techniques have been demonstrated in several studies to account for the spatial patterns of different vegetation types and moisture states, such that they could be valuable in constraining semi-distributed hydrological models (e.g. Savenije and Hrachowitz, 2017).

The Normalized Difference Infrared Index (NDII) is an index that detects canopy water content (Hardisky et al., 1983) which has been recently investigated for monitoring drought conditions (Moricz et al., 2018; Xulu et al., 2018). The index is indicative of differences in moisture capacities and has been shown to correspond with root zone soil moisture (RZSM) dynamics. Sriwongsitanon et al. (2016) proposed to use the NDII as a proxy for RZSM and showed its effectiveness in 8 sub-catchments of the Upper Ping River basins in Thailand. This is in agreement with the study carried out by Castelli et al. (2019) who found reasonable correlations between Landsat 7 NDII values and measured RZSM soil moisture contents of rainfed olive trees growing in the arid regions of south-eastern Tunisia, supporting the use of NDII as a proxy for soil water content in arid regions.

Mao and Liu (2019) found RZSM signatures to be well-correlated to NDII in most regions, except in river basins with high forest coverage, as well as those with low moisture stress, or those with developed the Water And Ecosystem Simulator (WAYS) which is a distributed model based on FLEXL to simulate discharge as well as root zone water storage (RZWS) on a global scale across 10 major basins comprising Congo, Nile, Niger, Yangtze, Ganges, Parana, Amazon, Mississippi, Murray-Darling, and Mekong. The model showed a good performance in simulating evaporation and discharge. It also could simulate RZWS in most of the regions through comparison with NDII (correlation (r) ranging from 0.951 and 0.713 with an average of 0.883). This is with the exception of some basins such as the Amazon, Murray Darling and Mississippi (r ranging from 0.552 and 0.677) which have high percentage of forest areas, trees intercepting deep groundwater (e.g. Eucalyptus) or plenty of precipitation with low moisture stress where NDII may not correctly reflect RZWS dynamics. The above studies reveal the worthwhileness of incorporating NDII to constrain semi-distributed models with the objective of enhancing the accuracy of runoff estimates at the sub-catchment scale.

Regarding the use of the Soil Water Index (SWI), which is partly model-based, as a proxy for root-zone soil moisture, Paulik et al. (2014) found reasonable correlations between in situ soil moisture data from 664 stations—available through the international Soil Moisture Network (ISMN)—and the SWI produced from ASCAT SSM estimates. The average of Pearson correlation coefficients was shown to be 0.54, with 64.4% of all time series greater than 0.5. SWI may be used as another index for the soil moisture state of a basin with or without moisture stress.

Among the wide range of existing lumped rainfall-runoff models, FLEXL has proven to be an adequate model for runoff estimation in a wide range of catchments (Fenicia et al., 2011; Fenicia et al., 2008; Gao et al., 2014; Kavetski and Fenicia, 2011; Tekleab et al., 2015). This model was further developed by Gharari et al. (2011) and Gao et al. (2016) to account for the spatial variability of landscape characteristics (FLEX-TOPO), useful for prediction in ungauged basins (Savenije, 2010). Moreover, Sriwongsitanon et al. (2016) demonstrated that catchment-scale soil moisture content in the rootzone of vegetation computed from FLEXL is correlated with the remotely sensed Normalized Difference Infrared Index (NDII), as a proxy for the equivalent water thickness (EWT) in the root zone, especially during periods of moisture stress.

This study ~~aims to utilize~~ the fundamental model structure of FLEXL, include distributed time lags and channel routing as used in URBS, and include distributed root zone soil moisture capacity per sub-catchment ~~so as to~~ create a new parsimonious semi-distributed FLEX model for flood and flow monitoring within the (ungauged) sub-catchments of the gauged Upper Ping River Basin. ~~Distribution of time lags is expected to improve hydrograph shape, particularly the timing and shape of the peaks, which would improve best-fit parameters, but it does not affect the partitioning of the hydrological fluxes or the water balance. Since the root zone storage is the main control on flux partitioning, the distribution of the root zone moisture storage capacity would potentially have a larger impact on model performance. Therefore, the spatial variation of the NDII, as an indicator of root zone moisture stress, has been used to distribute moisture storage capacities among sub-catchments, while the model-based SWI, as an estimator of moisture storage, was used for validation.~~

~~The main steps undertaken in the following sections are the following: (~~

~~1) To introduce the effect of runoff timing in a catchment with multiple sub-catchments, the travel times to the outfall of each individual sub-catchment are computed on the basis of topographical indicators and the routing of the discharge from the sub-catchment outfall to stations further downstream are computed using the Muskingum method. These time lags are then applied both in the FLEX-SD model system and in the well-established URBS model, for the purpose of comparison. These two semi-distributed models only account for timing, but not for the distribution of the moisture storage capacity — a crucial parameter in runoff generation. The distribution of time lags is expected to properly simulate hydrograph shape, particularly the timing and shape of the peaks of all sub-catchments within calibrated gauging station, but it does not affect the partitioning of the hydrological fluxes or the water balance as well as the accuracy of runoff estimates. (~~

2) Subsequently, the effect of distribution of the root zone moisture storage is studied in the FLEX-SD model, making use of the spatial distribution pattern of the maximum and minimum range of NDII values, and the annual average NDII values to construct 2 alternative models: FLEX-SD-NDII_{Max-Min} and FLEX-SD-NDII_{Avg}, respectively. (

5 3) Finally, as a validation of the models and to check if they are capable of representing the internal moisture states, the simulated root zone moisture storage is compared to the independent data-set of the Soil Wetness Index (SWI).

2 Study area and datasets

2.1 Study area

The Upper Ping River Basin (UPRB) is situated between latitude 17°14'30'' to 19°47'52''N and longitude 98° 4'30'' to 99°22'30''E in the provinces of Chiang Mai and Lamp-hun. The catchment area of the basin is approximately 25,370 km². The basin is dominated by well-forested, steep mountains in a generally north-south alignment (Sriwongsiton and Taesombat, 2011). The areal average annual rainfall and runoff of the basin from 2001-2016 are 1,224 mm/yr and 235 mm/yr, respectively. The land use for the UPRB in 2013 can be classified into 6 main classes comprising forest, irrigated agriculture, rainfed agriculture, bare land, water body, and others, which cover approximately 77.40%, 3.11%, 12.54%, 1.99%, 1.23%, and 3.73% of the catchment area, respectively (Land Development Department, LDD). The landform of the UPRB varies from an undulating to a rolling terrain with steep hills at elevations of 1,500–2,000 m, and valleys of 330–500 m (Mapiam and Sriwongsiton, 2009; Sriwongsiton, 2010). Chiang Dao district, north of Chiang Mai is the origin of the Ping River, which flows downstream to the south to become the inflow of the Bhumibol Dam – a large dam with an active storage capacity of about 9.7 billion m³ (Sriwongsiton, 2010). The climate of the basin is dominated by tropical monsoons. The southwest monsoon causes a rainy season between May and October and the northeast monsoon brings dry weather and low temperatures between November and April. Only 6,142 km² of the total area controlled by the runoff station P.1 (situated at the centre of Chiang Mai) is selected for this study (Fig. 1). The catchment area of the station P.1 is divided into 32 sub-catchments (Fig. 1) where the semi-distributed rainfall-runoff models are tested.

2.2 Rainfall data

25 Daily rainfall data from 48 non-automatic rain-gauge stations located within the UPRB and its surroundings from 2001-2016 were used in this study. These data are owned and operated by the Thai Meteorological Department and the Royal Irrigation Department. These data have been validated for their accuracy on monthly basis using double mass curve and some inaccurate data were removed from the time series before spatially averaging using an inverse distance square (IDS) to be applied as the forcing data of URBS, FLEXL, and FLEX-SD. Mean areal rainfall depth for each of 32 sub-catchments varies between 1,100 (S17) and 1,402 (S11) mm/yr as shown in Figure 1 (b) while the average rainfall depth of P.1 is approximately 1,224 mm/yr.

Formatted: Superscript

Formatted: Superscript

Formatted: Superscript

2.3 Runoff data

The Royal Irrigation Department (RID) operates 7 daily runoff stations in the study area between 2001 and 2016 as shown in Fig. 1. Catchment P.56A was rejected from the study because it is located upstream of Mae Ngat reservoir. Outflow data from the reservoir were used as input data in model calibration. Runoff data at the remaining 6 stations were used for the study since they are not affected by large reservoirs. The data have been checked for their accuracy by comparing them with average rainfall data covering their catchment areas at the same periods. Table 1 presents the catchment characteristics and hydrological data for these 6 gauging stations in the UPRB. In this study, the catchments of these 6 stations were divided into 32 sub-catchments (see Fig. 1) with areas ranging from 57 to 230 km². High variation of catchment size is due to the proximity between the locations of these runoff stations and the outlets of the tributaries. Runoff data have been checked for their accuracy by comparing the annual runoff coefficient between all stations. The comparison revealed that the runoff coefficients at P.20 in 2006 and 2011 are overestimated, while the runoff coefficient at P.21 in 2004 is underestimated and in 2007 and 2009 are overestimated due to incorrect rating curves (see Fig. 2). These inaccurate data would affect the results of model calibration.

2.4 NDII Data

The Normalized Difference Infrared Index (NDII) is a ratio of the near-infrared (NIR) and shortwave infrared (SWIR) bands, centred at 859 and 1,640 nm, respectively, as shown in Eq. (1). In this study, the NDII was calculated using the MODIS level 3 surface reflectance product (MOD09A1), which is available at 500 m resolution in an 8-day composite of the gridded level 2 surface reflectance products. Atmospheric correction has been carried out to improve the accuracy and can be downloaded from <ftp://e4ftl01.cr.usgs.gov/MOLT> (Vermote et al., 2011). The 8 day NDII values between 2002-2016 were averaged over each of 31 sub-catchments of the UPRB to be used for estimating model parameter within sub-catchment and to be compared to the 8 day average S_u (root zone storage) values extracted from the model results at each station.

$$NDII = \frac{(NIR - SWIR)}{(NIR + SWIR)} \quad (1)$$

2.5 SWI Data

The near real-time Soil Water Index (SWI) is derived from the reprocessed Surface Soil Moisture (SSM) data derived from the ASCAT sensor (Brocca et al., 2011; Paulik et al., 2014), which is a C-Band Scatterometer measuring at a frequency of 5.255 GHz in VV-polarisation (Paulik et al., 2014). The product makes use of a two-layer water balance model to describe the time series relationship between surface and profile soil moisture. This dataset of moisture conditions is available on a daily basis for eight characteristic time windows 1, 5, 10, 15, 20, 40, 60 and 100 days. The global scale SWI dataset is available at 0.1 degree, which is about 10 km resolution, within 3 days after observation and can be downloaded from the Copernicus Global Land Service website. The dataset is available from January 2007 onwards. Since the SWI dataset is not complete in 2007, only the data between 2008 and 2016 were used in this study. The characteristic time length is the only parameter in the SWI procedure. Bouaziz et al. (2020) specified the optimal T values (T_{opt}) by matching modelled time series of RZSM from a

Formatted: Complex Script Font: Times New Roman, 10 p
(Complex) Arabic (Saudi Arabia)

Formatted: Complex Script Font: Times New Roman, 10 p

Formatted: Complex Script Font: Times New Roman, 10 p
(Complex) Arabic (Saudi Arabia)

Formatted: Complex Script Font: Times New Roman, 10 p
(Complex) Arabic (Saudi Arabia), Subscript

Formatted: Complex Script Font: Times New Roman, 10 p
(Complex) Arabic (Saudi Arabia)

calibrated FLEXL model to several SWI products in 16 contrasting catchments in the Meuse river basin. They concluded that the characteristic time lengths are differentiated amongst land cover (% agriculture), soil properties (% silt), and runoff signatures (flashiness index). In Section 5.4.2 the appropriate time scale for the Ping basin will be determined in 40 days.

3 Theoretical B-background

3.1 FLEXL model

FLEXL is a lumped hydrological model comprising five reservoirs: a snow reservoir (S_w), an interception reservoir (S_i), an unsaturated soil reservoir (S_u), a fast-response reservoir (S_f), and a slow-response reservoir (S_s) (Gao et al., 2014). Excess rainfall from a snow reservoir, an interception reservoir, and an unsaturated soil reservoir is divided and routed into a fast-response reservoir and a slow-response reservoir using two lag functions. It includes the lag time from storm to peak flow (T_{lagF}) and the lag time of recharge from the root zone to the groundwater (T_{lagS}). Each reservoir has process equations that connect the fluxes entering or leaving the storage compartment to the storage in the reservoirs (so-called constitutive functions) (Sriwongsitanon et al., 2016). The water balance equations and constitutive equations for each conceptual reservoir are summarised in Fig. 3 and Table 2. The total number of model parameters is 11. Forcing data include daily average rainfall and potential evaporation derived by the Penman-Monteith equation.

3.1.1 Snow reservoir

The snow routine, not very relevant in Thailand, can play an important role in areas with snow. When there is snow cover and the temperature (T_i) is above T_t , the effective precipitation is equal to the sum of rainfall (P_i) and snowmelt (M_i). The snowmelt (M_i) is calculated by the melted water per day per degree Celsius above T_t (F_{DD}) (Eq. (2)). The snow reservoir uses the water balance equation, Eq. (3), where S_{w_i} (mm) is the storage of the snow reservoir.

3.1.2 Interception reservoir

Interception is more important in summer and autumn. The interception evaporation E_i was calculated by potential evaporation (E_{p_i}) and the storage in the interception reservoir (S_i), with a daily maximum storage capacity (I_{max}) (Eqs. (4), (5)). The interception reservoir uses the water balance equation, Eq. (6), presented in Table 2.

3.1.3 Root zone reservoir

The root zone routine, which is the core of the hydrological models, determines the amount of runoff generation. In this study, we applied the widely used beta function of the Xinanjiang model (Ren-Jun, 1992) to compute the runoff coefficient for each time step as a function of the relative soil moisture. In Eq. (7), C_r indicates the runoff coefficient, S_{u_i} is the storage in the root zone reservoir, S_{umax} is the maximum moisture holding capacity in the root zone and β is the parameter describing the spatial

Formatted: Complex Script Font: Times New Roman, 10 p

Formatted: Complex Script Font: Times New Roman, 10 p
(Complex) Arabic (Saudi Arabia)

Formatted: Complex Script Font: Times New Roman, 10 p

Formatted: Complex Script Font: Times New Roman, 10 p
(Complex) Arabic (Saudi Arabia)

Formatted: Complex Script Font: Times New Roman, 10 p

Formatted: Complex Script Font: Times New Roman, 10 p
(Complex) Arabic (Saudi Arabia)

process heterogeneity of the runoff threshold in the catchment. In Eq. (8), Pe_i indicates the effective rainfall and snowmelt into the root zone routine; Ru_i represents the generated flow during rainfall events. In Eq. (9), Su_i , $Sumax_i$ and potential evaporation (Ep_i) were used to determine actual evaporation from the root zone Ea_i ; Ce indicates the fraction of $Sumax$ above which the actual evaporation is equal to potential evaporation, here set to 0.5 as previously suggested by Savenije (1997) otherwise Ea_i is constrained by the water available in Su_i . The unsaturated soil reservoir uses the water balance equation, Eq. (10), presented in Table 2.

3.1.4 Fast response reservoir

In Eq. (11), Rf_i indicates the flow into the fast-response routine; D is a splitter to separate recharge from preferential flow. Equations (12) and (13) were used to describe the lag time between storm and peak flow. Rf_{t-i+1} is the generated fast runoff in the unsaturated zone at time $t - i + 1$, $TlagF$ is a parameter which represents the time lag between storm and fast runoff generation, $c_{lagF}(i)$ is the weight of the flow in $i - 1$ days before and Rfl_i is the discharge into the fast-response reservoir after convolution.

A linear-response reservoir, representing a linear relationship between storage and release, was applied to conceptualize the discharge from the surface runoff reservoir, fast response reservoirs and slow-response reservoirs. In Eq. (14), Qff_i is the surface runoff, with timescale Kff , active when the storage of the fast-response reservoir exceeds the threshold $Sfmax$. In Eq. (15), Qf_i represents the fast runoff; Sf_i represents the storage state of the fast response reservoirs; Kf is the timescales of the fast runoff. The fast response reservoir uses the water balance equation, Eq. (16), presented in Table 2.

3.1.5 Slow response reservoir

In Eq. (17), Rs_i indicates the recharge of the groundwater reservoir. Equations (18) and (19) were used to describe the lag time of recharge from the root zone to the groundwater. Rs_{t-i+1} is the generated slow runoff in the groundwater zone at time $t - i + 1$, $TlagS$ is a parameter which represents the lag time of recharge from the root zone to the groundwater, $c_{lagS}(i)$ is the weight of the flow in $i - 1$ days before and Rsl_i is the discharge into the slow-response reservoir after convolution. In Eq. (20), Qs_i represents the slow runoff; Ss_i represents the storage state of the groundwater reservoir; Ks is the timescales of the slow runoff. The slow response reservoir uses the water balance equation, Eq. (21), presented in Table 2.

3.2 URBS model

URBS was developed by Queensland Department of Natural Resources and Mines in 1990 based on the structures of RORB (Laurenson and Mein, 1990) and WBNM (Boyd et al., 1987). URBS is a semi-distributed rainfall-runoff model that can provide runoff estimates not only at the calibrated station but also at the outlet of every sub-catchment at any required location upstream. The calibrated catchment area needs to be divided into sub-catchments to obtain different areal rainfall and different catchment and channel travelling time.

Table 3 presents 5 main processes used in URBS comprising the calculation of the initial loss, proportional loss, excess rainfall, catchment routing and channel routing. Excess rainfall is calculated separately between pervious and impervious areas. For the pervious area, URBS assumes that there is the maximum initial loss rate (IL_{max}) to be reached before any rainfall becoming the effective rainfall (R_i^{eff}). The initial loss (IL_i) can be recovered when the rainfall rate (R_i) is less than the recovering loss rate (r/r) per time interval (δt) (see Eq. (22)).

Excess rainfall for each time step is calculated using Eq. (23) by weighting the excess rainfall between pervious and impervious area using a ratio of the cumulative infiltration (F_i) and the maximum infiltration capacity (F_{max}). The recovering rate is included by simply reducing the amount infiltrated after every time step using the reduction coefficient ($k_{\delta t}$) as shown in Eq. (24), and the pervious excess rainfall (R_i^{per}) is calculated using the Eq. (25), where pr is the proportional runoff coefficient. The remaining water $(1-pr)R_i^{eff}$ will infiltrate to the root zone storage (dF_i) (see Eq. (26)). Excess rainfall is then routed to the centroid of any sub-catchment using a nonlinear reservoir relationship ($S_i = KQ_i^m$). The parameter m is the catchment non-linearity and K is the catchment travel time, which can be calculated for different sub-catchment using the multiplication between the catchment lag time coefficient (β) and square root of each sub-catchment area (A) (see Eq. (27)).

Thereafter, the outflow at the centroid of each sub-catchment is routed along a reach downstream of each sub-catchment using the Muskingum equation ($S_i^{ch} = K_{ch}(XI + (1-X)Q_i)$). The parameter X is the Muskingum coefficient and K_{ch} is the channel travel time, which can be calculated for different sub-catchment using the multiplication between the channel lag coefficient (α) and the reach length (L) between the closest location in the channel to the centroid and the outlet of each sub-catchment (see Eq. (28)).

4 Methodology

4.1 Development of the semi-distributed FLEX models

The first step in distribution is to account for the timing of floods and the rooting of flood waves as a function of topographical factors. The resulting semi-distributed FLEX-SD model therefore is expected to better represent the shape of hydrographs, although it would not affect the partitioning of fluxes or the water balance. The root zone storage capacity is a strong control on partitioning, affecting both runoff generation and evaporation. Therefore, distribution of this parameter would potentially affect overall model performance more strongly than merely the timing of the peaks. Therefore, in a second step, the NDII, as a proxy for moisture storage, is used to assess the distribution of moisture storage among sub-catchments.

4.1.1 Accounting for distributed timing and channel-routing

FLEX-SD is set-up by applying lumped models for each sub-catchment, adding up to a semi-distributed model for a downstream calibration site. Therefore, the catchment area of any gauging station needs to be divided into sub-catchments. Runoff estimates at each sub-catchment can be simulated using the structure of the original FLEXL by calculating different excess rainfall for each sub-catchment. The excess rainfall of each sub-catchment is routed to its outlet using the lag time from rainfall to surface runoff ($TlagF$) and the lag time of recharge from the root zone to the groundwater ($TlagS$). In this study, $TlagF$ and $TlagS$ are calculated in hours instead of days to increase model performance. The lag time is distributed among sub-catchments using the following equations.

$$TlagF_{sub} = TlagF \sqrt{A_{sub}/A} \quad (29)$$

$$TlagS_{sub} = TlagS \sqrt{A_{sub}/A} \quad (30)$$

where, $Tlag$ is a lag time parameter for the entire catchment of a calibrated gauging station. The lag time of each sub-catchment ($Tlag_{sub}$) is scaled by the square root of each sub-catchment area divided by the overall catchment area (A).

Runoff estimates from an upstream sub-catchment is later routed from its outlet to the outlet of a downstream sub-catchment using the Muskingum method (Eq. (31)) before adding to the runoff estimates of the downstream sub-catchment.

$$S_{chnl-sub} = K_{sub} (XQ_{up} + (1-X)Q_{down}) \quad (31)$$

$$K_{sub} = \alpha L_{sub} \quad (32)$$

where, α and X are the delay time parameter and the channel routing parameter for the entire catchment, respectively. The delay time parameter of each sub-catchment (K_{sub}) can be calculated by the multiplication between α and the main channel length of each sub-catchment as shown in Equation (32).

4.1.2 Accounting for distributed root zone storage at sub-catchment scale using the maximum and minimum values of NDII (FLEX-SD-NDII_{MaxMinMaxMin} model)

The Normalized Difference Infrared Index (NDII) was used to estimate root zone storage capacity for each sub-catchment. The NDII values, which are available at 8 day intervals, were found to correlate well with the 8-day average root zone moisture content (Su) simulated by FLEXL during the dry period in eight sub-catchments in the UPRB (Sriwongsitanon et al., 2016).

The relation between NDII and Su can be described by an exponential function of the type: $ae^{b(NDII)}+c$, with c close to zero. The maximum value that Su can achieve is $Sumax$, the storage capacity of the root zone. The hypothesis is that the ecosystem creates sufficient storage to overcome a critical period of drought (Gao et al., 2014; Savenije and Hrachowitz, 2017). Every year has a maximum range of storage variation. If a sufficiently long NDII record is available, then the maximum of the annual ranges of the NDII should provide an estimate of the root zone storage capacity $Sumax$. By calibrating the hydrological FLEX model to discharge observations at the gauging stations, for each gauged catchment a $Sumax$ value can be calibrated. This is a representative $Sumax$ value for a particular gauging station, consisting of n sub-areas, indicated by $Sumax_n$.

$$Sumax_n = \frac{\sum_{i=1}^n (A_i Sumax_i)}{\sum_{i=1}^n A_i} \quad (33)$$

By using the NDII as proxy for root zone storage, we have developed the following equation for the proxy root zone storage capacity $Sumax'_i$ for a sub-area within a river basin consisting of 31 sub-catchments:

$$Sumax'_i = \frac{[e^{b \times NDII_{i,max}} - e^{b \times NDII_{i,min}}]_{max}}{[e^{b \times NDII_{n,max}} - e^{b \times NDII_{n,min}}]_{max}} \quad (34)$$

Where $Sumax'_i$ is a scaled proxy for the root zone storage capacity of each sub-catchment, and b is the remaining calibration parameter, because the constant c and the factor a of the exponential function drop out. The $NDII_{i,max}$ and $NDII_{i,min}$ represent the maximum and minimum values of NDII for each year of each sub-catchment, while the $NDII_{n,max}$ and $NDII_{n,min}$ indicate the maximum and minimum values of NDII for each year in the reference basin, in this case, the entire Upper Ping basin controlled by station P.1. The unscaled root zone storage capacity per sub-catchment then becomes:

$$Sumax_i = Sumax_n \frac{Sumax'_i}{Sumax'_n} \quad (35)$$

Where $Sumax_n$ is the calibrated value of the root zone storage capacity of the gauged catchment, and $Sumax'_n$ is the area weighted proxy for the root zone storage capacity.

$$Sumax'_n = \frac{\sum_{i=1}^n (A_i Sumax'_i)}{\sum_{i=1}^n A_i} \quad (36)$$

4.1.3 Accounting for distributed root zone storage at sub-catchment scale using average value of NDII (FLEX-SD-NDII_{Avg})

Instead of applying the maximum and minimum of the annual ranges of the NDII to distribute root zone storage at a sub-catchment scale, we tested the annual average NDII value of each sub-area to calculate $Sumax'_i$ as presented in the following equation.

$$Sumax'_i = \left(0.5 - \frac{R}{2}\right) + R \left(\frac{(e^{b \times NDII_i}) - (e^{b \times NDII_{i \rightarrow n}})_{min}}{(e^{b \times NDII_{i \rightarrow n}})_{max} - (e^{b \times NDII_{i \rightarrow n}})_{min}} \right) \quad (37)$$

Where $NDII_i$ represents the annual average NDII value of each sub-catchment, while $(e^{b \times NDII_{i \rightarrow n}})_{max}$ and $(e^{b \times NDII_{i \rightarrow n}})_{min}$ indicate the maximum and minimum values of exponential function produced by the annual average NDII value within 32

sub-catchments. The parameters b and R can be determined by model calibration. The parameter R is suggested to vary between 0.2 and 0.8 to force a scaled factor $Sumax'_i$ to be more than 0 and less than 1. The average NDII value is supposed to reflect the maximum moisture storage capacity as well, since a high maximum value also leads to a higher average, but is much easier to calculate. However, this method requires the introduction of the additional calibration parameter R .

5

4.2 Model Applications Applications of URBS, FLEXL, FLEX-SD, FLEX-SD-NDII_{Max-Min} and FLEX-SD-NDII_{Avg}

Firstly, FLEXL and the four semi-distributed models, URBS, FLEX-SD, FLEX-SD-NDII_{Max-Min} and FLEX-SD-NDII_{Avg} were calibrated (2001-2011) and validated (2012-2016) at the stations P.4A, P.20, P.21, P.75, P.67 and P.1 individually to provide baselines for comparison of model performances. Further, additional runoff estimates at the outlet of 31 sub-catchments, inclusive of the internal gauging stations upstream of P.1, were extracted from the four semi-distributed models. The runoff estimates at the above stations were compared to observed data and also for their comparability to the performance of FLEXL at individual stations.

10

URBS, FLEX-SD, FLEX-SD-NDII_{Max-Min} and FLEX-SD-NDII_{Avg} were calibrated (2001-2011) and validated (2012-2016) at P.1 station located in the city of Chiang Mai. Since these models are semi-distributed rainfall runoff models, they can provide runoff estimates in any required locations upstream of P.1 station, resulting in runoff estimates for P.4A, P.20, P.21, P.75 and P.67. As benchmarks for analysis, the calibrated FLEXL model was also used to estimate runoff at these 5 stations. In addition, all semi-distributed models were calibrated and validated at these 5 stations for a fair comparison with the results of the locally calibrated FLEXL model at each internal station (presented in Annex A). The model parameters of the calibrated models were

15

determined using the MOCEM-UA (Multi-Objective Shuffled Complex Evolution Metropolis-University of Arizona) algorithm (Vrugt et al., 2003) by finding the Pareto-optimal solutions defined by three objective functions of the Kling-Gupta Efficiencies for high flows, low flows, and the flow duration (KGE_{F_h} , KGE_{F_l} and KGE_{F_d}), respectively. KGE_{F_d} is analysed using the following equations, where \bar{X} is the average observed discharge, \bar{Y} is the average simulated discharge, S_X is the standard deviation of observed discharge, S_Y is the standard deviation of simulated discharge, and r is the linear correlation between observations and simulations. KGE_{F_l} can be calculated using the logarithm of flows to emphasize low flows. The Nash-Sutcliffe Efficiency (NSE) is an independent statistical indicator, which is not utilised in the objective function but merely used to summarised model performance. The model calculates at daily time steps, but this is disaggregated to hourly to take into account the time lags. The output is again aggregated to daily time steps.

20

25

$$KGE = 1 - ED \quad (38)$$

30

$$ED = \sqrt{(r - 1)^2 + (\alpha - 1)^2 + (\beta - 1)^2} \quad (39)$$

Formatted: Subscript

Formatted: Subscript

Formatted: Subscript

Formatted: Subscript

Formatted: Subscript

Formatted: Subscript

$$\alpha = S_y/S_x \quad (40)$$

$$\beta = \bar{Y}/\bar{X} \quad (41)$$

5 The results of this section are presented in Sections 5.1 and 5.2.

Additionally, to test the efficacy of the distribution of moisture capacities by NDII, we investigated the relationship between the proportion of evergreen forests and the *Sumax* values produced by FLEX-SD-NDII_{Avg} and FLEX-SD-NDII_{MaxMin} in each sub-catchment. The results are presented in Section 5.3.

4.3 Estimation of Uncertainty in FLEX-SD-based Models

10 In hydrological models, inherent uncertainties caused by imperfect model structures and model parameters are unavoidable (Solomatine, D.P. and Shrestha, D.L., 2009). To identify uncertainty of developed models, FLEX-SD, FLEX-SD-NDII_{MaxMin} and FLEX-SD-NDII_{Avg} were calibrated (2001-2011) and validated (2012-2016) at P.1 station using 50,000 random parameter sets. The 5% best-performing parameter sets were identified as feasible (Hulsman et al., 202019) and utilized to evaluate uncertainties. The results of KGE_E, KGE_L and KGE_F at the calibrated station (P.1) and at 5 upstream stations (P.20, P.4A,

15 P.21, P.75 and P.67) were assessed.

4.4 Relationship between the average root zone soil moisture storage (*Su_t*) and the average NDII and SWI

Sriwongsitanon et al. (2016) suggested that NDII can be used as a proxy for soil moisture storage in hydrology. Here, 8-day average NDII values were compared to 8-day average root zone moisture storage (*Su_t*) derived at the six gauging stations, as calculated by FLEXL, FLEX-SD, FLEX-SD-NDII_{MaxMin} and FLEX-SD-NDII_{Avg}. The *Su* estimates were compared to the SWI product at the daily time scale. The *Su*-SWI relationship was examined for all characteristic time lengths to deduce the optimal time length which best represents RZSM dynamics in the UPRB. The results of *Su*-NDII and *Su*-SWI were aggregated to present these relationships at the seasonal basis. The Coefficient of Determination (*R*²) and NSE were used as objective functions. Subsequently, for the FLEX-SD-based models, their *Su* time series were extracted at the outlets of 31 sub-catchments to be compared to time series of NDII and the optimal time length of SWI.

20

25 **5 Results**

5.1 Model Performances Accuracy of runoff estimates simulated by URBS, FLEXL, FLEX-SD, FLEX-SD-NDII_{Max-Min} and FLEX-SD-NDII_{Avg}

The assessment of model performances during the calibration and validation periods are presented in two sub-sections. Section 5.1.1 presents the results at internal gauging stations through the calibration/validation at all stations and from all models.

30 Section 5.1.2 shows the results at internal gauging stations from the semi-distributed models through calibration/validation at

Formatted: Complex Script Font: 14 pt

Formatted: Heading 2

Formatted: Font: Italic, Complex Script Font: Not Italic

Formatted: Font: Italic, Complex Script Font: Not Italic, Subscript

P.1, which were compared to the corresponding performance of FLEXL through calibration/validation at all stations. A discussion of the model parameters provided in Section 5.1.3. Figures A1-A3 provides a comparison between performances undertaken at all stations and at P.1 only, in terms of accumulated flows, hydrographs, and duration curves, respectively. In the following sections, the term average refers to the average across all gauging stations (P.4A, P.20, P.67, P.75, P.21, P.1).

5.1.1 Performance of all models by Calibration/Validation at all Stations

For the calibration period (Fig. 4(a)), similar overall accuracy was produced by all models, with URBS and FLEXL showing NSE of 0.69 and 0.73, respectively, and the three FLEX-SD-based models (FLEX-SD-NDII_{Avg}, FLEX-SD and FLEX-SD-NDII_{MaxMin}) yielding NSE of 0.76. However, FLEXL provided slightly lower average KGE_L in some stations. For the validation period (Fig. 4(b)), lower overall accuracy was achieved by FLEXL (NSE = 0.53) and URBS (NSE = 0.59), and with notably lower KGE_L at some stations. Meanwhile, the FLEX-SD-based models showed NSE of 0.65-0.66. All models provided similar KGE_E and KGE_F during both periods.

In conclusion, all developed FLEX-SD-based models can simulate runoff with similar accuracy or perform even better than the lumped model, FLEXL, and the established semi-distributed model, URBS.

5.1.2 Performance of semi-distributed models by Calibration/Validation at P.1.

As aforementioned, the performance of FLEXL at each gauging station provides a baseline comparison for the results of the semi-distributed models in predictive mode. Over the calibration period (Fig. 5(a)), the FLEX-SD-based models produced similar accuracies (average NSE = 0.72-0.75), while URBS performed slightly poorer (NSE = 0.68). This is comparable, if not slightly better, than FLEXL (NSE = 0.73). However, in terms of the KGE_E indicator, FLEXL (KGE_E = 0.86) performs notably better than the semi-distributed models (KGE_E = 0.78-0.82). For the validation period (Fig. 5(b)), the FLEX-SD-based models (NSE = 0.67-0.70) and URBS (NSE = 0.65) performed notably better than FLEXL (NSE = 0.53).

As shown in Fig. A1, the semi-distributed models are not capable of closing the water balance in four stations except at the most downstream stations – P.67 and P.1. Additionally, the calibration/validation performed at all stations also closes the water balance better than achieved in predictive mode, although this may be due to over-fitting. Nonetheless, the fact that the validation mode of all semi-distributed models obtains more accurate results than the lumped and calibrated FLEXL model indicates a higher predictive capacity of the semi-distributed models.

Needless to say, issues such as flow regulation and water withdrawals pose challenges to these semi-distributed models. This is apparent at P.75, where outflows from Mae Ngat Dam were potentially abstracted for agricultural demands but were yet unaccounted for, causing notable overestimations of observed flows. This is reinforced in Fig. A3, which shows the lowest observed flows to be predominantly below modelled flows. P.4A also revealed overestimated flows, which drains a mountainous catchment with evergreen forest. In contrast, flow underestimations were seen in P.21 and P.20, which are

Formatted: No bullets or numbering

intensively used catchments with rating problems (see Fig. 2). The lumped models are apparently not yet capable to distinguish well between different landscapes. A landscape-based model as suggested by Gharari et al. (2011) and Savenije (2010) could be the next step for improvement.

5.1.3 Discussion of Model Parameters

- 5 The performance criteria of the runoff estimates simulated by URBS, FLEXL, FLEX-SD, FLEX-SD-NDII_{Max-Min} and FLEX-SD-NDII_{Avg} calibrated on P.1 runoff data for the period (2001–2011), and for the validation period (2012–2016), are presented in Table 4 and Table 5, respectively. Model parameters of these models are presented in Table A1. Figures 4, 5 and 6 present the output of the five models for all stations compared to observations, as accumulated flows, hydrographs on logarithmic scale, and duration curves, respectively. For comparison, the results of the calibrated and validated models at each of the 6 individual stations are presented in Figures A1, A2 and A3. Of course, these calibrated models close the water balance better, but this may be due to over fitting. Table 4 shows that FLEXL, FLEX-SD, FLEX-SD-NDII_{Max-Min} and FLEX-SD-NDII_{Avg} calibrated at P.1 produce similar overall accuracy with an average NSE of 0.73, 0.73, 0.72 and 0.75, respectively during the calibration period, while URBS obtained a lower NSE of 0.68. However, FLEXL acquired higher KGE values compared to other models. Table 5 surprisingly shows that FLEXL attains the lowest NSE value of 0.53 during validation, compared to NSE values of 0.70, 0.68, 0.67 and 0.65 produced by FLEX-SD-NDII_{Avg}, FLEX-SD, FLEX-SD-NDII_{Max-Min}, and URBS, respectively. It should be realized that FLEXL was calibrated individually for each sub-catchment, while the other models were used in predictive mode. The fact that in the validation mode all semi-distributed models obtain more accurate results than the lumped and calibrated FLEXL model indicates a higher predictive capacity of the semi-distributed models.
- 10
- 15
- 20 Figure 4 clearly shows that the distributed models are not capable of closing the water balance in four stations except at P.1 and P.67 located in the main Ping. While FLEXL, which is calibrated at each individual station can mimic the pattern, this may be due to over fitting. In P.75, the models over estimate the observed flow. This is due to flow regulation and water withdrawals in the managed parts of the sub-catchments (there is the large Mae Ngad dam upstream of P.75). The duration curves in Figure 6 confirm this and also show that the observed lowest flow is below the modelled flow, almost throughout.
- 25 This is likely due to water abstractions for urban and agricultural water supply. In contrast, the models underestimate the flows in P.21 and P.20, which are intensively used catchments with rating problems. On the other hand, the flow is over estimated at P.4A, which drains a mountainous catchment with evergreen forest. The lumped models are apparently not yet capable to distinguish well between these different landscapes. A landscape-based model as suggested by Gharari et al. (2011) and Savenije (2010) could be the next step for improvement.

30

The model parameters used in FLEXL, FLEX-SD and FLEX-SD-NDII_{Max-Min} and FLEX-SD-NDII_{Avg} are summarized in Table A1. The FLEX-SD-based models provides different values for *TlagF* (the time lag between storm and fast runoff generation),

and $TlagS$ (the lag time of recharge from the root zone to the groundwater); the other parameters are kept the same as the calibrated values for P.1. Since $TlagF$ and $TlagS$ were designed to be related to the catchment area, the parameter values for each station are more reasonable compared to the values given by FLEXL. It can be noted that the values of $TlagF$ obtained by FLEX-SD-NDII_{Avg} are much closer to the ones presented by FLEX-SD compared to the values obtained by FLEX-SD-

5 NDII_{Max-Min}.

~~The $Sumax$ values generated by FLEX-SD-NDII_{Avg} and FLEX-SD-NDII_{MaxMin} are quite different between the 31 sub-catchments. A large part of the landscape within the Upper Ping River Basin is covered by evergreen forest which may affect the soil moisture of each sub-catchment. The relationships between the percentage of evergreen forest and $Sumax$ in 31 sub-catchments calibrated and validated by FLEX-SD-NDII_{Avg} and FLEX-SD-NDII_{MaxMin} are presents in Figure A4. The figure displays quite high R^2 correlation of 0.69 introduced by FLEX-SD-NDII_{Avg} compared to a small R^2 value of 0.01 exhibits by FLEX-SD-NDII_{MaxMin}. It seems that FLEX-SD-NDII_{Avg} introduces more realistic $Sumax$ values in forested landscapes.~~

10

In general, ~~the FLEX-SD-NDII models~~ provides lower $Sumax$ estimates than the other models, constraining evaporation in the dry season ~~(which provides more realistic recessions in Figure 5)~~, but compensatinges for this reduction by a smaller β value, so as to limit excessive flood generation. Since these parameters jointly control Eq. (7), they can compensate for each other, leading to equifinality. If one of the parameters is constrained by additional information, as is the case here using the NDII, then this is no longer possible. The performance with respect to best fit parameters may reduce in the process, but the model has gained realism and hence predictive power.

15

20

We see that the FLEXL-SD-NDII models show the highest realism (illustrated ~~clearly in Figure 5 and Figure A2 in the appendix A~~) but not a very good performance in the sub-catchment P.20, although still better than the other ~~semi-distributedSD~~ models. P.20 remains a difficult sub-catchment to predict due to its flow regulation and water consumption. Also, we see that adding constraints to model calibration does not always improve best-fit performance, as compared to free calibration, but that realism can be improved. ~~To further test the realism of the models, in the following section the outputs of the models are compared to observations of NDII and the global scale SWI dataset for verification.~~

25

5.2 Relationship between $Sumax$ and percentage of evergreen forests at the sub-catchment scale.

~~The relationship between modelled $Sumax$ values and the proportion of evergreen forests in each sub-catchment has been presented in Fig. 6. R^2 of 0.69 and 0.01 were yielded by FLEX-SD-NDII_{Avg} and FLEX-SD-NDII_{MaxMin}, respectively, indicating that $Sumax$ values from the former model increases with greater vegetation coverage. With this unforeseen distinguishing power between sub-catchments of varying land use compositions, it is worth investigating the merit of implementing FLEX-SD-NDII_{Avg} in the ungauged basins. To further test the realism of the models, the outputs of the models were compared to observations of NDII and the global scale SWI dataset for verification as described in Section 5.3.~~

30

Formatted: No bullets or numbering

5.3 Uncertainty in runoff estimation using FLEX-SD, FLEX-SD-NDII_{MaxMin} and FLEX-SD-NDII_{Avg}

Figure 7 displays the 2,500 parameter sets selected to demonstrate the uncertainty (KGE_E , KGE_F and KGE_L) at the six gauging stations. Results of all indicators are similar at P.67 and P.1. At Station P.75, KGE_L values are similar, while KGE_E and KGE_F provided by FLEX-SD-NDII_{MaxMin} are slightly higher than the others. At P.21, FLEX-SD performed marginally better than the others for all indicators. The most notable observations are at P.4A and P.20, where FLEX-SD-NDII_{Avg} is shown to outperform the others in terms of KGE_E and KGE_F . This is reinforced by the observed and calculated hydrographs in Fig. A4, where this model shows the narrowest uncertainty band at these stations. Moreover, the uncertainty bands in the flow duration curves of Fig. A5 show FLEX-SD-NDII_{Avg} produced the narrowest bands at P.4A and P.21, but FLEX-SD showed the best performance at P.20 and P.67. In summary, all models show similar uncertainties, however, FLEX-SD-NDII_{Avg} reveals significantly better performance for upstream sub-catchments and not much difference for other areas compared to the other two models.

5.4 The relationship between the average root zone soil moisture storage (Su) and the average NDII and SWI

5.4.1 Su-NDII relationships

Figure 8 shows the R^2 and NSE during the wet and dry seasons for all six stations generated by 3 FLEX-SD models. Figure 8(a) shows that the time series of NDII correlates well with Su values during the dry season by giving average R^2 value of 0.75-0.79. The average NSE value given by these models are 0.50-0.58, respectively. During the wet season these correlations are lower (average $R^2 = 0.41-0.46$, NSE = 0.44-0.49).

The same procedure was also carried out for all 31 sub-catchments and the results shown in Fig. 8(b). During the dry season, the average $R^2 = 0.71-0.74$, but FLEX-SD-NDII_{Avg} provided notably higher NSE (0.52) than FLEX-SD (0.41) and FLEX-SD-NDII_{MaxMin} (0.45). The relationships are significantly lower in the wet season (average $R^2 = 0.36-0.41$; average NSE = 0.36-0.40). All in all, FLEX-SD-NDII_{Avg} provided higher R^2 and NSE than FLEX-SD-NDII_{MaxMin} in both seasons. These results confirm the study carried out by Sriwongsitanon et al. (2016) that NDII is a reasonable index to indicate root zone soil moisture during the dry season.

It is worth noting that FLEX-SD-NDII_{Avg} was able to differentiate the signatures in catchments of various soil moisture capacities. For a number of sub-catchments, particularly those with more evergreen forest (e.g., S14 = 72.2%, S23 = 58.8%, S29 = 44.7%), estimates of Su from FLEX-SD-NDII_{Avg} provides notably higher NSE than others. Figure 9 presents the time-series of simulated root zone moisture storage (Su), NDII and SWI (discussed in following section) for a selection of contrasting sub-catchments. NDII signatures are well correlated with Su in sub-catchments with low percentages of evergreen forest (S4, S6, S9, S15 and S32). Low correlations were found in evergreen forest-rich sub-catchments (S14, S23 and S29). The evergreen forest probably experiences less moisture stress compared to other land use land cover (LULC), in which situation NDII does not relate as well to simulated root zone soil moisture.

5.4.2 Su-SWI40 relationships

Through testing all available characteristic time lengths (TL) of SWI, the TL of 40 days produced the optimal Su-SWI relationship across the six gauging stations. This was thereby used for subsequent investigation and referred to as SWI40. Figure 10 shows the R^2 and NSE at all six stations simulated by the FLEX-SD-based models. Figure 10(a) shows that SWI40 correlates well with Su values during the dry season ($R^2 = 0.86-0.89$ and $NSE = 0.76-0.81$). During the wet season, these correlations are in the same order of magnitude as in the dry season ($R^2 = 0.87-0.89$ and $NSE = 0.80-0.84$). The results for all 31 sub-catchments are shown in Fig. 10(b) which show average R^2 of 0.86-0.87 and NSE of 0.78-0.79 during the dry season. During the wet season, R^2 of 0.87 and NSE of 0.79-0.81 were yielded.

Despite the overall consistency in average performance amongst these models and limited seasonality, it is however evident that FLEX-SD-NDII_{Avg} shows the most variability across the 31 sub-catchments. In addition to the sensitivity of NDII to the proportion of evergreen forests, Figure 9 also reveals the sensitivity of SWI40 to it. This is reflected in the notable time lag of the Su time series from SWI40 in the productive sub-catchments (e.g., S14, S23 and S29). This observation was not apparent with Su derived from FLEX-SD nor FLEX-SD-NDII_{MaxMin}.

Sriwongsitanon et al. (2016) suggested that NDII can be used as a proxy for soil moisture storage in hydrology. Therefore, the 8-day average NDII values were compared to the 8-day average root zone moisture storage (Su_t) as calculated by FLEXL, FLEX-SD, FLEX-SD-NDII_{Max-Min} and FLEX-SD-NDII_{Avg}. Table 6 shows the coefficients of the exponential relationships and the coefficients of determination (R^2) together with the NSE for the wet season, and the dry season for all six stations. The table shows that the time series of NDII values correlate well with Su values during the dry season by giving R^2 -value (average of all sub-catchments) of 0.75, 0.76, 0.79, and 0.78 for the 4 models respectively. The NSE value given by these models are 0.50, 0.53, 0.57, and 0.58, respectively. During the wet season these correlations are much worse, resulting in average R^2 -value of 0.43, 0.41, 0.46, and 0.46 respectively, while the NSE value are 0.44, 0.49, 0.46, and 0.48, respectively. The same procedure was also carried out for all 31 sub-catchments and the results shown in Table 7 which indicates that during the dry season, the average R^2 -value produced by FLEX-SD, FLEX-SD-NDII_{Max-Min} and FLEX-SD-NDII_{Avg} are 0.71, 0.74, and 0.74, respectively, and NSE are 0.41, 0.45, and 0.52, respectively. During the wet season, R^2 -value are 0.36, 0.41, and 0.41, respectively, and NSE are 0.38, 0.36, and 0.40, respectively. FLEX-SD-NDII_{Avg} provides the highest R^2 - and NSE values for all seasons. Detailed information for 31 sub-catchments presents in Table A2. The Table confirms that FLEX-SD-NDII_{Avg} performs slightly better than FLEX-SD-NDII_{MaxMin}, but this is not surprising as it has one more calibration parameter (R), which provides an additional degree of freedom.

It is to be noted that some sub-catchments show much lower R^2 - and NSE values compared to the rest, which may be the result of land use/land cover. The evergreen forest probably experiences less moisture stress compared to other land use/land cover, in which situation the NDII does not relate as well to root zone soil moisture. Therefore, Figure A5 displays the dry season

Formatted: Normal

Formatted: Font: Italic, Complex Script Font: Italic

relationships between percent of evergreen forest and NSE values from the relationships between the average scaling NDH values and simulated root zone moisture storage (S_u) in 31 sub-basins calibrated and validated by FLEX-SD, FLEX-SD-NDH_{MaxMin}, FLEX-SD-NDH_{Avg}. The figure obviously shows that R^2 provided by these models are quite high with the values of 0.85, 0.52, and 0.80, respectively. The results indicate that the relationship with the average root zone soil moisture storage is affected by the ecology of the river basin. It should be noted that the NSE values contributed by FLEX-SD-NDH_{Avg} for 31 sub-catchments are generally higher than those of produced by FLEX-SD-NDH_{MaxMin}, and especially by FLEX-SD. The results confirm the power of NDII to capture the spatial variation of root zone soil moisture within the sub-catchment scale. Figure A6 presents the corresponding scatter plots for six stations and it clearly shows that the correlation is much better in the dry season than in the wet season. This is not surprising, as it was argued by Sriwongsitanon et al. (2016) that the relation between NDII and root zone soil moisture can only be observed by this remote sensing product when the vegetation is experiencing moisture stress. Hence correlations between root zone soil moisture and NDII are poor during the wet season. Because the FLEX-SD-NDII was constrained by the spatial variability of NDII ranges, the good correlation between S_u and NDII during the dry season may not be surprising. Therefore, an additional test was done, testing the modelled S_u values at daily time step with the daily SWI values, for all models.

Table 8 and Figure A7 shows that the time series of SWI40 correlates well with S_u values during the dry season by giving R^2 value of 0.86, 0.89, 0.87, and 0.88 simulated by FLEXL, FLEX-SD, FLEX-SD-NDH_{MaxMin}, FLEX-SD-NDH_{Avg} respectively, and NSE value of 0.76, 0.79, 0.81, and 0.81, respectively. During the wet season these correlations are in the same order of magnitude as in the dry season with the average R^2 value of 0.87, 0.88, 0.89, and 0.88, respectively, with NSE value of 0.80, 0.84, 0.83, and 0.83, respectively. The results reveal that seasons and model types do not influence the S_u -SWI relationship. All FLEX models, essentially using the same runoff generation procedure, have shown their ability to simulate S_u in correspondence with SWI.

Detailed information for 31 sub-catchments is displayed in Table 9 and Table A3. The correlation does not significantly deviate among different models for all seasons. We also show the time series plots of the average NDII (Scaling), average SWI (Scaling) and the average root zone moisture storage (S_u) calculated by all models for six runoff stations in the wet and the dry seasons separately in Figures A8 and A9, respectively. One should realise, however, that the SWI is partly model based and that this may affect the good correspondence during the wet season. It can therefore be concluded that the NDII is a suitable parameter to constrain hydrological models during moisture recession, but that it works less well under wet conditions. The SWI, being partly model based, is less attractive as a model constraint, but does not suffer from a drawback during wet conditions, and hence serves well as an assessment criterion, particularly during wet conditions. As a result, the NDII appears to be useful to constrain hydrological models during dry conditions and both SWI and NDII appear to be useful to test model performance and to assess moisture states of river basins.

6 Discussion

Inspired by the significance of S_{umax} in governing the hydrological cycle, we investigated the utilization of NDII to constrain our formulated FLEX-SD model with the objective of distributing the parameter of interest across the UPRB's 31 sub-catchments. The distribution of S_{umax} , particularly as achieved by FLEX-SD-NDII_{Avg}, helped produce better-informed runoff estimates for the gauged and ungauged sub-catchments than FLEX-SD, FLEX-SD-NDII_{MaxMin}, and URBS. The analysis of model uncertainties reinforces the improvements to flow estimation in ungauged sub-catchments, particularly in forest-rich sub-catchments. As explained below, this study has raised a few points worthy of discussion:

1. With the consequentially better representation of S_{u} , the Su-NDII relationship yielded has become more informative of the underlying degree of aridity – that is, arid and productive sub-catchments exhibit greater differences than presented by FLEX-SD and FLEX-SD-NDII_{MaxMin}. The increased variation challenges the preconception from the study by Sriwongsitanon et al. (2016) that NDII is a suitable proxy for RZSM dynamics in the dry season, as it was hereby shown to barely correspond with S_{u} in evergreen forests under any circumstances.
2. Upon testing the accuracy of derived S_{u} against SWI, we realize the potential of implementing SWI to indicate moisture states of river basins. Although such variation in Su-SWI may be perceived as unpreferable (as shown in Fig. 10), it is arguably inevitable to see SWI40 exhibit less agreement in catchments characterized by unique S_{u} signatures (e.g., forest-rich catchments), and that this is also indicative of the underlying aridity. That being said, appropriately manipulating the SWI's sole parameter, T, to specific catchments could widen the potential of implementing SWI to indicate moisture states in river basins of contrasting characteristics.

7.6 Conclusion

Most lumped rainfall-runoff models are controlled by a gauging station at the outfall on which it is calibrated. Runoff estimation at any location upstream requires indirect approaches such as model parameter transfer from gauged stations to ungauged locations, or applying relationships between model parameters and catchment characteristics to the ungauged locations. By using any of these approaches, uncertainty in runoff estimation for ungauged catchments is unavoidable. A semi-distributed hydrological model could offer a better alternative. Besides considering taking into account lag times and flood routing (as in FLEX-SD), it has been shown that it is required to account for the spatial variation of the moisture holding capacity of the root zone. Therefore, the model was constrained by using NDII patterns (particularly average NDII as to produce the FLEX-SD-NDII_{Avg}) as a proxy for the spatial variation of root zone moisture leading to distributed S_{umax} -values among sub-catchments. We concluded that the maximum of a series of annual ranges (NDII_{MaxMin}) and annual average (NDII_{Avg}) of NDII values offers an effective proxy for estimating the appropriate S_{umax} values in the different sub-catchments. It was shown that the two FLEX-SD-NDII models significantly improved the relationship between NDII and the modelled

Formatted: Font: Italic, Complex Script Font: Italic

Formatted: Font: Italic, Complex Script Font: Italic

Formatted: Subscript

Formatted: Subscript

Formatted: Font: Italic, Complex Script Font: Italic

Formatted: Subscript

Formatted: Font: Italic, Complex Script Font: Italic

Formatted: Font: Italic, Complex Script Font: Italic, Subscript

Formatted: Font: Italic, Complex Script Font: Italic

Formatted: Font: Italic, Complex Script Font: Italic, Subscript

Formatted: Font: Italic, Complex Script Font: Italic

Formatted: Font: Italic, Complex Script Font: Italic, Subscript

root zone moisture storage (S_{tz}) of all 31 sub-catchments. Moreover, the time-series of the SWI correlated very well with the modelled root zone moisture storage (S_{tz}) of all sub-basins controlled by runoff stations.

The model parameters provided by the semi-distributed FLEX models are more realistic compared to the original FLEX since they are distributed according to catchment characteristics comprising catchment area, reach length, and the remote sensing indices (NDII and SWI).

With the inclusion of NDII, the estimated catchment-scale root zone soil moisture (S_{tz}) has been shown to be increasingly sensitive to the underlying degree of aridity, which is arguably more representative of the hydrological responses across heterogeneous sub-catchments. Such knowledge should be used in further studies to explore the opportunities of implementing the model-based SWI to estimate soil moisture in different land use land cover. A next step in the analysis is to account for diversity in landscape composition and related model structures among sub-catchments (Gao et al., 2016), which would allow for a distinction between the main rainfall runoff mechanisms belonging to different landscape types. This study confirms the result of the earlier study by Sriwongsitanon et al. (2016) who concluded that NDII can be used as a proxy for catchment-scale root zone moisture deficit when plants are exposed to water stress. However, during the wet season when soil moisture is replenished as a result of rainfall, NDII values are no longer well correlated with soil moisture. However, the partly model-based SWI proved to be a reliable index to estimate soil moisture both under water stressed and wet conditions.

Appendix A

Table A1

Figure A1 to Figure A5
Table A1 to A3
Fig. A1 to Fig. A9

Acknowledgements

The authors would like to express our sincere gratitude to Faculty of Engineering, Kasetsart University for financially supporting this research. We are also indebted to the Royal Irrigation Department and Thai Meteorology Department for providing the hydrological data. We would also like to thank the reviewers for their invaluable feedback for the revision of this manuscript.
~~The authors would like to express our sincere gratitude to Faculty of Engineering, Kasetsart University for financially supporting this research. We are also indebted to the Royal Irrigation Department and Thai Meteorology Department for providing the hydrological data.~~

Formatted: Complex Script Font: Times New Roman, (Complex) Arabic (Saudi Arabia), English (United Kingdom)

References

- Bao, A. M., Liu, H. L., Chen, X., and Pan, X. I.: The effect of estimating areal rainfall using self-similarity topography method on the simulation accuracy of runoff prediction, *Hydrol. Processes*, 25, 3506-3512, [doi:10.1002/hyp.8078](https://doi.org/10.1002/hyp.8078), 2011.
- 5 [Bouaziz, L. J. E., Steele-Dunne, S. C., Schellekens, J., Weerts, A. H., Stam, J., Sprokkereef, E., Winsemius, H. H. C., Savenije, H. H. G., and Hrachowitz, M.: Improved understanding of the link between catchment-scale vegetation accessible storage and satellite-derived Soil Water Index, *Water Resour. Res.*, 56, e2019WR026365, \[doi:10.1029/2019WR026365\]\(https://doi.org/10.1029/2019WR026365\), 2020.](https://doi.org/10.1029/2019WR026365)
- Boyd, M.J., Bates, B.C., Pilgrim, D.H., and Cordery, I.: WBNM: A General Runoff Routing Model Computer Programs and User Guide, Water Research Laboratory, The University of New South Wales, 1987.
- 10 Brocca, L., Hasenauer, S., Lacava, T., Melone, F., Moramarco, T., Wagner, W., Dorigo, W., Matgen, P., Martínez-Fernández, J., and Llorens, P.: Soil moisture estimation through ASCAT and AMSR-E sensors: An intercomparison and validation study across Europe, *Remote Sens. Environ.*, 115, 3390-3408, [doi:10.1016/j.rse.2011.08.003](https://doi.org/10.1016/j.rse.2011.08.003), 2011.
- Carroll, D.: URBS a Rainfall Runoff Routing Model for flood forecasting and design version 4.00., 2004.
- 15 [Castelli, G., Oliveira, L. A. A., Abdelli, F., Dhaou, H., Bresci, E., and Ouassar, M.: Effect of traditional check dams \(jessour\) on soil and olive trees water status in Tunisia, *Science of The Total Environment*, 690, 226-236, \[doi:10.1016/j.scitotenv.2019.06.514\]\(https://doi.org/10.1016/j.scitotenv.2019.06.514\), 2019.](https://doi.org/10.1016/j.scitotenv.2019.06.514)
- Euser, T., Hrachowitz, M., Winsemius, H. C., and Savenije, H. H. G.: The effect of forcing and landscape distribution on performance and consistency of model structures, *Hydrol. Processes*, 29, 3727-3743, <https://doi.org/10.1002/hyp.10445>, 2015.
- 20 Fencia, F., Savenije, H. H. G., Matgen, P., and Pfister, L.: Understanding catchment behavior through stepwise model concept improvement, *Water Resour. Res.*, 44, <https://doi.org/10.1029/2006WR005563>, 2008.
- Fencia, F., Kavetski, D., and Savenije, H. H. G.: Elements of a flexible approach for conceptual hydrological modeling: 1. Motivation and theoretical development, *Water Resour. Res.*, 47, [W11510, doi:10.1029/2010WR010174](https://doi.org/10.1029/2010WR010174), <https://doi.org/10.1029/2010WR010174>, 2011.
- 25 Gao, H., Hrachowitz, M., Schymanski, S. J., Fencia, F., Sriwongsitanon, N., and Savenije, H. H. G.: Climate controls how ecosystems size the root zone storage capacity at catchment scale, *Geophys. Res. Lett.*, 41, 7916-7923, <https://doi.org/10.1002/2014GL061668>, 2014.
- Gao, H., Hrachowitz, M., Sriwongsitanon, N., Fencia, F., Gharari, S., and Savenije, H. H. G.: Accounting for the influence of vegetation and landscape improves model transferability in a tropical savannah region, *Water Resour. Res.*, 52, 7999-8022, <https://doi.org/10.1002/2016WR019574>, 2016.
- 30 Gharari, S., Hrachowitz, M., Fencia, F., and Savenije, H. H. G.: Hydrological landscape classification: investigating the performance of HAND based landscape classifications in a central European meso-scale catchment, *Hydrol. Earth Syst. Sci.*, 15, 3275-3291, <https://doi.org/10.5194/hess-15-3275-2011>, 2011.
- 35 [Hardisky, M. A., Klemas V. and Smart, R. M.: The influence of soil salinity, growth form, and leaf moisture on the spectral radiance of *Spartina alterniflora* canopies, *Photogrammetric Engineering and Remote Sensing*, 49, 77-83, 1983.](https://doi.org/10.1016/0167-6369(83)90001-0)
- Hawkins, R. H.: Asymptotic Determination of Curve Numbers from Rainfall—Runoff Data, 67-76, 1990.
- [Hulsman, P., Winsemius, H. C., Michailovsky, C. I., Savenije, H. H. G., and Hrachowitz, M.: Using altimetry observations combined with GRACE to select parameter sets of a hydrological model in a data-scarce region, *Hydrol. Earth Syst. Sci.*, 24, 3331-3359, \[doi:10.5194/hess-24-3331-2020\]\(https://doi.org/10.5194/hess-24-3331-2020\), 2020](https://doi.org/10.5194/hess-24-3331-2020)
- 40 Kavetski, D., and Fencia, F.: Elements of a flexible approach for conceptual hydrological modeling: 2. Application and experimental insights, *Water Resour. Res.*, 47, [W11511, https://doi.org/10.1029/2011WR010748](https://doi.org/10.1029/2011WR010748), 2011.
- Laurenson, E.M., Mein, R.G.: Version 4 Runoff Routing Program User Manual, Department of Civil Engineering, Monash University, Australia, 1990.
- Lewis, D., Singer, M. J., and Tate, K. W.: Applicability of SCS curve number method for a California oak woodlands watershed, *J. Soil Water Conserv.*, 55, 226-230, 2000.
- 45 Malone, T.: Using URBS for Real Time Flood Modelling: 25th Hydrology & Water Resources Symposium, 2nd International Conference on Water Resources & Environment Research, 1999.
- Malone, T., Johnston, A., Perkins, J., and Sooriyakumaran, S.: HYMODEL-a Real Time Flood Forecasting System: 28th International Hydrology and Water Resources Symposium: About Water; Symposium Proceedings, 2003.

Formatted: Font: (Default) +Body (Times New Roman), Complex Script Font: +Body (Times New Roman)

Formatted: Thai Distributed Justification

Formatted: Font: (Default) +Body (Times New Roman), 1 pt, Font color: Auto, Complex Script Font: +Body (Times New Roman), English (United Kingdom), Check spelling and grammar

Formatted: Font: (Default) +Body (Times New Roman), Complex Script Font: +Body (Times New Roman)

Formatted: Font: (Default) +Body (Times New Roman), 1 pt, Font color: Auto, Complex Script Font: +Body (Times New Roman), English (United Kingdom), Check spelling and grammar

Formatted: Font: (Default) +Body (Times New Roman), Complex Script Font: +Body (Times New Roman)

Formatted: Font: (Default) +Body (Times New Roman), 1 pt, Font color: Auto, Complex Script Font: +Body (Times New Roman), English (United Kingdom), Check spelling and grammar

Formatted: Font: (Default) +Body (Times New Roman), Complex Script Font: +Body (Times New Roman)

Formatted: Font: (Default) +Body (Times New Roman), 1 pt, Font color: Auto, Complex Script Font: +Body (Times New Roman), English (United Kingdom), Check spelling and grammar

Formatted: Font: (Default) +Body (Times New Roman), Complex Script Font: +Body (Times New Roman)

Formatted: Font: (Default) +Body (Times New Roman), 1 pt, Font color: Auto, Complex Script Font: +Body (Times New Roman), English (United Kingdom), Check spelling and grammar

Formatted: Font: (Default) +Body (Times New Roman), Complex Script Font: +Body (Times New Roman)

Formatted: Font: (Default) +Body (Times New Roman), 1 pt, Font color: Auto, Complex Script Font: +Body (Times New Roman), English (United Kingdom), Check spelling and grammar

Formatted: Font: (Default) +Body (Times New Roman), Complex Script Font: +Body (Times New Roman)

Formatted: Font: (Default) +Body (Times New Roman), 1 pt, Font color: Auto, Complex Script Font: +Body (Times New Roman), English (United Kingdom), Check spelling and grammar

Formatted: Font: (Default) +Body (Times New Roman), Complex Script Font: +Body (Times New Roman)

Formatted: Font: (Default) +Body (Times New Roman), 1 pt, Font color: Auto, Complex Script Font: +Body (Times New Roman), English (United Kingdom), Check spelling and grammar

Formatted: Font: (Default) +Body (Times New Roman), Complex Script Font: +Body (Times New Roman)

Malone, T.: Roadmap mission for the development of a flood forecasting system for the Lower Mekong River, Mekong River Commission Flood Management and Mitigation Programme, Technical Component-Main Report, 72, 2006.

Mao, G., and Liu, J.: WAYS v1: a hydrological model for root zone water storage simulation on a global scale, *Geosci. Model Dev.*, 12, 5267–5289, doi:10.5194/gmd-12-5267-2019, 2019.

5 Mapiam, P., and Sriwongsitanon, N.: Estimation of the URBS model parameters for flood estimation of ungauged catchments in the upper Ping river basin, Thailand, *ScienceAsia*, 35, 49-56, doi:10.2306/scienceasia1513-1874.2009.35.049, 2009.

Mapiam, P. P., Sharma, A., and Sriwongsitanon, N.: Defining the Z–R relationship using gauge rainfall with coarse temporal resolution: implications for flood forecasting, *J. Hydrol. Eng.*, 19, 04014003, doi:10.1061/(ASCE)HE.1943-5584.0000616, 2014.

10 Mishra, S. K., Jain, M. K., Bhunya, P. K., and Singh, V. P.: Field applicability of the SCS-CN-based Mishra–Singh general model and its variants, *Water Resour. Manage.*, 19, 37-62, doi:10.1007/s11269-005-1076-3, 2005.

Moricz, N., Garamszegi, B., Rasztovits, E., Bidlo, A., Horvath, A., Jagicza, A., Illes, G., Vekerdy, Z., Somogyi, Z., and Galos, B.: Recent Drought-Induced Vitality Decline of Black Pine (*Pinus nigra* Arn.) in South-West Hungary—Is This Drought-Resistant Species under Threat by Climate Change?, *Forests*, 9(7), 414, doi:10.3390/f9070414, 2018.

15 Paulik, C., Dorigo, W., Wagner, W., and Kidd, R.: Validation of the ASCAT Soil Water Index using in situ data from the International Soil Moisture Network, *Int. J. Appl. Earth Obs. Geoinf.*, 30, 1-8, doi:10.1016/j.jag.2014.01.007, 2014.

Ren-Jun, Z.: The Xinanjiang model applied in China, *J. Hydrol.*, 135, 371-381, 1992.

20 Rodriguez, F., Morena, F., and Andrieu, H.: Development of a distributed hydrological model based on urban databanks—production processes of URBS, *Water Sci. Technol.*, 52, 241-248, doi:10.2166/wst.2005.0139, 2005.

Savenije, H. H. G.: Determination of evaporation from a catchment water balance at a monthly time scale, *Hydrol. Earth Syst. Sci.*, 1, 93-100, doi:10.5194/hess-1-93-1997, 1997.

Savenije, H. H. G.: HESS Opinions "Topography driven conceptual modelling (FLEX-Topo)", *Hydrol. Earth Syst. Sci.*, 14, 2681–2692, <https://doi.org/10.5194/hess-14-2681-2010>, 2010.

25 Savenije, H. H. G. and Hrachowitz, M.: HESS Opinions "Catchments as meta-organisms – a new blueprint for hydrological modelling", *Hydrol. Earth Syst. Sci.*, 21, 1107-1116, <https://doi.org/10.5194/hess-21-1107-2017>, 2017.

Solomatine, D. P., and Shrestha, D. L.: A novel method to estimate model uncertainty using machine learning techniques, *Water Resour. Res.*, 45, W00B11, doi:10.1029/2008WR006839, 2009.

30 Sriwongsitanon, N.: Flood Forecasting System Development for the Upper Ping River Basin, *Kasetsart J. (Nat. Sci.)*, 44, pp-717-731, 2010.

Sriwongsitanon, N., and Taesombat, W.: Effects of land cover on runoff coefficient, *J. Hydrol.*, 410, 226-238, doi:10.1016/j.jhydrol.2011.09.021, 2011.

Sriwongsitanon, N., Gao, H., Savenije, H. H. G., Maekan, E., Saengsawang, S., and Thianpopirug, S.: Comparing the Normalized Difference Infrared Index (NDII) with root zone storage in a lumped conceptual model, *Hydrol. Earth Syst. Sci.*, 20, 3361, doi:10.5194/hess-20-3361-2016, 2016.

35 Suresh Babu, P., and Mishra, S. K.: Improved SCS-CN–inspired model, *J. Hydrol. Eng.*, 17, 1164-1172, doi:10.1061/(ASCE)HE.1943-5584.0000435, 2011.

Tekleab, S., Uhlenbrook, S., Savenije, H. H. G., Mohamed, Y., and Wenninger, J.: Modelling rainfall–runoff processes of the Chemoga and Jedeb meso-scale catchments in the Abay/Upper Blue Nile basin, Ethiopia, *Hydrol. Sci. J.*, 60, 2029-2046, doi:10.1080/02626667.2015.1032292, 2015.

40 Tingsanchali, T., and Gautam, M. R.: Application of tank, NAM, ARMA and neural network models to flood forecasting, *Hydrol. Processes*, 14, 2473-2487, [https://doi.org/10.1002/1099-1085\(20001015\)14:14<2473::AID-HYP109>3.0.CO;2-J](https://doi.org/10.1002/1099-1085(20001015)14:14<2473::AID-HYP109>3.0.CO;2-J), 2000.

45 Vaitiekuniene, J.: Application of rainfall-runoff model to set up the water balance for Lithuanian river basins, *Environmental research, engineering and management*, 1, 34-44, 2005.

Vermote, E. F., Kotchenova, S. Y., and Ray, J. P.: MODIS Surface Reflectance user's guide, version 1.3, MODIS Land Surface Reflectance Science Computing Facility, 2011.

Vrugt, J. A., Gupta, H. V., Bastidas, L. A., Bouten, W., and Sorooshian, S.: Effective and efficient algorithm for multiobjective optimization of hydrologic models, *Water Resour. Res.*, 39, 1214, doi:10.1029/2002WR001746, 2003.

Formatted: Font: (Default) +Body (Times New Roman), 1 pt, Complex Script Font: +Body (Times New Roman), English (United Kingdom), Check spelling and grammar

Formatted: Font: (Default) +Body (Times New Roman), Complex Script Font: +Body (Times New Roman)

Xulu, S., Peerbhay, K., Gebreslasie, M., and Ismail, R.: Drought Influence on Forest Plantations in Zululand, South Africa, Using MODIS Time Series and Climate Data, Forests, 9(9), 528, doi:10.3390/f9090528, 2018.

Yahya, B. M., Devi, N. M., and Umrikar, B.: Flood hazard mapping by integrated GIS-SCS model, International Journal of Geomatics and Geosciences, 1, 489, 2010.

- 5 Yew Gan, T., Dlamini, E. M., and Biftu, G. F.: Effects of model complexity and structure, data quality, and objective functions on hydrologic modeling, J. Hydrol., 192, 81-103, [https://doi.org/10.1016/S0022-1694\(96\)03114-9](https://doi.org/10.1016/S0022-1694(96)03114-9), 1997.

Tables and Figures

Formatted: Font: (Default) +Body (Times New Roman), Complex Script Font: +Body (Times New Roman)

Formatted: Font: (Default) +Body (Times New Roman), 1 pt, Complex Script Font: +Body (Times New Roman)

Formatted: Heading 1

Table 1: Catchment characteristics and hydrological data for 6 gauging stations in the study area

Runoff Station	P.20	P.75	P.4A	P.67	P.21	P.1
Area (km ²)	1,309	3,029	1,954	5,333	516	6,142
Altitude range (m)	993	1,035	686	1,058	581	1,067
Length main channel (km)	89	126	143	155	52	185
Average channel slope	0.006	0.005	0.004	0.004	0.01	0.004
Average rainfall (mm/yr)	1,227	1,250	1,176	1,221	1,220	1,224
Rainfall Range (mm/yr)	926 – 1,640	900 – 1,643	829 – 1,449	866 – 1,570	728 – 1,606	847 – 1,565
Average runoff (mm/yr)	324.8	233.6	186.6	229.2	261.8	235.2
Runoff Range (mm/yr)	94.2 – 672.4	67.0 – 480.1	37.3 – 455.2	34.0 – 495.5	80.2 - 522.4	54.2 – 494.1
Irrigated Area (%)	15.7	18.1	9.4	15.1	17.4	15
Evergreen Forest (%)	10.2	9.6	39.7	20.0	22.1	19.8
Forest Area (%)	76.0	74.0	82.1	76.1	67.8	73.9
% Runoff Average	25.9	18.2	15.1	18	20.7	18.5
% Runoff Range	10.2 - 51.7	7.4 - 34.2	4.5 - 31.4	3.9 - 34.6	11.0 - 32.5	6.4 - 33.9

Table 2: Constitutive and water balance equations used in FLEXL

No.	Reservoir	Constitutive equations	Equation	Water balance equations	Equation
1	Snow	$M_i = \begin{cases} F_{DD}(T_i - T_t) & ; T_i > T_t \\ 0 & ; T_i \leq T_t \end{cases}$	(2)	$\frac{dS_w}{dt} = P_{S_i} - M_i$	(3)
2	Interception	$Ei_i = \begin{cases} Ep_i & ; Si_i > 0 \\ 0 & ; Si_i = 0 \end{cases}$	(4)	$\frac{dSi}{dt} = Pr_i - Ei_i - Ptf_i$	(6)
		$Ptf_i = \begin{cases} 0 & ; Si_i < I_{max} \\ Pr_i & ; Si_i \geq I_{max} \end{cases}$	(5)		
3	Unsaturated soil	$Cr_i = 1 - \left(1 - \frac{Su_{i-1}}{Sumax}\right)^\beta$	(7)	$\frac{dSu}{dt} = Pe_i(1 - Cr_i) - Ea_i$	(10)
		$Ru_i = Pe_i Cr_i$	(8)		
		$Ea_i = (Ep_i - Ei_i) \min\left(\frac{Su_i}{Sumax \cdot Ce}, 1\right)$	(9)		
4	Fast response	$Rf_i = Ru_i D$	(11)	$\frac{dSf}{dt} = Rf_i - Qff_i - Qf_i$	(16)
		$c_{lagF}(j) = \frac{j}{\sum_{u=1}^{TlagF} u}$	(12)		
		$Rf_i = \sum_{j=1}^{TlagF} C_{lagF}(j) \cdot Rf_{i-j-1}$	(13)		
		$Qff_i = \frac{\max(0, Sf_i - Sf_{max})}{Kff}$	(14)		
		$Qf_i = \frac{Sf_i}{Kf}$	(15)		
5	Slow response	$Rs_i = Ru_i(1 - D)$	(17)	$\frac{dSs}{dt} = Rs_i - Qs_i$	(21)
		$c_{lagS}(j) = \frac{j}{\sum_{u=1}^{TlagS} u}$	(18)		
		$Rs_i = \sum_{j=1}^{TlagS} C_{lagS}(j) \cdot Rs_{i-j-1}$	(19)		
		$Qs_i = \frac{Ss_i}{Ks}$	(20)		

Table 3: Constitutive equations used in URBS

Processes	Constitutive Equations	Equation
Initial Loss	$IL_i = \begin{cases} IL_{i-1} & ; R_{i-1} > rlr \cdot \delta t \\ IL_{i-1} + rlr \cdot \delta t - R_{i-1} & ; R_{i-1} \leq rlr \cdot \delta t \\ IL_{max} & ; IL_{i-1} > IL_{max} \end{cases}$	(22)
Proportional Loss and Excess Rainfall	$R_i^E = \frac{F_i}{F_{max}} C_{imp} R_i + \left(1 - \frac{F_i}{F_{max}}\right) R_i^{per}$	(23)
	$F_i = k_{\delta t} F_{i-1} + dF_i$	(24)
	$R_i^{per} = pr(R_i^{eff})$	(25)
	$dF_i = (1-pr)R_i^{eff}$	(26)
Catchment Routing	$S_i = \beta \sqrt{A} Q_i^m$	(27)
Channel Routing	$S_i^{ch} = \alpha L (X I_i + (1-X) Q_i)$	(28)

Table 4: Statistical indicators at each station for calibration period provided by FLEXL and semi-distributed models. Best performance underlined.

Station	Model	Calibration period (2001–2011)							
		Statistical indicators for calibrate at each station				Statistical indicators for calibrate at station P.1			
		NSE	KGE _E	KGE _L	KGE _R	NSE	KGE _E	KGE _L	KGE _R
P.20	(1) URBS	0.59	0.79	0.30	0.91	0.58	0.63	0.49	0.70
	(2) FLEXL	0.66	<u>0.82</u>	0.50	0.96	<u>0.66</u>	<u>0.82</u>	<u>0.50</u>	<u>0.96</u>
	(3) FLEX-SD	0.66	<u>0.83</u>	0.51	0.96	0.62	0.59	0.38	0.63
	(4) FLEX-SD-NDH _{Max-Min}	0.67	<u>0.83</u>	0.65	<u>0.98</u>	0.59	0.50	<u>0.50</u>	0.54
	(5) FLEX-SD-NDH _{Avg}	<u>0.67</u>	0.82	<u>0.73</u>	0.96	0.64	0.67	0.40	0.72
P.75	(1) URBS	0.76	0.87	0.81	0.96	0.68	0.81	0.78	0.87
	(2) FLEXL	0.73	0.86	0.65	0.97	0.73	0.86	0.65	<u>0.97</u>
	(3) FLEX-SD	0.79	0.89	0.82	0.97	0.77	0.87	0.83	0.93
	(4) FLEX-SD-NDH _{Max-Min}	<u>0.80</u>	<u>0.90</u>	<u>0.84</u>	<u>0.98</u>	<u>0.80</u>	<u>0.88</u>	0.82	0.94
	(5) FLEX-SD-NDH _{Avg}	0.79	<u>0.90</u>	0.83	<u>0.98</u>	0.75	0.82	<u>0.84</u>	0.86
P.4A	(1) URBS	0.64	0.82	0.63	<u>0.98</u>	0.64	0.79	0.57	0.89
	(2) FLEXL	<u>0.71</u>	0.84	<u>0.71</u>	0.93	0.71	<u>0.84</u>	<u>0.71</u>	<u>0.93</u>
	(3) FLEX-SD	<u>0.71</u>	<u>0.85</u>	0.58	0.95	0.68	0.75	0.65	0.79
	(4) FLEX-SD-NDH _{Max-Min}	<u>0.71</u>	<u>0.84</u>	0.64	0.94	0.65	0.70	0.62	0.74
	(5) FLEX-SD-NDH _{Avg}	0.70	0.84	0.67	0.93	<u>0.71</u>	0.83	0.68	0.90
P.67	(1) URBS	0.72	0.86	0.73	<u>0.97</u>	0.77	0.84	0.70	0.90
	(2) FLEXL	0.76	0.87	<u>0.75</u>	0.95	0.76	<u>0.87</u>	<u>0.75</u>	<u>0.95</u>
	(3) FLEX-SD	<u>0.80</u>	<u>0.90</u>	0.72	0.96	0.82	<u>0.87</u>	0.70	0.91
	(4) FLEX-SD-NDH _{Max-Min}	0.78	0.88	0.72	0.95	<u>0.83</u>	0.86	0.71	0.89
	(5) FLEX-SD-NDH _{Avg}	0.79	0.89	0.72	0.96	<u>0.83</u>	<u>0.87</u>	0.71	0.90
P.21	(1) URBS	0.64	0.82	0.48	0.95	0.60	0.77	0.53	0.84
	(2) FLEXL	0.70	0.85	<u>0.88</u>	<u>0.98</u>	<u>0.70</u>	<u>0.85</u>	<u>0.88</u>	<u>0.98</u>
	(3) FLEX-SD	<u>0.74</u>	0.86	0.82	0.93	0.61	0.78	0.37	0.86
	(4) FLEX-SD-NDH _{Max-Min}	0.73	<u>0.87</u>	0.85	0.97	0.61	0.76	0.45	0.85
	(5) FLEX-SD-NDH _{Avg}	0.72	0.86	0.73	0.95	0.66	0.74	0.38	0.80
P.1	(1) URBS	0.80	0.90	0.76	0.97	0.80	0.90	0.76	0.97
	(2) FLEXL	0.82	0.90	0.76	0.98	0.82	0.90	0.76	0.98
	(3) FLEX-SD	0.86	<u>0.93</u>	0.75	0.97	0.86	<u>0.93</u>	0.75	0.97
	(4) FLEX-SD-NDH _{Max-Min}	<u>0.87</u>	<u>0.93</u>	<u>0.77</u>	0.98	<u>0.87</u>	<u>0.93</u>	<u>0.77</u>	0.98
	(5) FLEX-SD-NDH _{Avg}	<u>0.87</u>	<u>0.93</u>	<u>0.77</u>	<u>0.99</u>	<u>0.87</u>	<u>0.93</u>	<u>0.77</u>	<u>0.99</u>
Average	(1) URBS	0.69	0.84	0.62	<u>0.96</u>	0.68	0.79	0.64	0.86
	(2) FLEXL	0.73	0.86	0.71	<u>0.96</u>	0.73	<u>0.86</u>	<u>0.71</u>	<u>0.96</u>
	(3) FLEX-SD	<u>0.76</u>	<u>0.87</u>	0.70	<u>0.96</u>	0.73	0.80	0.61	0.85
	(4) FLEX-SD-NDH _{Max-Min}	<u>0.76</u>	<u>0.87</u>	<u>0.74</u>	<u>0.96</u>	0.72	0.77	0.64	0.82
	(5) FLEX-SD-NDH _{Avg}	<u>0.76</u>	<u>0.87</u>	<u>0.74</u>	<u>0.96</u>	<u>0.75</u>	0.81	0.63	0.86

Table 5: Statistical indicators at each station for validation period provided by FLEXL and semi-distributed models. Best performance underlined.

Station	Model	Validation period (2012–2016)							
		Statistical indicators for calibrate at each station				Statistical indicators for calibrate at station P.1			
		NSE	KGE _E	KGE _L	KGE _R	NSE	KGE _E	KGE _L	KGE _R
P.20	(1) URBS	0.44	0.80	0.31	0.90	0.72	0.66	<u>0.52</u>	0.70
	(2) FLEXL	0.43	0.82	0.52	0.92	0.43	<u>0.82</u>	<u>0.52</u>	<u>0.92</u>
	(3) FLEX-SD	0.46	<u>0.83</u>	0.52	0.92	0.77	0.59	0.39	0.62
	(4) FLEX-SD-NDH _{Max-Min}	<u>0.50</u>	<u>0.83</u>	0.64	<u>0.94</u>	0.76	0.47	<u>0.52</u>	0.53
	(5) FLEX-SD-NDH _{Avg}	0.49	<u>0.83</u>	<u>0.74</u>	0.92	0.74	0.67	0.42	0.71
P.75	(1) URBS	0.70	0.84	0.79	0.96	0.72	0.81	0.76	0.87
	(2) FLEXL	0.33	0.74	0.60	0.91	0.33	0.74	0.60	0.91
	(3) FLEX-SD	<u>0.79</u>	<u>0.89</u>	0.81	0.97	0.76	<u>0.87</u>	<u>0.82</u>	0.93
	(4) FLEX-SD-NDH _{Max-Min}	0.78	0.88	<u>0.82</u>	0.97	0.78	<u>0.87</u>	0.81	<u>0.94</u>
	(5) FLEX-SD-NDH _{Avg}	0.78	0.88	0.81	<u>0.98</u>	0.73	0.82	<u>0.82</u>	0.86
P.4A	(1) URBS	0.55	0.75	<u>0.72</u>	<u>0.98</u>	0.55	0.74	0.62	0.88
	(2) FLEXL	0.58	0.77	0.70	0.93	0.58	<u>0.77</u>	<u>0.70</u>	<u>0.93</u>
	(3) FLEX-SD	<u>0.59</u>	<u>0.78</u>	0.66	0.94	0.46	0.68	0.64	0.79
	(4) FLEX-SD-NDH _{Max-Min}	<u>0.59</u>	<u>0.78</u>	<u>0.68</u>	<u>0.94</u>	0.44	<u>0.63</u>	<u>0.62</u>	<u>0.73</u>
	(5) FLEX-SD-NDH _{Avg}	0.55	0.77	0.69	0.93	<u>0.59</u>	0.76	0.69	0.90
P.67	(1) URBS	0.65	0.83	<u>0.76</u>	<u>0.96</u>	<u>0.71</u>	0.82	0.73	0.90
	(2) FLEXL	0.51	0.78	<u>0.76</u>	0.92	0.51	0.78	<u>0.76</u>	<u>0.92</u>
	(3) FLEX-SD	<u>0.70</u>	<u>0.85</u>	0.75	0.95	<u>0.71</u>	<u>0.83</u>	0.72	0.90
	(4) FLEX-SD-NDH _{Max-Min}	0.69	0.84	<u>0.76</u>	0.93	0.69	0.81	0.73	0.88
	(5) FLEX-SD-NDH _{Avg}	0.67	0.83	0.74	0.95	<u>0.71</u>	0.82	0.74	0.89
P.21	(1) URBS	0.54	0.78	0.49	0.94	0.50	0.72	0.50	0.84
	(2) FLEXL	0.66	0.82	<u>0.88</u>	<u>0.98</u>	<u>0.66</u>	<u>0.82</u>	<u>0.88</u>	<u>0.98</u>
	(3) FLEX-SD	<u>0.67</u>	<u>0.83</u>	0.80	0.93	0.61	0.76	0.36	0.85
	(4) FLEX-SD-NDH _{Max-Min}	0.65	<u>0.83</u>	0.84	0.97	0.60	0.74	0.45	0.85
	(5) FLEX-SD-NDH _{Avg}	0.65	0.82	<u>0.72</u>	0.95	0.64	0.73	0.38	0.80
P.1	(1) URBS	0.68	0.84	0.74	0.97	0.68	0.84	0.74	0.97
	(2) FLEXL	0.66	0.85	0.71	0.97	0.66	0.85	0.71	0.97
	(3) FLEX-SD	0.74	<u>0.88</u>	0.73	0.97	0.74	<u>0.88</u>	0.73	0.97
	(4) FLEX-SD-NDH _{Max-Min}	0.75	<u>0.88</u>	0.74	<u>0.98</u>	0.75	<u>0.88</u>	0.74	<u>0.98</u>
	(5) FLEX-SD-NDH _{Avg}	<u>0.76</u>	<u>0.88</u>	<u>0.75</u>	<u>0.98</u>	<u>0.76</u>	<u>0.88</u>	<u>0.75</u>	<u>0.98</u>
Average	(1) URBS	0.59	0.81	0.63	<u>0.95</u>	0.65	0.76	0.65	0.86
	(2) FLEXL	0.53	0.80	0.70	0.94	0.53	<u>0.80</u>	<u>0.70</u>	<u>0.94</u>
	(3) FLEX-SD	<u>0.66</u>	<u>0.84</u>	0.71	<u>0.95</u>	0.68	0.77	0.61	0.84
	(4) FLEX-SD-NDH _{Max-Min}	<u>0.66</u>	<u>0.84</u>	<u>0.75</u>	<u>0.95</u>	0.67	0.73	0.64	0.82
	(5) FLEX-SD-NDH _{Avg}	0.65	<u>0.84</u>	0.74	<u>0.95</u>	<u>0.70</u>	0.78	0.63	0.86

5 **Table 6: Exponential relationships between NDH values and simulated root zone moisture storage (S_{rz}) in six sub-basins controlled by runoff stations. Best performance in bold.**

Station	Model	Dry season				Wet season			
		a	b	R^2	NSE	a	b	R^2	NSE
P.20	FLEXL	65.1	5.7	0.83	0.66	37.0	7.9	0.48	0.51
	FLEX-SD	25.6	9.0	0.79	0.60	14.0	11.7	0.43	0.52
	FLEX-SD-NDH _{Max-Min}	133.8	4.5	0.81	0.60	81.6	6.2	0.48	0.46
	FLEX-SD-NDH _{Avg}	42.1	7.3	0.84	0.67	23.2	9.9	0.47	0.54
P.75	FLEXL	208.2	3.9	0.79	0.47	126.1	5.4	0.44	0.38
	FLEX-SD	23.3	9.5	0.80	0.62	12.0	12.4	0.43	0.53
	FLEX-SD-NDH _{Max-Min}	123.1	4.9	0.82	0.61	71.6	6.7	0.48	0.46
	FLEX-SD-NDH _{Avg}	44.1	7.5	0.84	0.68	23.1	10.1	0.47	0.54
P.4A	FLEXL	22.0	9.2	0.69	0.40	12.6	11.9	0.38	0.40
	FLEX-SD	6.4	12.8	0.69	0.30	5.3	15.0	0.36	0.41
	FLEX-SD-NDH _{Max-Min}	36.7	7.8	0.74	0.45	25.0	10.0	0.41	0.44
	FLEX-SD-NDH _{Avg}	51.7	7.0	0.71	0.43	32.2	9.2	0.41	0.42
P.67	FLEXL	16.5	10.2	0.79	0.56	6.6	14.3	0.43	0.51
	FLEX-SD	13.9	11.0	0.79	0.56	7.1	14.4	0.45	0.54
	FLEX-SD-NDH _{Max-Min}	72.6	6.3	0.82	0.63	39.5	8.7	0.51	0.53
	FLEX-SD-NDH _{Avg}	51.1	7.0	0.82	0.62	26.5	9.8	0.49	0.53
P.21	FLEXL	71.9	5.9	0.64	0.33	39.6	7.5	0.38	0.29
	FLEX-SD	8.5	12.4	0.69	0.54	4.7	14.5	0.35	0.40
	FLEX-SD-NDH _{Max-Min}	56.1	7.2	0.70	0.49	30.7	8.9	0.39	0.36
	FLEX-SD-NDH _{Avg}	52.9	7.2	0.68	0.45	28.5	8.9	0.38	0.34
P.1	FLEXL	11.7	11.5	0.79	0.57	4.8	15.6	0.44	0.53
	FLEX-SD	13.1	11.3	0.78	0.58	6.4	14.8	0.46	0.54
	FLEX-SD-NDH _{Max-Min}	69.4	6.5	0.81	0.63	36.3	9.1	0.51	0.53
	FLEX-SD-NDH _{Avg}	49.8	7.2	0.81	0.62	24.8	10.1	0.50	0.52
Average	FLEXL	-	-	0.75	0.50	-	-	0.43	0.44
	FLEX-SD	-	-	0.76	0.53	-	-	0.41	0.49
	FLEX-SD-NDH _{Max-Min}	-	-	0.79	0.57	-	-	0.46	0.46
	FLEX-SD-NDH _{Avg}	-	-	0.78	0.58	-	-	0.46	0.48

Note: $S_{rz} = ae^{b(NDH)}$

Table 7: Exponential relationships between the NDH values and simulated root zone moisture storage (Sr) in 31 ungauged sub-basins. Best performance in bold.

Model	Dry season		-	Wet season	
	R^2	NSE		R^2	NSE
FLEX-SD	0.71	0.41	-	0.36	0.38
FLEX-SD-NDH _{Max-Min}	0.74	0.45	-	0.41	0.36
FLEX-SD-NDH _{Avg}	0.74	0.52	-	0.41	0.40

10

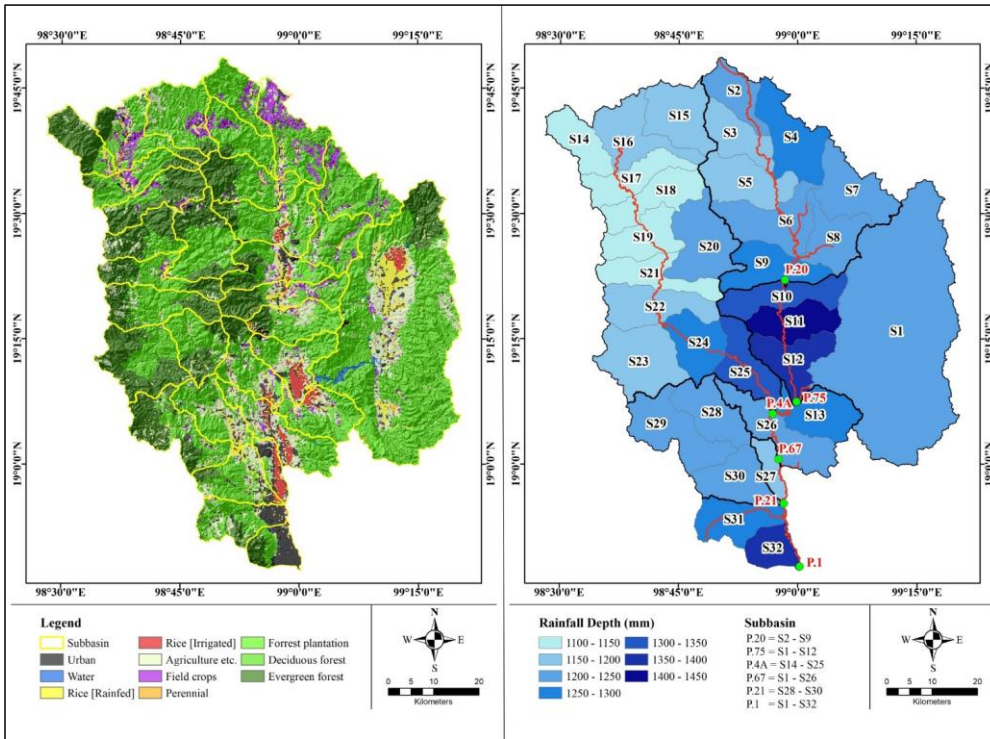
Table 8: Exponential relationships between the daily SWI040 values and simulated root zone moisture storage (Sr) in six sub-basins controlled by runoff stations. Best performance in bold.

Station	Model	Dry season				-	Wet season			
		a	b	R^2	NSE		a	b	R^2	NSE
P.20	FLEXL	55.4	0.024	0.88	0.84	-	36.3	0.030	0.91	0.88
	FLEX-SD	20.2	0.037	0.87	0.79	-	15.1	0.042	0.88	0.86
	FLEX-SD-NDH _{Max-Min}	118.7	0.019	0.85	0.78	-	78.8	0.024	0.90	0.84
	FLEX-SD-NDH _{Avg}	34.4	0.031	0.91	0.85	-	24.0	0.037	0.91	0.89
P.75	FLEXL	190.6	0.016	0.85	0.75	-	126.2	0.021	0.90	0.82
	FLEX-SD	20.9	0.037	0.89	0.81	-	15.6	0.043	0.89	0.87
	FLEX-SD-NDH _{Max-Min}	116.1	0.019	0.87	0.81	-	76.5	0.025	0.91	0.85
	FLEX-SD-NDH _{Avg}	40.3	0.029	0.92	0.86	-	27.4	0.036	0.92	0.89
P.4A	FLEXL	47.9	0.026	0.85	0.78	-	26.6	0.033	0.86	0.77
	FLEX-SD	19.7	0.036	0.89	0.81	-	14.8	0.040	0.89	0.83
	FLEX-SD-NDH _{Max-Min}	71.8	0.022	0.89	0.84	-	49.3	0.027	0.89	0.83
	FLEX-SD-NDH _{Avg}	92.9	0.020	0.84	0.76	-	59.5	0.025	0.85	0.77
P.67	FLEXL	22.5	0.035	0.91	0.82	-	12.6	0.043	0.91	0.84
	FLEX-SD	20.1	0.037	0.90	0.81	-	15.4	0.042	0.90	0.86
	FLEX-SD-NDH _{Max-Min}	88.8	0.021	0.89	0.84	-	60.2	0.026	0.91	0.86
	FLEX-SD-NDH _{Avg}	63.4	0.024	0.89	0.84	-	41.9	0.030	0.91	0.85
P.21	FLEXL	97.4	0.019	0.74	0.57	-	55.3	0.025	0.77	0.66
	FLEX-SD	16.8	0.039	0.87	0.73	-	10.2	0.047	0.83	0.77
	FLEX-SD-NDH _{Max-Min}	82.1	0.023	0.84	0.73	-	47.5	0.030	0.82	0.74
	FLEX-SD-NDH _{Avg}	77.3	0.023	0.81	0.69	-	43.6	0.030	0.80	0.71
P.1	FLEXL	17.1	0.038	0.92	0.81	-	10.6	0.046	0.90	0.85
	FLEX-SD	19.5	0.037	0.90	0.80	-	14.6	0.043	0.90	0.85
	FLEX-SD-NDH _{Max-Min}	86.5	0.022	0.89	0.83	-	57.4	0.027	0.90	0.85
	FLEX-SD-NDH _{Avg}	63.1	0.024	0.89	0.83	-	40.8	0.030	0.90	0.84
Average	FLEXL	-	-	0.86	0.76	-	-	-	0.87	0.80
	FLEX-SD	-	-	0.89	0.79	-	-	-	0.88	0.84
	FLEX-SD-NDH _{Max-Min}	-	-	0.87	0.81	-	-	-	0.89	0.83
	FLEX-SD-NDH _{Avg}	-	-	0.88	0.81	-	-	-	0.88	0.83

Note: $Sr = ae^{b(SWI)}$

Table 9: Exponential relationships between the daily SWI040 values and simulated root zone moisture storage (S_{rz}) in 31 ungauged sub-basins for semi-distributed models. Best performance in bold.

Model	Dry-season		Wet season	
	R^2	NSE	R^2	NSE
FLEX-SD	0.87	0.78	0.87	0.81
FLEX-SD-NDH _{Max-Min}	0.86	0.78	0.87	0.79
FLEX-SD-NDH _{Avg}	0.87	0.79	0.87	0.79



(a) Topography for each sub-catchment of the UPRB (b) Rainfall depth for each sub-catchment of the UPRB

Figure 11: Topography and mean annual rainfall depth for each sub-catchment of the UPRB

25

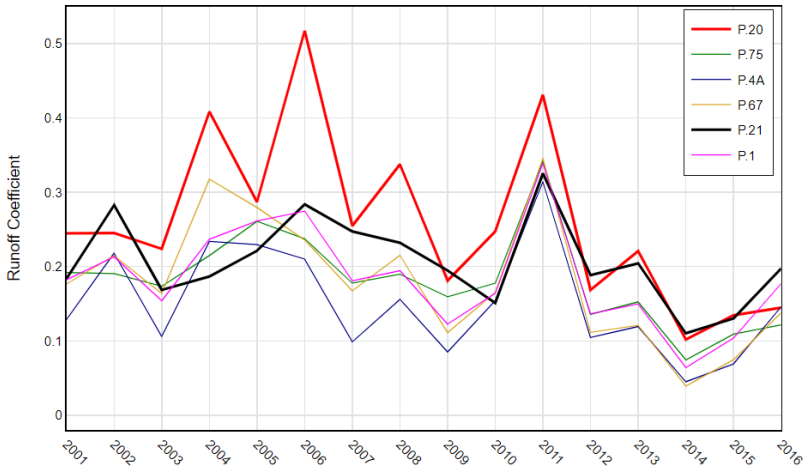
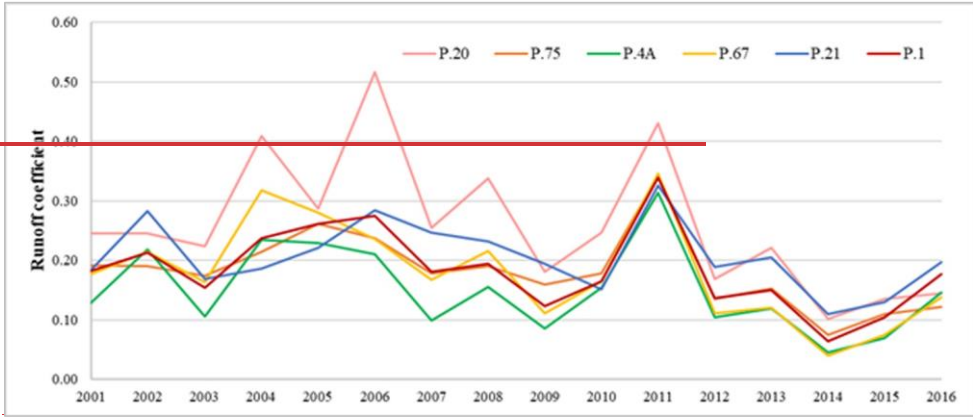


Figure 2: Runoff coefficient of each station

Figure 2: Runoff coefficient of each station

Formatted: Font: 9 pt, Bold, Complex Script Font: 9 pt, B

Formatted: Left

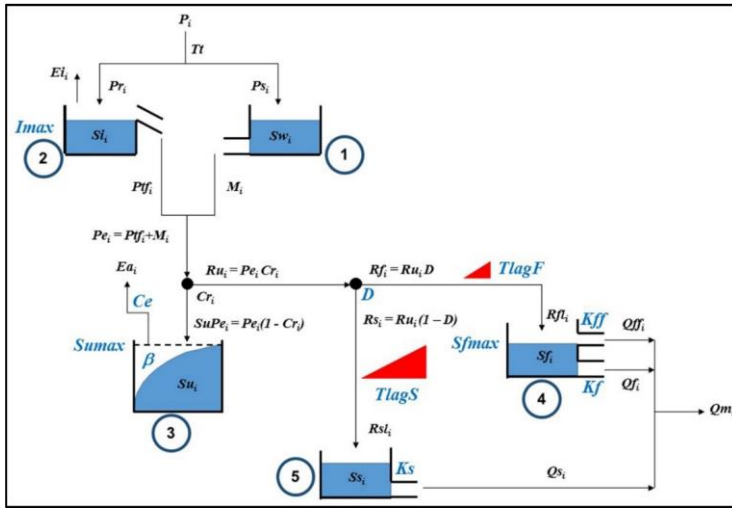
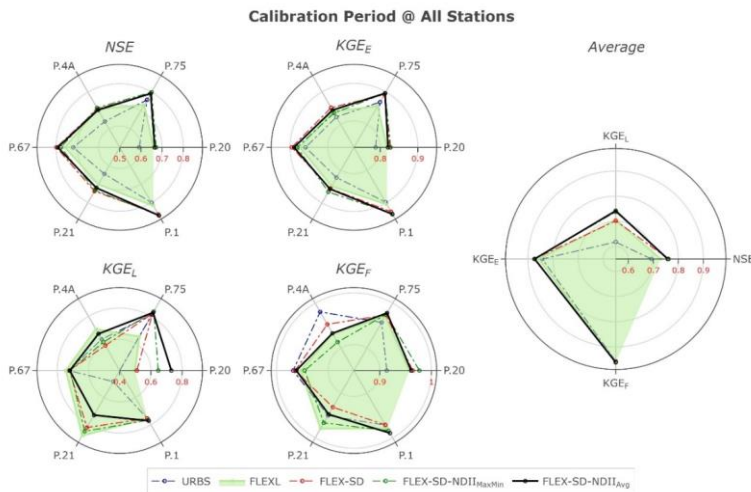
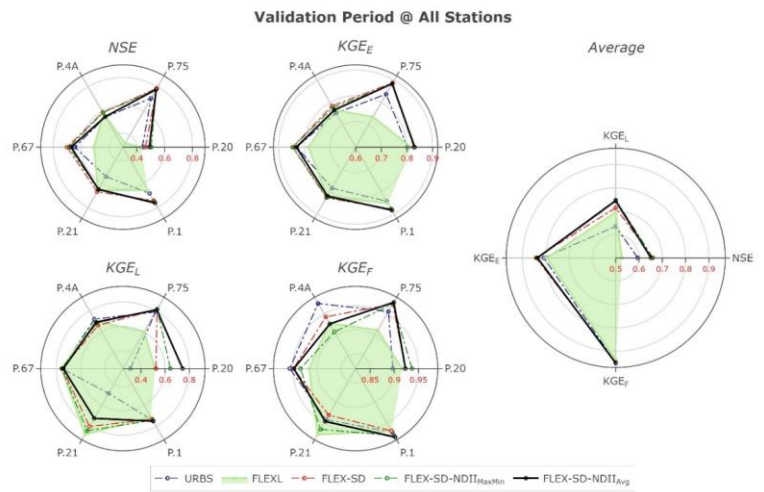


Figure 3: Model structure of FLEXL model





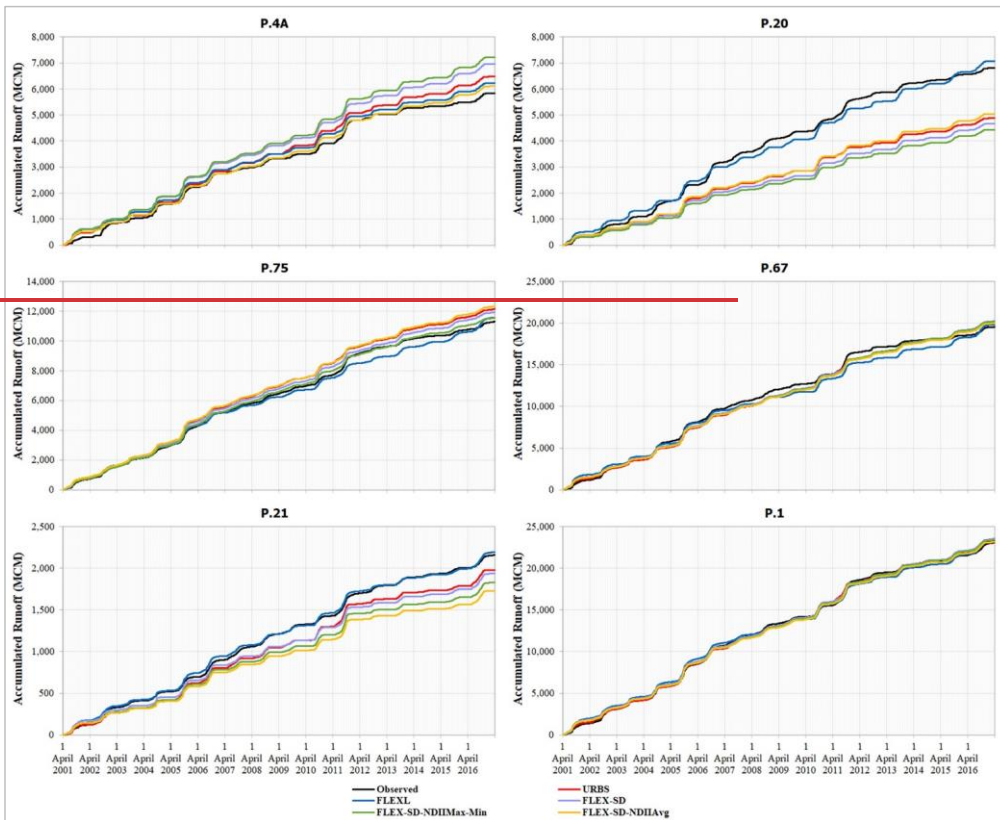


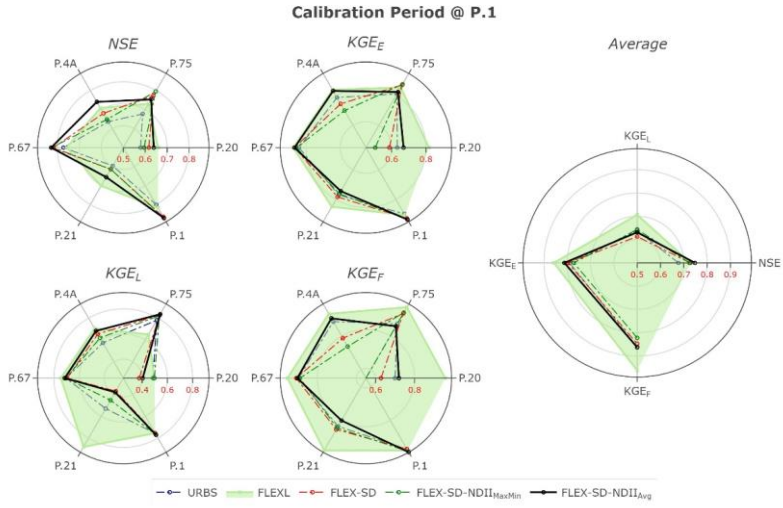
Figure 4: Comparison of the statistical indicators by (a) calibration and (b) validation at each station using FLEXL and 4 semi-distributed models Figure 4: — Accumulated simulated and observed runoff at all stations produced by FLEXL calibration at each station and by semi-distributed model calibration at P.1

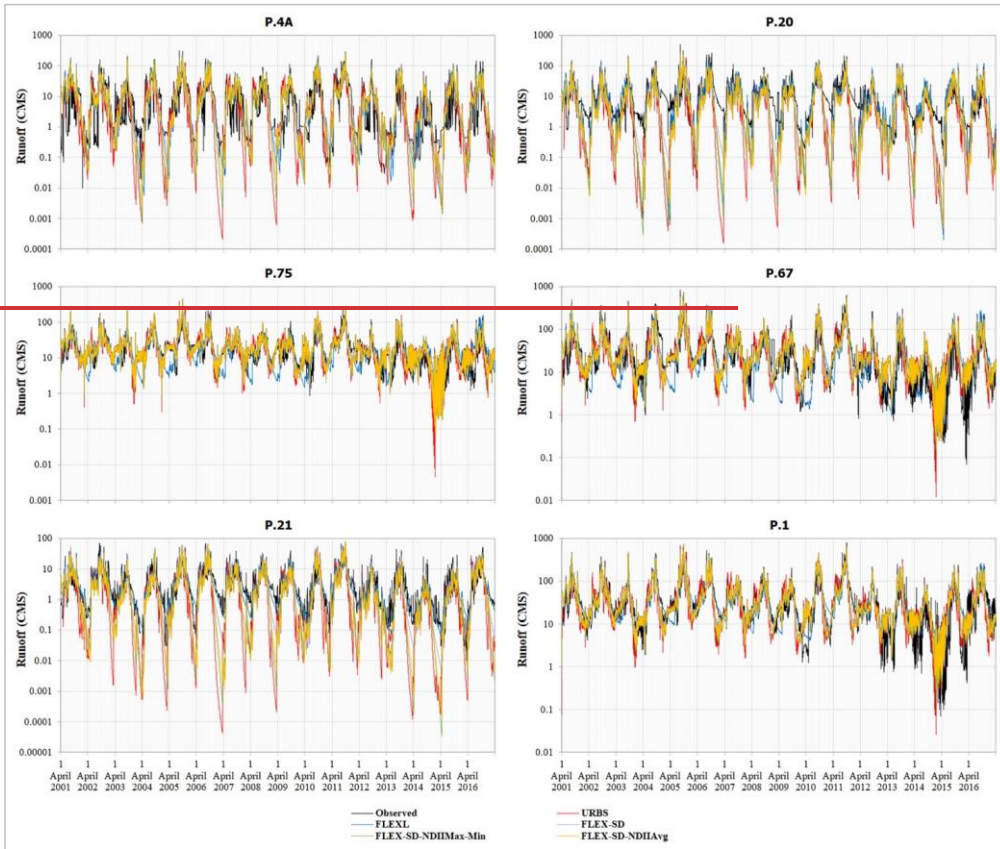
Formatted: Thai Distributed Justification

40

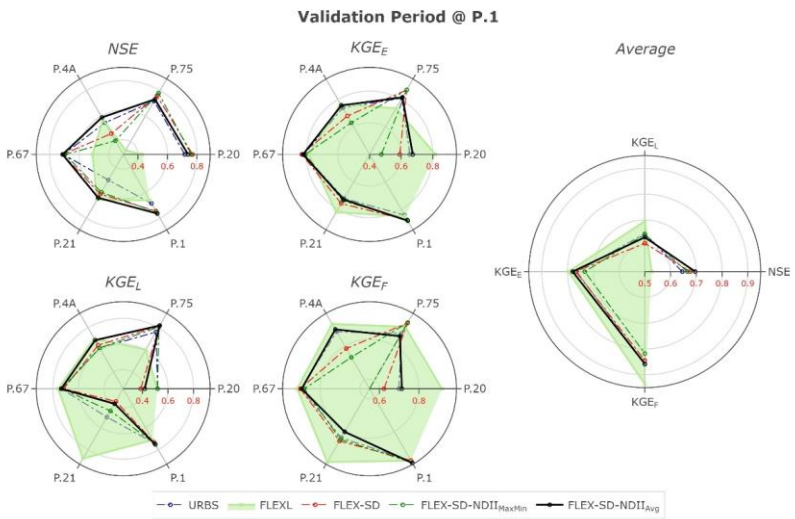
45

Formatted: Indent: Left: 0 cm, First line: 0 cm





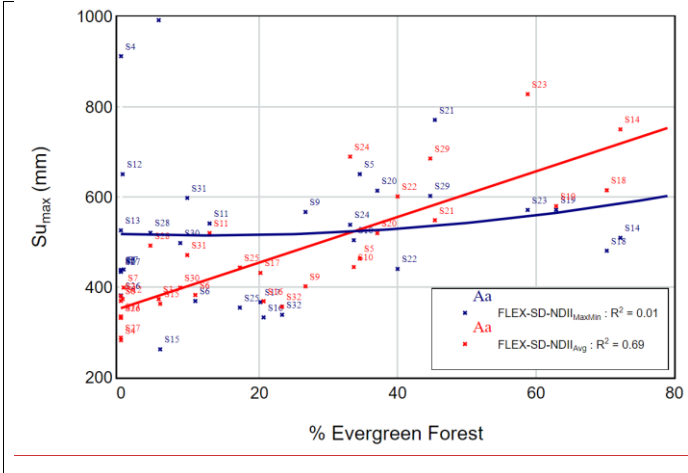
Formatted: Centered



50 **Figure 5:** Comparison between the statistical indicators by calibration (a) and validation (b) at each station using FLEXL and by calibration and validation at P.1 using 4 semi-distributed models Figure 5: Hydrograph of simulated and observed runoff at 6 stations produced by FLEXL calibrated at each station and by semi-distributed model calibrated only at P.1

Formatted: Indent: Left: 0 cm, First line: 0 cm

Formatted: Thai Distributed Justification



Formatted: Centered

55

60

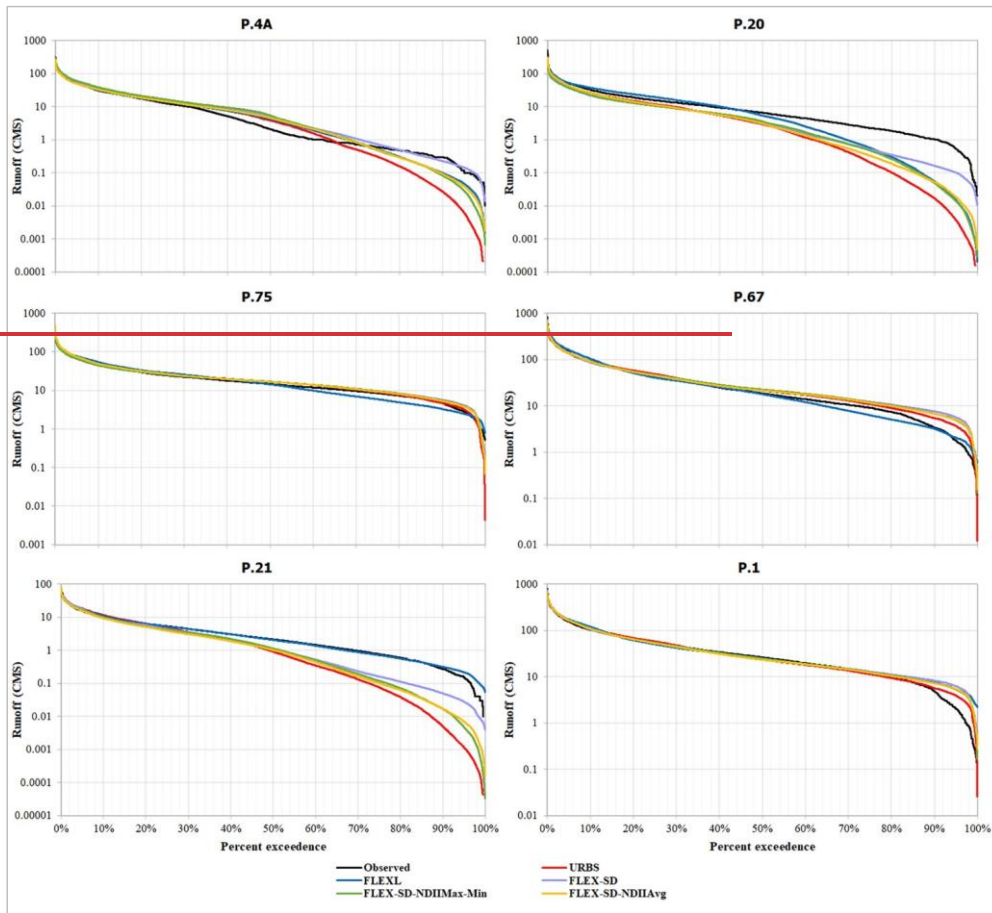


Figure 6: Relationships between percentage of evergreen forest and modelled *Sumax* in 31 sub-catchments as calibrated and validated by FLEX-SD-NDII_{avg} and FLEX-SD-NDII_{max-min}. The topography of UPRB is presented alongside. Flow duration curves of simulated and observed runoff at 6 stations produced by FLEXL calibrated at each station and by semi-distributed model calibrated only at P.1

Formatted: Indent: Left: 0 cm, First line: 0 cm

Formatted: Font: Italic, Complex Script Font: Italic

Formatted: Thai Distributed Justification

Formatted: Subscript

Formatted: Subscript

Formatted: Thai Distributed Justification, Indent: Left: 0 Hanging: 1.5 cm

65

70

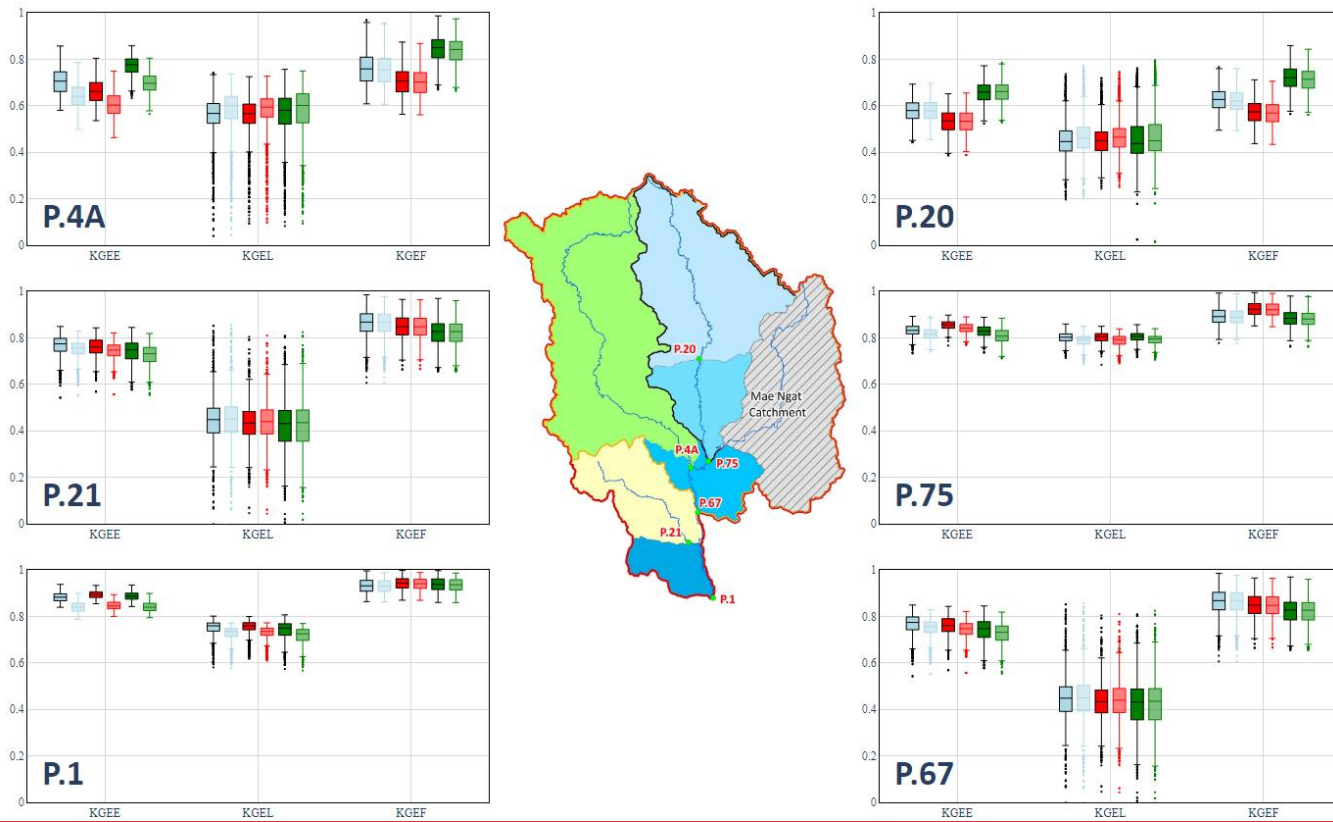


Figure 7: Comparison of box plots of the KGE_E , KGE_I , and KGE_F at 6 gauging stations provided by 3 FLEX-SD models using 5% best-performing parameter sets. Full boxes indicate calibration, transparent boxes validation. Blue, Red and Green indicate FLEX-SD, FLEX-SD-NDII_{MaxMin} and FLEX-SD-NDII_{Avg}, respectively

75

Formatted: Font: 9 pt, Com
 Formatted: Font: 9 pt, Com
 Formatted: Font: 9 pt, Com
 Formatted: Font: 9 pt, Com
 Formatted: Font: 9 pt, Com
 Formatted: Font: 9 pt, Com
 Formatted: Thai Distributed
 Hanging: 1.5 cm, Line spac
 Formatted: Font: 9 pt, Com
 Formatted: Font: 9 pt, Com
 Formatted: Font: 9 pt, Com
 Formatted: Font: 9 pt, Com

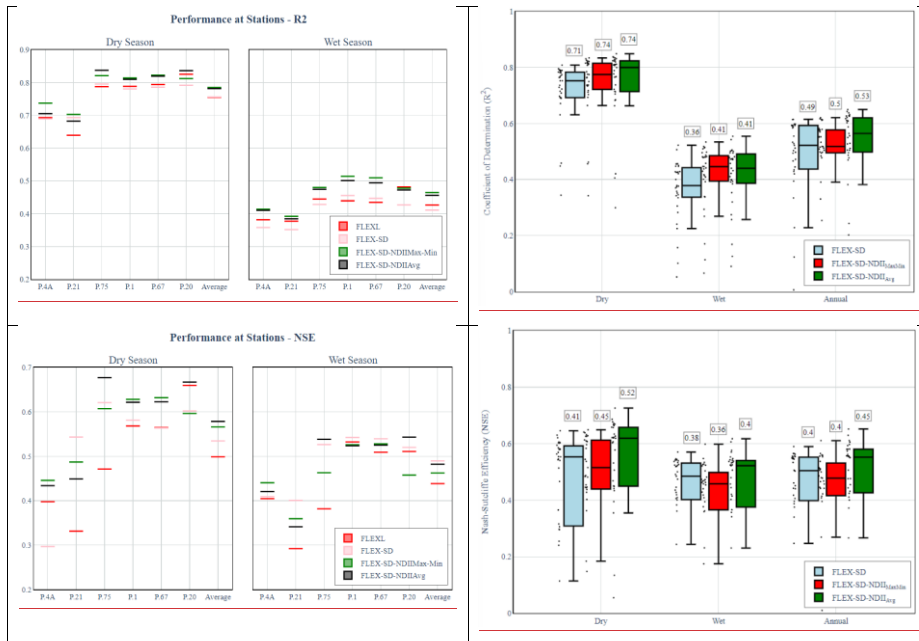


Figure 8: R^2 and NSE values from the exponential relationships between NDII values and simulated root zone moisture storage (S_u) during the wet and dry seasons for six sub-basins (a) and 31 sub-catchments (b) generated by 3 FLEX-SD models

Formatted: Font: 9 pt, Complex Script Font: 9 pt

Formatted: Font: 9 pt, Complex Script Font: 9 pt

Formatted: Font: 9 pt, Complex Script Font: 9 pt, Super

Formatted: Font: 9 pt, Complex Script Font: 9 pt

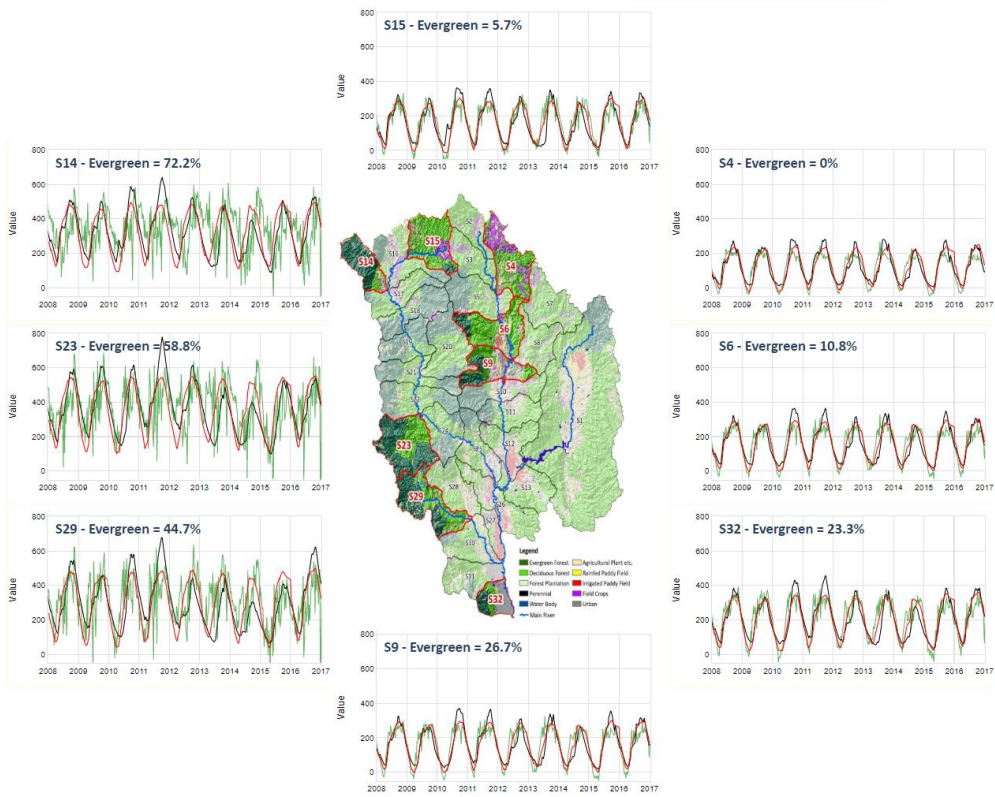


Figure 9: Comparison between simulated root zone moisture storage (Su), NDI and SWI for 8 sample sub-catchments with different percentage of evergreen forest

Formatted: Thai Distributed Justification

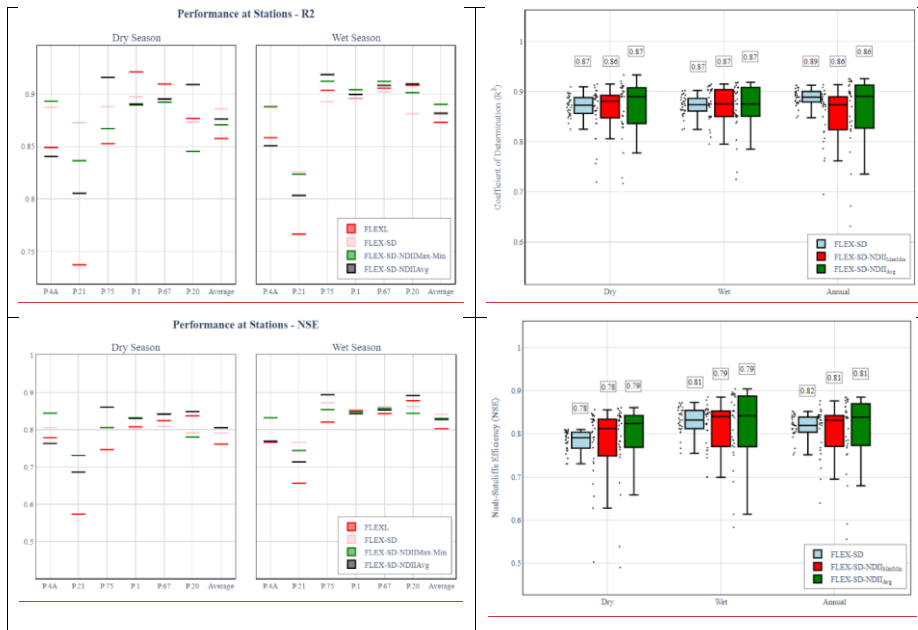
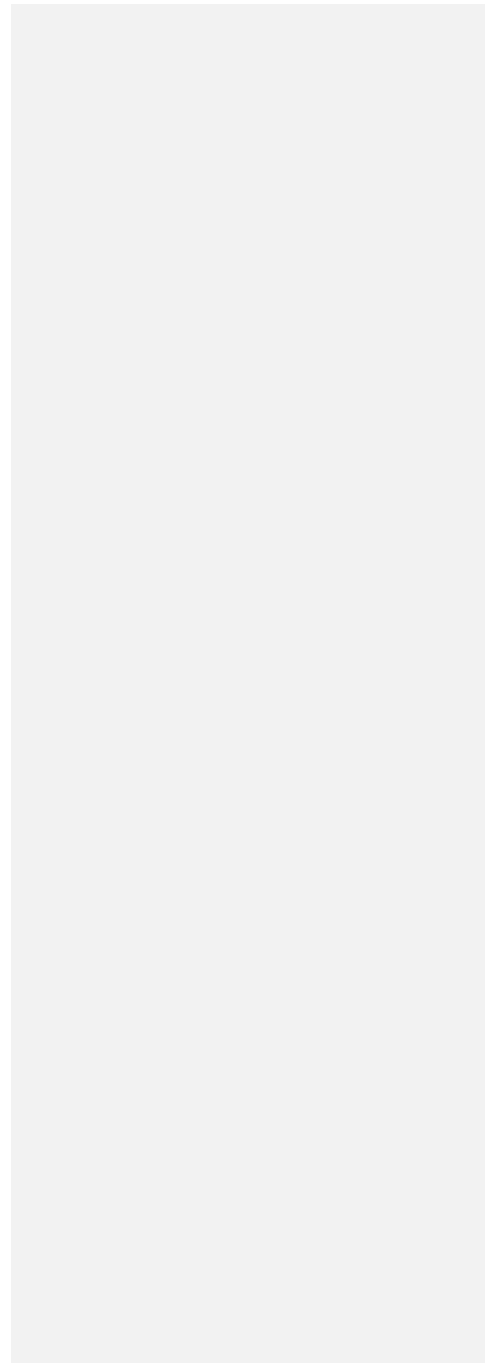


Figure 10: R^2 and NSE values from the exponential relationships between SWI40 and simulated root zone moisture storage (Su) during the wet and dry seasons for six sub-basins (a) and 31 sub-catchments (b) generated by 3 FLEX-SD models

Formatted: Superscript

Formatted: Indent: Left: 0 cm, Hanging: 1.75 cm, Line spacing: 1.5 lines, Tab stops: 1.75 cm, Left

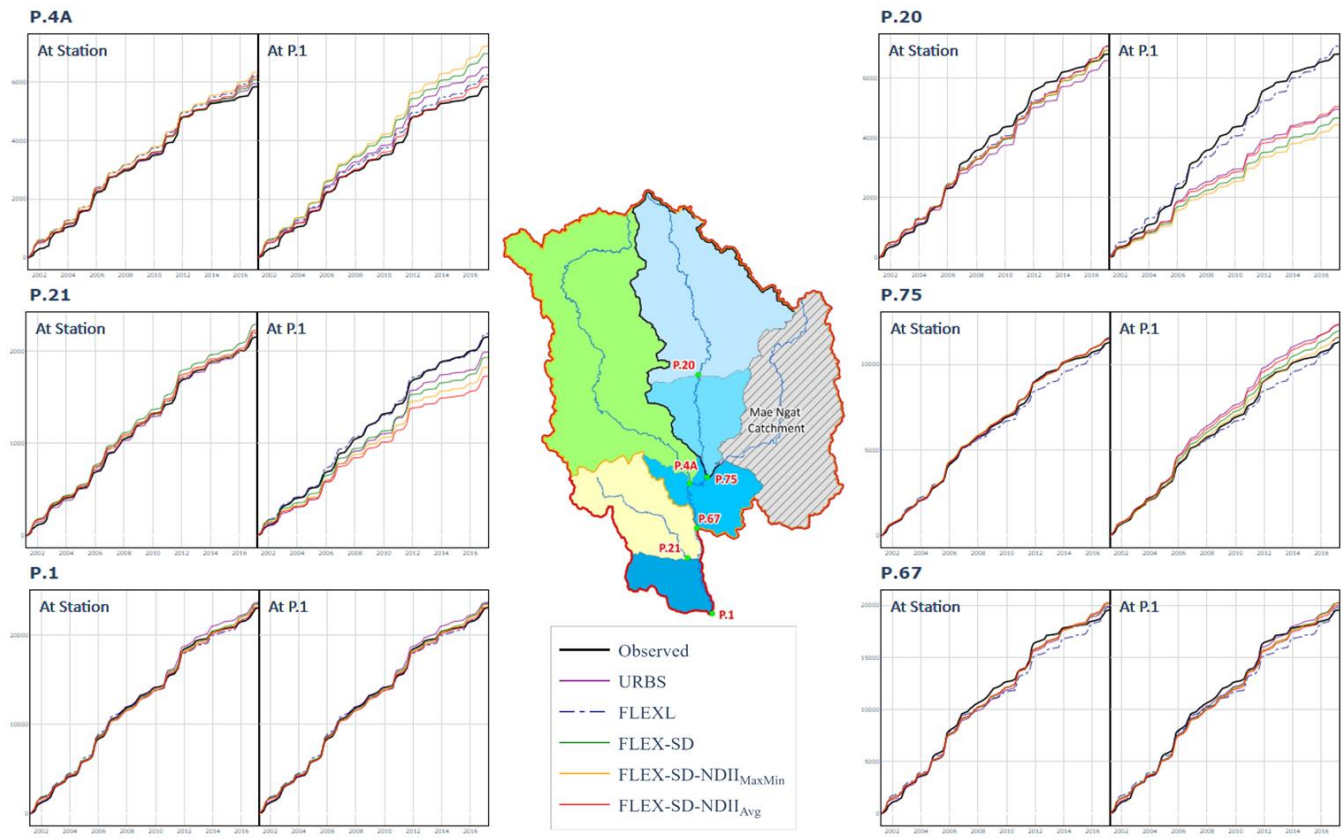
|



90 **Table A1: Model parameters of FLEXL (calibrated at all stations) and FLEX-SD and FLEX-SD-NDII (calibrated only at P.1)**

Station	Model - Case	I_{max} (mm)	S_{umax} (mm)	C_e	β	D	K_f	K_s	T_{lagF} (hr)	T_{lagS} (hr)	S_{fmax} (mm)	K_{ff}	α	X	b	R
P.1	(1) FLEXL	1.59	475.80	0.93	0.22	0.69	37.87	111.42	3.33	20.07	3.22	6.85				
	(2) FLEX-SD	3.51	435.48	0.69	0.48	0.82	8.12	36.68	5.03	56.42	8.63	3.47	0.30	0.19		
	(3) FLEX-SD-NDII _{Inter}	2.22	476.49	0.96	0.26	0.72	13.27	16.58	3.58	79.46	7.46	4.30	0.22	0.10	12.76	
	$\frac{I_{min}I_{max}}{I_{avg}}$ (4) FLEX-SD-NDII _{AVG}	3.18	464.87	0.95	0.31	0.62	4.53	19.90	5.35	22.53	2.81	3.50	0.38	0.14	15.50	0.49
P.20	(1) FLEXL	2.85	411.45	0.89	0.68	0.72	6.37	41.52	2.64	73.69	14.12	3.09				
	(2) FLEX-SD	*	*	*	*	*	*	*	3.71	41.62	*	*	*	*		
	(3) FLEX-SD-NDII _{Inter}	*	599.76	*	*	*	*	*	2.64	58.61	*	*	*	*	*	
	$\frac{I_{min}I_{max}}{I_{avg}}$ (4) FLEX-SD-NDII _{AVG}	*	380.45	*	*	*	*	*	3.94	16.62	*	*	*	*	*	*
P.75	(1) FLEXL	1.98	514.21	0.86	0.30	0.55	11.08	165.45	4.09	15.35	1.11	8.00				
	(2) FLEX-SD	*	*	*	*	*	*	*	6.44	72.19	*	*	*	*		
	(3) FLEX-SD-NDII _{Inter}	*	462.51	*	*	*	*	*	4.58	101.66	*	*	*	*	*	
	$\frac{I_{min}I_{max}}{I_{avg}}$ (4) FLEX-SD-NDII _{AVG}	*	409.31	*	*	*	*	*	6.84	28.82	*	*	*	*	*	*
P.4A	(1) FLEXL	4.19	429.49	0.86	0.38	0.91	13.34	43.48	4.29	30.12	8.13	7.27				
	(2) FLEX-SD	*	*	*	*	*	*	*	3.71	41.56	*	*	*	*		
	(3) FLEX-SD-NDII _{Inter}	*	483.50	*	*	*	*	*	2.64	58.53	*	*	*	*	*	
	$\frac{I_{min}I_{max}}{I_{avg}}$ (4) FLEX-SD-NDII _{AVG}	*	563.47	*	*	*	*	*	3.94	16.60	*	*	*	*	*	*
P.67	(1) FLEXL	3.53	358.74	0.75	0.41	0.76	16.30	175.56	3.03	51.90	8.52	7.38				
	(2) FLEX-SD	*	*	*	*	*	*	*	5.26	59.03	*	*	*	*		
	(3) FLEX-SD-NDII _{Inter}	*	469.08	*	*	*	*	*	3.75	83.13	*	*	*	*	*	
	$\frac{I_{min}I_{max}}{I_{avg}}$ (4) FLEX-SD-NDII _{AVG}	*	460.79	*	*	*	*	*	5.59	23.57	*	*	*	*	*	*
P.21	(1) FLEXL	4.88	759.96	0.88	1.14	0.70	11.71	42.09	2.48	23.98	9.40	4.77				
	(2) FLEX-SD	*	*	*	*	*	*	*	3.79	42.50	*	*	*	*		
	(3) FLEX-SD-NDII _{Inter}	*	547.29	*	*	*	*	*	2.70	59.85	*	*	*	*	*	
	$\frac{I_{min}I_{max}}{I_{avg}}$ (4) FLEX-SD-NDII _{AVG}	*	543.68	*	*	*	*	*	4.03	16.97	*	*	*	*	*	*

Note: * Same parameter values as P.1 for FLEX-SD and FLEX-SD-NDII



95 **Figure A1: Accumulated simulated and observed runoff (unit: MCM) of all models produced by calibration and validation at (1) each station ("At Station") and (2) at P.I. Note that FLEXL is the only lumped model and was thereby only calibrated at each station.**

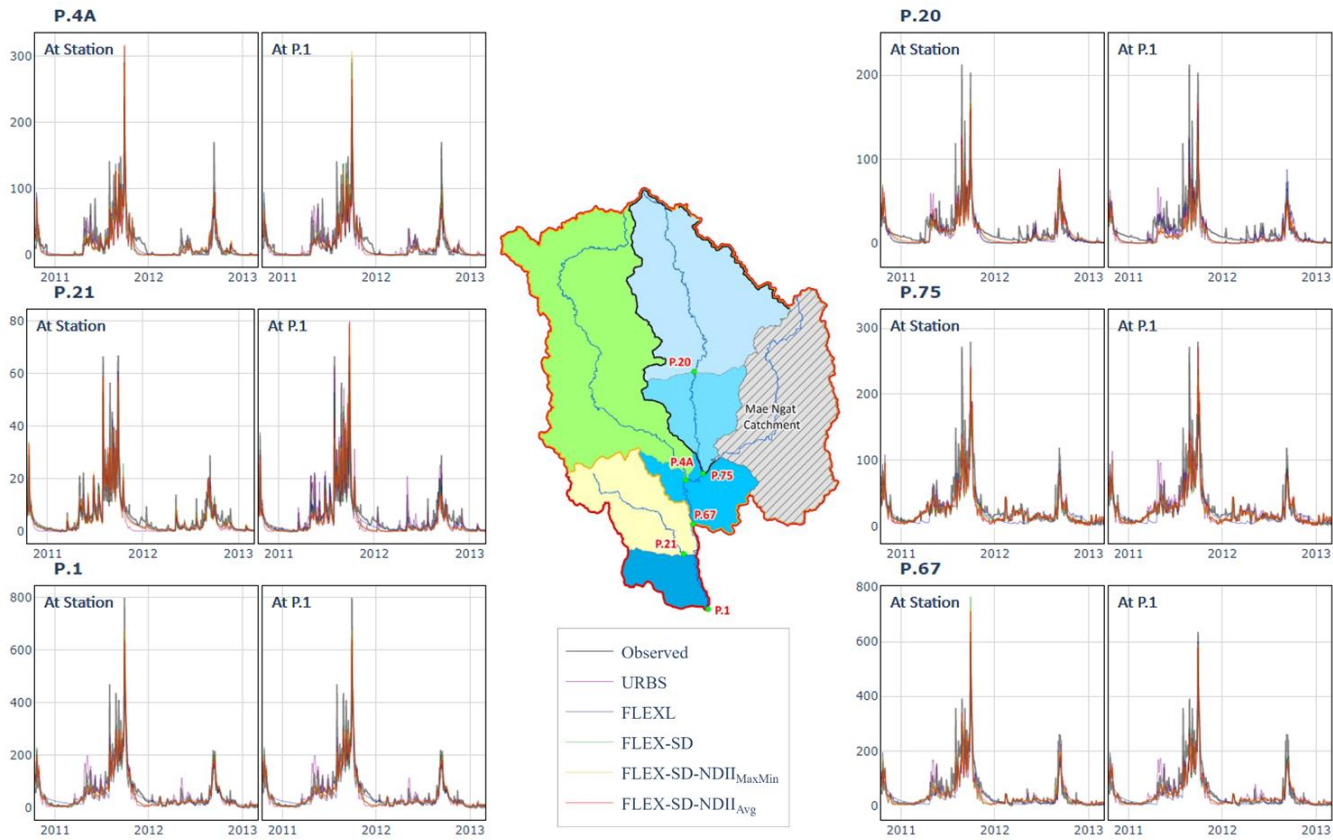
Formatted: Centered

Formatted: Font: 10 pt, Bold

Formatted: Font: 10 pt, Bold

Formatted: Font: 10 pt, Bold

Formatted: Indent: Left: 0 stops: 1.75 cm, Left + Not a



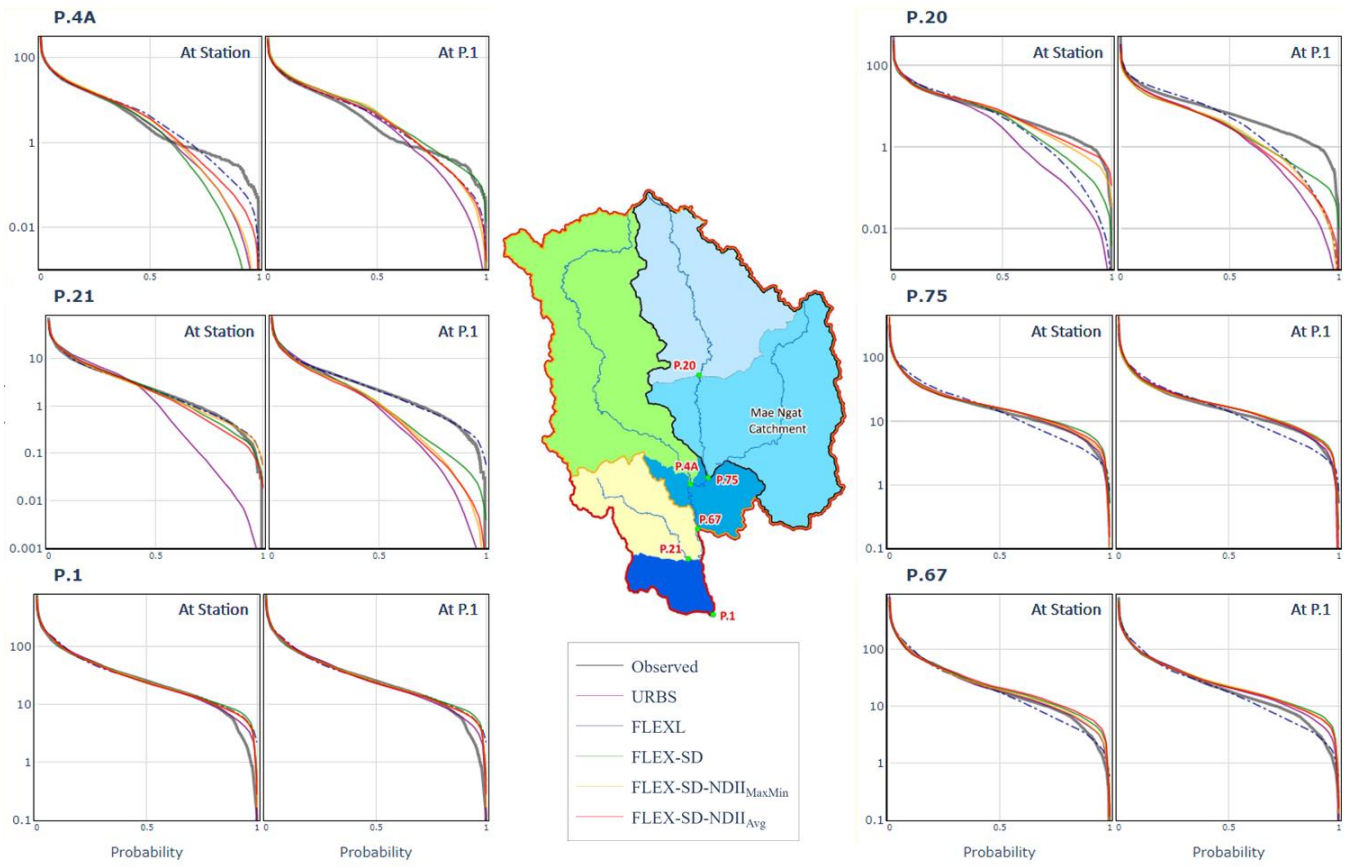
100 **Figure A2: Hydrographs of simulated and observed runoff (unit: cms) of all models at all stations produced by calibration and validation at (1) each station ("At Station") and (2) at P.1. Note that FLEXL is the only lumped model and was thereby only calibrated at each station.**

Formatted: Font: 10 pt, Bold

Formatted: Font: 10 pt, Bold

Formatted: Indent: Left: 0 stops: 2.25 cm, Left + Not a

Formatted: Font: 10 pt, Bold



105

Figure A3: Flow duration curves of simulated and observed runoff of all models at all stations produced by calibration and validation at (1) each station (“At Station”) and (2) at P.1. Note that FLEXL is the only lumped model and was thereby only calibrated at each station.

Formatted: Font: 10 pt, Bold, Check spelling and grammar

Formatted: Font: 10 pt, Bold, Check spelling and grammar

Formatted: Indent: Left: 0.5 in, stops: 1.75 cm, Left + Not a paragraph

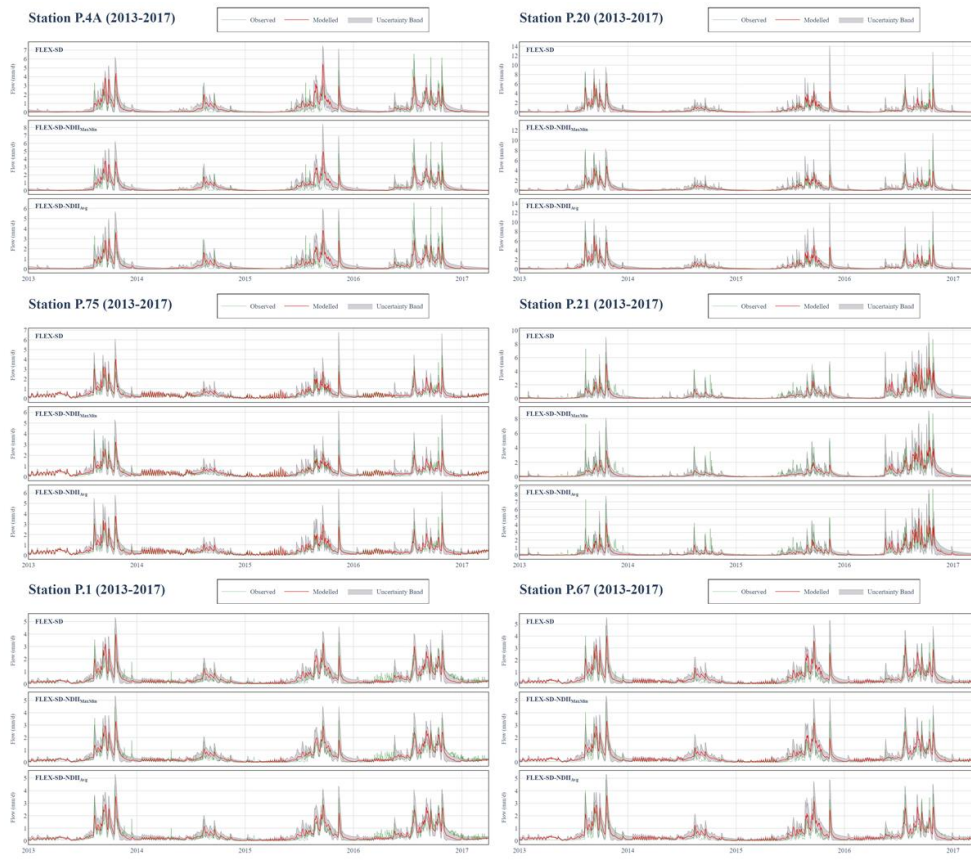
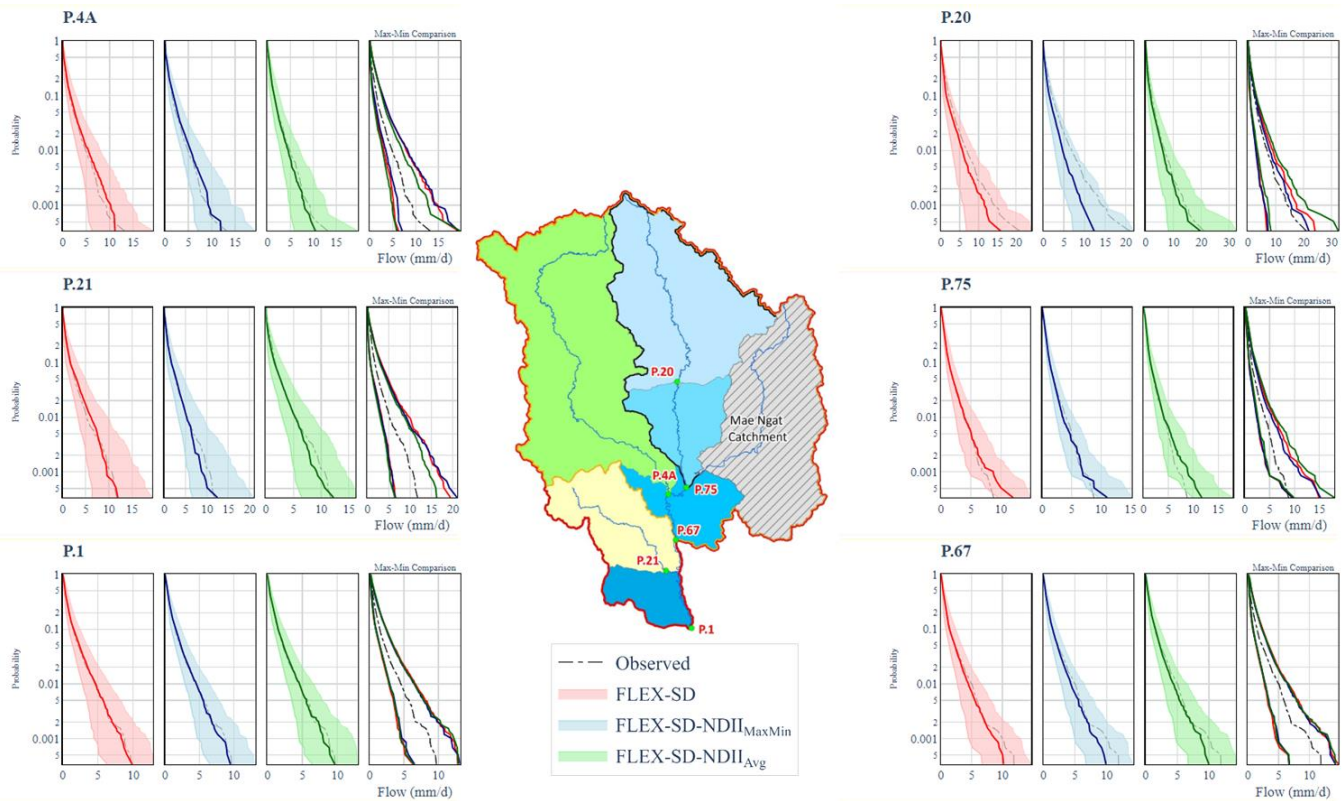


Figure A4: Comparison of the observed and calculated hydrographs at 6 stations acquired from the 5% best performing parameter combinations generated by 3 FLEX-SD models

Formatted: Font: 10 pt, Bold, Complex Script Font: 10 pt, Bold

Formatted: Font: 10 pt, Bold, Complex Script Font: 10 pt, Bold

Formatted: Indent: Left: 0 cm, Hanging: 1.75 cm, Tab stops: 1.75 cm, Left + Not at 2 cm



Formatted: Font: 10 pt, Bold
 Formatted: Centered, Tab stops: Not at 1.5 cm
 Formatted: Left: 2.36 cm, Bottom: 1.65 cm, Width: 2.36 cm

Formatted: Font: 9 pt, Com
 Formatted: Centered
 Formatted: Centered, Inde
 Tab stops: Not at 1.5 cm
 Formatted: Line spacing: 1
 Formatted: Line spacing: 1
 Formatted: Centered, Line
 Formatted: Line spacing: 1
 Formatted: Line spacing: 1
 Formatted: Line spacing: 1

115 **Table A2: Exponential relationships between the average NDII values and simulated root zone moisture storage (S_R) in 31 sub-basins. Best performance in bold.**

Station	Model	Dry-season				Wet-season			
		α	b	R^2	NSE	α	b	R^2	NSE
	FLEX-SD	22.1	9.5	0.74	0.54	15.5	11.5	0.34	0.49
Sub-2	FLEX-SD-NDII _{Max-Min}	56.5	6.8	0.81	0.65	37.7	8.7	0.42	0.52
	FLEX-SD-NDII _{Avg}	35.9	8.0	0.80	0.63	24.2	9.9	0.39	0.53

	FLEX-SD	19.4	10.0	0.72	0.51	-	14.1	12.1	0.33	0.50
Sub-3	FLEX-SD-NDH _{Max-Min}	170.6	4.1	0.71	0.48	-	119.2	5.3	0.44	0.43
	FLEX-SD-NDH _{Avg}	31.4	8.5	0.79	0.60	-	21.9	10.5	0.39	0.54
	FLEX-SD	57.1	6.9	0.77	0.65	-	31.4	8.9	0.31	0.48
Sub-4	FLEX-SD-NDH _{Max-Min}	364.2	2.4	0.69	0.15	-	242.6	3.1	0.34	0.17
	FLEX-SD-NDH _{Avg}	39.3	7.6	0.83	0.73	-	24.9	9.5	0.35	0.62
	FLEX-SD	24.8	9.5	0.75	0.59	-	14.4	12.2	0.37	0.53
Sub-5	FLEX-SD-NDH _{Max-Min}	203.8	3.9	0.74	0.44	-	129.5	5.2	0.45	0.39
	FLEX-SD-NDH _{Avg}	39.2	7.8	0.81	0.66	-	23.1	10.4	0.44	0.57
	FLEX-SD	24.7	9.4	0.77	0.60	-	13.8	12.2	0.43	0.54
Sub-6	FLEX-SD-NDH _{Max-Min}	162.5	4.2	0.78	0.54	-	101.5	5.8	0.49	0.45
	FLEX-SD-NDH _{Avg}	39.4	7.7	0.83	0.67	-	22.3	10.4	0.48	0.58
	FLEX-SD	25.6	8.0	0.77	0.55	-	15.7	9.9	0.24	0.36
Sub-7	FLEX-SD-NDH _{Max-Min}	64.5	5.8	0.82	0.63	-	40.6	7.2	0.29	0.36
	FLEX-SD-NDH _{Avg}	47.1	6.4	0.81	0.61	-	28.6	8.1	0.27	0.36
	FLEX-SD	29.5	7.6	0.78	0.55	-	17.3	9.7	0.28	0.41
Sub-8	FLEX-SD-NDH _{Max-Min}	71.1	5.4	0.83	0.64	-	43.4	7.1	0.34	0.41
	FLEX-SD-NDH _{Avg}	48.3	6.2	0.82	0.62	-	28.5	8.2	0.32	0.41
	FLEX-SD	25.6	9.0	0.79	0.60	-	14.0	11.7	0.43	0.52
Sub-9	FLEX-SD-NDH _{Max-Min}	133.8	4.5	0.81	0.60	-	81.6	6.2	0.48	0.46
	FLEX-SD-NDH _{Avg}	42.1	7.3	0.84	0.67	-	23.2	9.9	0.47	0.54
	FLEX-SD	24.4	9.2	0.79	0.61	-	13.2	12.0	0.43	0.52
Sub-10	FLEX-SD-NDH _{Max-Min}	125.6	4.7	0.81	0.61	-	75.4	6.5	0.48	0.47
	FLEX-SD-NDH _{Avg}	42.5	7.4	0.83	0.67	-	23.1	10.0	0.47	0.54
	FLEX-SD	23.5	9.3	0.79	0.60	-	12.4	12.2	0.43	0.52
Sub-11	FLEX-SD-NDH _{Max-Min}	121.0	4.8	0.82	0.61	-	71.4	6.7	0.48	0.47
	FLEX-SD-NDH _{Avg}	45.4	7.2	0.83	0.66	-	24.2	9.9	0.47	0.53
	FLEX-SD	23.3	9.5	0.80	0.62	-	12.0	12.4	0.43	0.53
Sub-12	FLEX-SD-NDH _{Max-Min}	123.1	4.9	0.82	0.61	-	71.6	6.7	0.48	0.46
	FLEX-SD-NDH _{Avg}	44.1	7.5	0.84	0.68	-	23.1	10.1	0.47	0.54

Formatted

Formatted

Formatted

Formatted

Formatted

Formatted

Formatted

Formatted

Formatted

Formatted

Formatted

Formatted

Formatted

Formatted

Formatted

Formatted

Formatted

Formatted

Formatted

Formatted

Formatted

Formatted

Formatted

Formatted

Formatted

Formatted

Formatted

Formatted

Formatted

Formatted

Formatted

Formatted

Formatted

Formatted

Formatted

Formatted

Formatted

Formatted

Formatted

Formatted

Formatted

Formatted

	FLEX-SD	24.4	9.4	0.81	0.63	-	12.2	12.4	0.45	0.54
Sub-13	FLEX-SD-NDH _{Max-Min}	123.4	4.9	0.83	0.61	-	70.4	6.8	0.50	0.47
	FLEX-SD-NDH _{Avg}	44.2	7.4	0.85	0.69	-	22.7	10.1	0.50	0.55

Note: $S_{ij} = ae^{ln(NDH)}$

Formatted: Centered, Line

Formatted: Line spacing: 1

Formatted: Line spacing: 1

Formatted: Line spacing: 1

Formatted: Line spacing: 1

Formatted: Centered, Line

Table A2: continued

Station	Model	Dry-season				-	Wet-season			
		<i>a</i>	<i>b</i>	<i>R</i> ²	<i>NSE</i>	-	<i>a</i>	<i>b</i>	<i>R</i> ²	<i>NSE</i>
Sub-14	FLEX-SD	2.8	12.7	0.34	-1.12	-	73.9	2.7	0.05	-0.74
	FLEX-SD-NDII _{Max-Min}	23.7	7.8	0.34	-0.80	-	121.8	2.7	0.07	-0.58
	FLEX-SD-NDII _{Avg}	73.6	5.3	0.30	-0.47	-	162.7	2.8	0.09	-0.41
Sub-15	FLEX-SD	18.9	10.3	0.71	0.55	-	19.3	11.2	0.51	0.57
	FLEX-SD-NDII _{Max-Min}	9.3	11.9	0.76	0.48	-	15.3	11.6	0.50	0.60
	FLEX-SD-NDII _{Avg}	27.3	9.0	0.78	0.62	-	26.2	10.0	0.54	0.61
Sub-16	FLEX-SD	17.4	10.9	0.75	0.59	-	17.2	11.8	0.52	-0.05
	FLEX-SD-NDII _{Max-Min}	14.3	11.0	0.81	0.58	-	18.1	11.4	0.53	-0.10
	FLEX-SD-NDII _{Avg}	26.0	9.5	0.81	0.66	-	24.1	10.5	0.55	-0.09
Sub-17	FLEX-SD	9.5	12.4	0.73	0.47	-	10.2	13.5	0.45	0.52
	FLEX-SD-NDII _{Max-Min}	17.1	10.3	0.78	0.52	-	18.1	11.3	0.48	0.55
	FLEX-SD-NDII _{Avg}	36.3	8.2	0.77	0.58	-	30.0	9.7	0.51	0.55
Sub-18	FLEX-SD	7.8	12.7	0.71	0.37	-	8.6	14.0	0.42	0.47
	FLEX-SD-NDII _{Max-Min}	18.7	9.8	0.76	0.45	-	18.4	11.2	0.46	0.50
	FLEX-SD-NDII _{Avg}	38.8	7.9	0.74	0.51	-	30.7	9.6	0.48	0.51
Sub-19	FLEX-SD	7.2	12.8	0.70	0.32	-	7.7	14.3	0.40	0.45
	FLEX-SD-NDII _{Max-Min}	23.0	9.2	0.75	0.43	-	20.7	10.8	0.45	0.48
	FLEX-SD-NDII _{Avg}	39.7	7.8	0.72	0.47	-	30.1	9.6	0.46	0.48
Sub-20	FLEX-SD	10.9	10.9	0.63	0.25	-	10.4	12.0	0.22	0.24
	FLEX-SD-NDII _{Max-Min}	90.0	5.5	0.66	0.36	-	68.3	6.6	0.27	0.23
	FLEX-SD-NDII _{Avg}	53.9	6.6	0.66	0.35	-	41.0	7.8	0.26	0.23
Sub-21	FLEX-SD	7.6	12.5	0.69	0.31	-	6.9	14.5	0.38	0.44
	FLEX-SD-NDII _{Max-Min}	42.3	7.4	0.73	0.45	-	30.9	9.5	0.44	0.47
	FLEX-SD-NDII _{Avg}	42.3	7.5	0.71	0.45	-	28.8	9.7	0.43	0.46
Sub-22	FLEX-SD	7.4	12.4	0.69	0.30	-	6.5	14.6	0.37	0.43
	FLEX-SD-NDII _{Max-Min}	39.8	7.5	0.74	0.44	-	28.4	9.7	0.43	0.46
	FLEX-SD-NDII _{Avg}	44.4	7.3	0.71	0.44	-	29.1	9.6	0.42	0.44

Formatted

Formatted

Formatted

Formatted

Formatted

Formatted

Formatted

Formatted

Formatted

Formatted

Formatted

Formatted

Formatted

Formatted

Formatted

Formatted

Formatted

Formatted

Formatted

Formatted

Formatted

Formatted

Formatted

Formatted

Formatted

Formatted

Formatted

Formatted

Formatted

Formatted

Formatted

Formatted

Formatted

Formatted

Formatted

Formatted

Formatted

Formatted

Formatted

Formatted

Formatted

Formatted

	FLEX-SD	2.5	13.8	0.45	-0.31	-	18.6	7.8	0.10	-0.33
Sub-23	FLEX-SD-NDH _{Max-Min}	32.8	7.6	0.46	-0.05	-	68.3	5.2	0.11	-0.24
	FLEX-SD-NDH _{Avg}	88.1	5.4	0.41	0.05	-	117.8	4.2	0.13	-0.18
	FLEX-SD	6.0	12.9	0.67	0.24	-	5.4	14.9	0.35	0.38
Sub-24	FLEX-SD-NDH _{Max-Min}	37.9	7.7	0.72	0.40	-	26.6	9.8	0.40	0.42
	FLEX-SD-NDH _{Avg}	52.9	6.9	0.68	0.39	-	33.9	9.0	0.40	0.40
	FLEX-SD	6.4	12.8	0.69	0.30	-	5.3	15.0	0.36	0.41
Sub-25	FLEX-SD-NDH _{Max-Min}	36.7	7.8	0.74	0.45	-	25.0	10.0	0.41	0.44
	FLEX-SD-NDH _{Avg}	51.7	7.0	0.71	0.43	-	32.2	9.2	0.41	0.42
	FLEX-SD	13.9	11.0	0.79	0.56	-	7.1	14.4	0.45	0.54
Sub-26	FLEX-SD-NDH _{Max-Min}	72.6	6.3	0.82	0.63	-	39.5	8.7	0.51	0.53
	FLEX-SD-NDH _{Avg}	51.1	7.0	0.82	0.62	-	26.5	9.8	0.49	0.53

Note: $S_H = ae^{h(NDH)}$

Formatted: Centered, Line

Formatted: Line spacing: 1

Formatted: Line spacing: 1

Formatted: Line spacing: 1

Formatted: Line spacing: 1

Formatted: Centered, Line

Formatted: Line spacing: 1

Formatted: Line spacing: 1

Formatted: Line spacing: 1

Formatted: Line spacing: 1

Formatted: Line spacing: 1

Formatted: Centered, Line

Formatted: Line spacing: 1

Formatted: Line spacing: 1

Formatted: Line spacing: 1

Formatted: Line spacing: 1

Formatted: Centered, Line

Formatted: Line spacing: 1

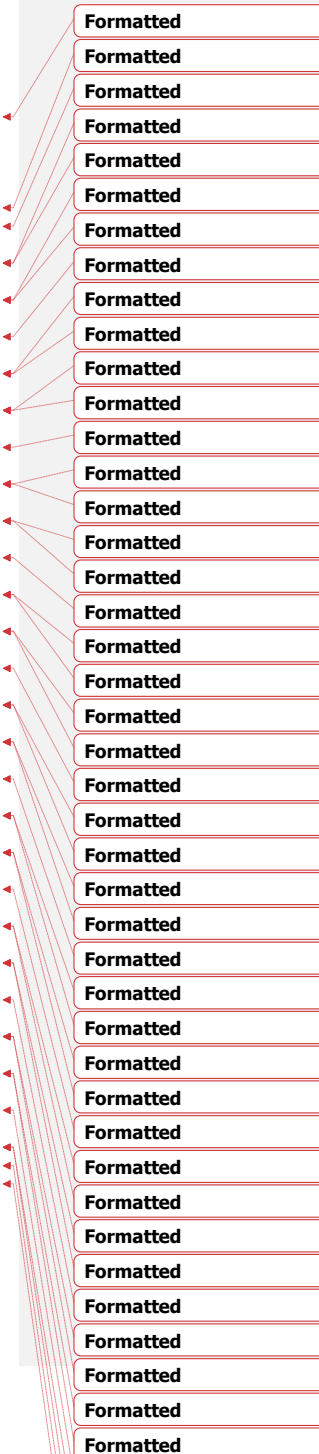
Formatted: Line spacing: 1

Formatted: Line spacing: 1

Formatted: Centered, Line

Table A3: Exponential relationships between the daily SWI040 values and simulated root zone moisture storage (S_r) in 31 sub-basins. Best performance in bold.

Station	Model	Dry-season				-	Wet-season			
		<i>a</i>	<i>b</i>	R^2	<i>NSE</i>		<i>a</i>	<i>b</i>	R^2	<i>NSE</i>
Sub-2	FLEX-SD	23.4	0.036	0.85	0.76	-	18.4	0.041	0.86	0.84
	FLEX-SD-NDH _{Max-Min}	58.1	0.026	0.91	0.86	-	41.8	0.031	0.90	0.89
	FLEX-SD-NDH _{Avg}	37.1	0.030	0.91	0.84	-	27.6	0.035	0.90	0.89
Sub-3	FLEX-SD	21.8	0.037	0.84	0.76	-	17.1	0.041	0.86	0.83
	FLEX-SD-NDH _{Max-Min}	177.0	0.015	0.76	0.66	-	122.5	0.019	0.85	0.78
	FLEX-SD-NDH _{Avg}	34.4	0.031	0.90	0.84	-	25.4	0.036	0.90	0.87
Sub-4	FLEX-SD	21.7	0.037	0.86	0.77	-	14.7	0.044	0.85	0.85
	FLEX-SD-NDH _{Max-Min}	259.9	0.013	0.72	0.50	-	168.2	0.018	0.81	0.70
	FLEX-SD-NDH _{Avg}	13.7	0.040	0.93	0.77	-	12.5	0.044	0.85	0.90
Sub-5	FLEX-SD	21.2	0.037	0.86	0.78	-	15.7	0.042	0.88	0.85
	FLEX-SD-NDH _{Max-Min}	190.8	0.015	0.76	0.63	-	125.8	0.020	0.85	0.76
	FLEX-SD-NDH _{Avg}	34.0	0.030	0.91	0.84	-	24.3	0.036	0.91	0.89
Sub-6	FLEX-SD	20.8	0.037	0.86	0.79	-	15.7	0.042	0.88	0.85
	FLEX-SD-NDH _{Max-Min}	150.6	0.017	0.81	0.71	-	100.8	0.021	0.88	0.81
	FLEX-SD-NDH _{Avg}	33.8	0.031	0.91	0.85	-	24.2	0.036	0.91	0.89
Sub-7	FLEX-SD	17.2	0.038	0.87	0.75	-	10.6	0.047	0.85	0.84
	FLEX-SD-NDH _{Max-Min}	48.2	0.027	0.90	0.83	-	28.5	0.036	0.90	0.87
	FLEX-SD-NDH _{Avg}	34.0	0.031	0.89	0.81	-	19.3	0.040	0.88	0.85
Sub-8	FLEX-SD	18.0	0.038	0.87	0.77	-	11.7	0.046	0.86	0.85
	FLEX-SD-NDH _{Max-Min}	49.9	0.027	0.90	0.84	-	30.7	0.035	0.90	0.88
	FLEX-SD-NDH _{Avg}	32.2	0.032	0.90	0.82	-	19.5	0.040	0.88	0.87
Sub-9	FLEX-SD	20.2	0.037	0.87	0.79	-	15.1	0.042	0.88	0.86
	FLEX-SD-NDH _{Max-Min}	118.7	0.019	0.85	0.78	-	78.8	0.024	0.90	0.84
	FLEX-SD-NDH _{Avg}	34.4	0.031	0.91	0.85	-	24.0	0.037	0.91	0.89
Sub-10	FLEX-SD	20.5	0.037	0.88	0.80	-	15.3	0.042	0.88	0.87
	FLEX-SD-NDH _{Max-Min}	114.9	0.019	0.85	0.79	-	76.3	0.024	0.91	0.85



	FLEX-SD-NDH _{Avg}	36.8	0.030	0.91	0.85	-	25.3	0.036	0.91	0.89
	FLEX-SD	20.7	0.037	0.88	0.80	-	15.5	0.042	0.89	0.87
Sub-11	FLEX-SD-NDH _{Max-Min}	113.4	0.019	0.86	0.80	-	75.2	0.025	0.91	0.85
	FLEX-SD-NDH _{Avg}	41.0	0.029	0.91	0.86	-	27.7	0.035	0.92	0.89
	FLEX-SD	20.9	0.037	0.89	0.81	-	15.6	0.043	0.89	0.87
Sub-12	FLEX-SD-NDH _{Max-Min}	116.1	0.019	0.87	0.81	-	76.5	0.025	0.91	0.85
	FLEX-SD-NDH _{Avg}	40.3	0.029	0.92	0.86	-	27.4	0.036	0.92	0.89
	FLEX-SD	20.6	0.038	0.89	0.80	-	15.6	0.043	0.89	0.87
Sub-13	FLEX-SD-NDH _{Max-Min}	112.7	0.020	0.87	0.81	-	74.4	0.025	0.91	0.86
	FLEX-SD-NDH _{Avg}	38.6	0.030	0.92	0.86	-	26.7	0.036	0.92	0.90

Note: $Su = ae^{b(SWT)}$

Formatted: Line spacing: 1

Formatted: Centered, Line

Formatted: Line spacing: 1

Formatted: Line spacing: 1

Formatted: Line spacing: 1

Formatted: Line spacing: 1

Formatted: Centered, Line

Formatted: Line spacing: 1

Formatted: Line spacing: 1

Formatted: Line spacing: 1

Formatted: Line spacing: 1

Formatted: Centered, Line

Formatted: Line spacing: 1

Formatted: Line spacing: 1

Formatted: Line spacing: 1

Formatted: Line spacing: 1

Formatted: Centered, Line

Table A3: continued

Station	Model	Dry-season				-	Wet-season			
		α	b	R^2	NSE	-	α	b	R^2	NSE
Sub-14	FLEX-SD	19.1	0.035	0.89	0.80	-	17.7	0.037	0.87	0.82
	FLEX-SD-NDH _{Max-Min}	76.0	0.022	0.89	0.85	-	56.2	0.025	0.87	0.81
	FLEX-SD-NDH _{Avg}	158.9	0.015	0.78	0.66	-	110.7	0.018	0.79	0.69
Sub-15	FLEX-SD	22.3	0.036	0.82	0.77	-	18.2	0.039	0.86	0.80
	FLEX-SD-NDH _{Max-Min}	42.1	0.040	0.91	0.74	-	16.5	0.038	0.82	0.85
	FLEX-SD-NDH _{Avg}	31.5	0.031	0.89	0.83	-	24.9	0.035	0.87	0.84
Sub-16	FLEX-SD	22.7	0.035	0.85	0.79	-	19.6	0.038	0.86	0.04
	FLEX-SD-NDH _{Max-Min}	49.7	0.035	0.91	0.79	-	22.1	0.035	0.85	0.00
	FLEX-SD-NDH _{Avg}	33.0	0.031	0.89	0.84	-	27.0	0.034	0.87	0.01
Sub-17	FLEX-SD	21.0	0.035	0.85	0.78	-	18.5	0.038	0.86	0.81
	FLEX-SD-NDH _{Max-Min}	33.0	0.029	0.90	0.83	-	30.3	0.031	0.87	0.85
	FLEX-SD-NDH _{Avg}	59.5	0.024	0.86	0.82	-	44.8	0.027	0.86	0.81
Sub-18	FLEX-SD	20.6	0.035	0.85	0.78	-	17.8	0.038	0.86	0.81
	FLEX-SD-NDH _{Max-Min}	39.3	0.027	0.89	0.83	-	33.3	0.031	0.87	0.85
	FLEX-SD-NDH _{Avg}	68.5	0.022	0.84	0.79	-	49.4	0.026	0.85	0.79
Sub-19	FLEX-SD	20.2	0.036	0.85	0.78	-	17.2	0.038	0.86	0.81
	FLEX-SD-NDH _{Max-Min}	47.8	0.026	0.88	0.83	-	38.0	0.029	0.88	0.84
	FLEX-SD-NDH _{Avg}	72.0	0.022	0.83	0.78	-	50.6	0.026	0.85	0.79
Sub-20	FLEX-SD	20.6	0.036	0.88	0.81	-	13.3	0.042	0.88	0.82
	FLEX-SD-NDH _{Max-Min}	121.3	0.019	0.84	0.74	-	73.8	0.024	0.85	0.76
	FLEX-SD-NDH _{Avg}	77.6	0.022	0.85	0.77	-	44.5	0.029	0.86	0.77
Sub-21	FLEX-SD	20.2	0.036	0.86	0.79	-	16.1	0.039	0.87	0.82
	FLEX-SD-NDH _{Max-Min}	74.1	0.022	0.86	0.82	-	53.4	0.026	0.87	0.82
	FLEX-SD-NDH _{Avg}	74.0	0.022	0.84	0.78	-	49.5	0.027	0.85	0.78
Sub-22	FLEX-SD	19.9	0.036	0.87	0.79	-	15.6	0.039	0.87	0.82
	FLEX-SD-NDH _{Max-Min}	71.0	0.022	0.87	0.83	-	50.5	0.026	0.88	0.82
	FLEX-SD-NDH _{Avg}	77.1	0.022	0.83	0.78	-	50.6	0.026	0.85	0.78

Formatted

Formatted

Formatted

Formatted

Formatted

Formatted

Formatted

Formatted

Formatted

Formatted

Formatted

Formatted

Formatted

Formatted

Formatted

Formatted

Formatted

Formatted

Formatted

Formatted

Formatted

Formatted

Formatted

Formatted

Formatted

Formatted

Formatted

Formatted

Formatted

Formatted

Formatted

Formatted

Formatted

Formatted

Formatted

Formatted

Formatted

Formatted

Formatted

Formatted

Formatted

Formatted

	FLEX-SD	18.2	0.037	0.91	0.81	-	9.6	0.045	0.88	0.80
Sub-23	FLEX-SD-NDH _{Max-Min}	95.6	0.020	0.89	0.79	-	53.8	0.027	0.85	0.75
	FLEX-SD-NDH _{Avg}	187.5	0.014	0.73	0.49	-	113.8	0.019	0.72	0.58
	FLEX-SD	19.7	0.036	0.88	0.80	-	14.8	0.040	0.88	0.83
Sub-24	FLEX-SD-NDH _{Max-Min}	75.8	0.022	0.88	0.83	-	51.5	0.026	0.88	0.82
	FLEX-SD-NDH _{Avg}	96.7	0.020	0.83	0.75	-	61.9	0.024	0.84	0.76
	FLEX-SD	19.7	0.036	0.89	0.81	-	14.8	0.040	0.89	0.83
Sub-25	FLEX-SD-NDH _{Max-Min}	71.8	0.022	0.89	0.84	-	49.3	0.027	0.89	0.83
	FLEX-SD-NDH _{Avg}	92.9	0.020	0.84	0.76	-	59.5	0.025	0.85	0.77
	FLEX-SD	20.1	0.037	0.90	0.81	-	15.4	0.042	0.90	0.86
Sub-26	FLEX-SD-NDH _{Max-Min}	88.8	0.021	0.89	0.84	-	60.2	0.026	0.91	0.86
	FLEX-SD-NDH _{Avg}	63.4	0.024	0.89	0.84	-	41.9	0.030	0.91	0.85

Note: $S_{it} = a e^{b(SWT)}$

Formatted: Centered, Line

Formatted: Line spacing: 1

Formatted: Line spacing: 1

Formatted: Line spacing: 1

Formatted: Line spacing: 1

Formatted: Centered, Line

Formatted: Line spacing: 1

Formatted: Line spacing: 1

Formatted: Line spacing: 1

Formatted: Line spacing: 1

Formatted: Line spacing: 1

Formatted: Centered, Line

Formatted: Line spacing: 1

Formatted: Line spacing: 1

Formatted: Line spacing: 1

Formatted: Line spacing: 1

Formatted: Centered, Line

Formatted: Line spacing: 1

Formatted: Line spacing: 1

Formatted: Line spacing: 1

Formatted: Centered, Tab

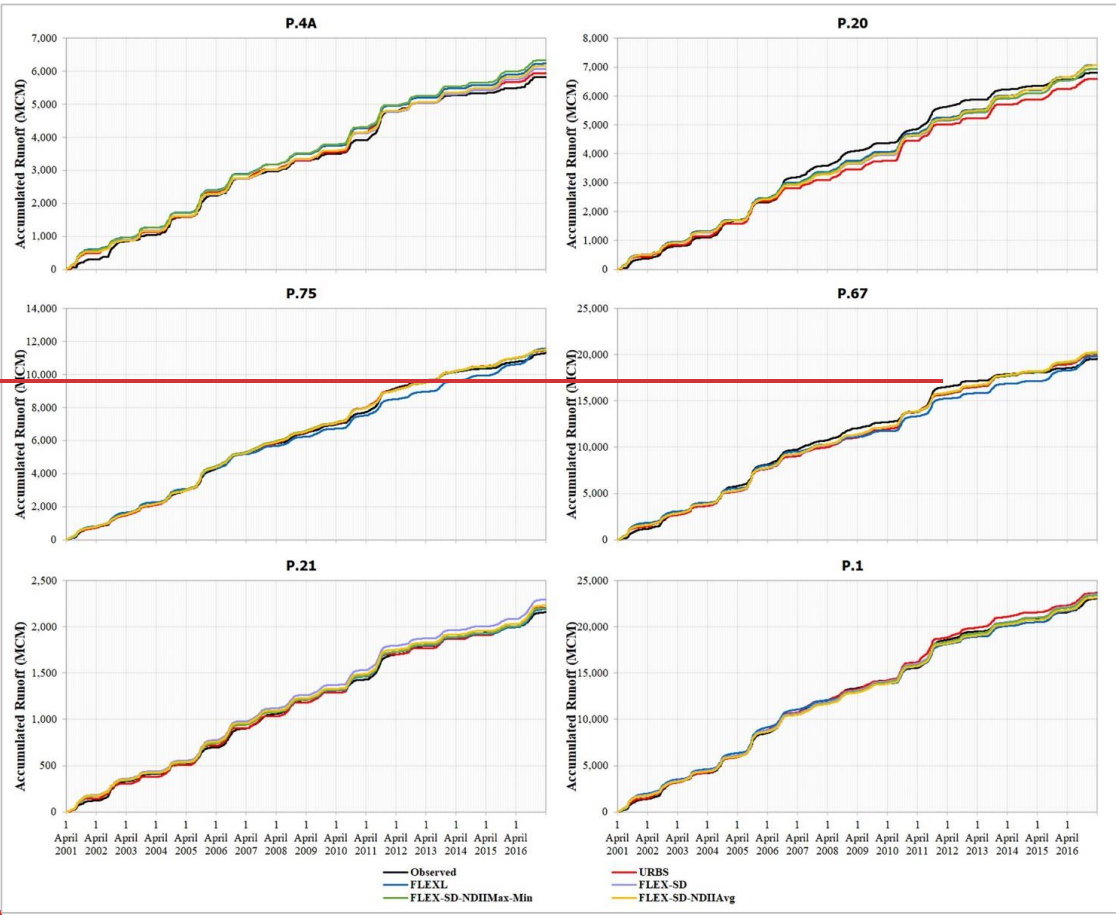
Table A3: continued

Station	Model	Dry-season				-	Wet-season			
		a	b	R^2	NSE		a	b	R^2	NSE
Sub-27	FLEX-SD	20.0	0.037	0.90	0.81	-	15.4	0.042	0.90	0.86
	FLEX-SD-NDH _{Max-Min}	88.2	0.021	0.89	0.84	-	59.7	0.026	0.91	0.86
	FLEX-SD-NDH _{Avg}	62.6	0.024	0.90	0.84	-	41.5	0.030	0.91	0.85
Sub-28	FLEX-SD	16.2	0.039	0.88	0.73	-	9.3	0.048	0.84	0.78
	FLEX-SD-NDH _{Max-Min}	70.8	0.024	0.86	0.77	-	40.0	0.031	0.85	0.77
	FLEX-SD-NDH _{Avg}	57.0	0.025	0.85	0.75	-	30.3	0.034	0.84	0.75
Sub-29	FLEX-SD	17.5	0.038	0.86	0.74	-	10.5	0.046	0.82	0.76
	FLEX-SD-NDH _{Max-Min}	104.6	0.020	0.81	0.68	-	60.4	0.026	0.80	0.70
	FLEX-SD-NDH _{Avg}	127.5	0.018	0.72	0.54	-	72.3	0.024	0.74	0.61
Sub-30	FLEX-SD	16.8	0.039	0.87	0.73	-	10.2	0.047	0.83	0.77
	FLEX-SD-NDH _{Max-Min}	82.1	0.023	0.84	0.73	-	47.5	0.030	0.82	0.74
	FLEX-SD-NDH _{Avg}	77.3	0.023	0.81	0.69	-	43.6	0.030	0.80	0.71
Sub-31	FLEX-SD	19.6	0.037	0.90	0.80	-	14.8	0.042	0.90	0.85
	FLEX-SD-NDH _{Max-Min}	88.1	0.021	0.89	0.83	-	58.5	0.027	0.90	0.85
	FLEX-SD-NDH _{Avg}	64.1	0.024	0.89	0.83	-	41.5	0.030	0.90	0.84
Sub-32	FLEX-SD	19.5	0.037	0.90	0.80	-	14.6	0.043	0.90	0.85
	FLEX-SD-NDH _{Max-Min}	86.5	0.022	0.89	0.83	-	57.4	0.027	0.90	0.85
	FLEX-SD-NDH _{Avg}	63.1	0.024	0.89	0.83	-	40.8	0.030	0.90	0.84
Average	FLEX-SD	-	-	0.87	0.78	-	-	-	0.87	0.81
	FLEX-SD-NDH _{Max-Min}	-	-	0.86	0.78	-	-	-	0.87	0.79
	FLEX-SD-NDH _{Avg}	-	-	0.87	0.79	-	-	-	0.87	0.79

Figure A5: Comparison of the observed and calculated flow duration curves at 6 stations acquired from the 5% best performing parameter combinations generated by 3 FLEX-SD models Note: $S_u = aeb(SWI)$

A vertical column of 20 'Formatted' text boxes on the right side of the page. Each box is connected to a row in the table above by a red arrow, indicating that the content of each box is derived from the corresponding row of the table.

Formatted: Font: Bold, Con
Roman, 10 pt, Bold, (Comple
(United Kingdom)



135 **Figure A1: Accumulated simulated and observed runoff at all stations produced by all models calibration and validation at each station**

Formatted: Font: 10 pt, Co

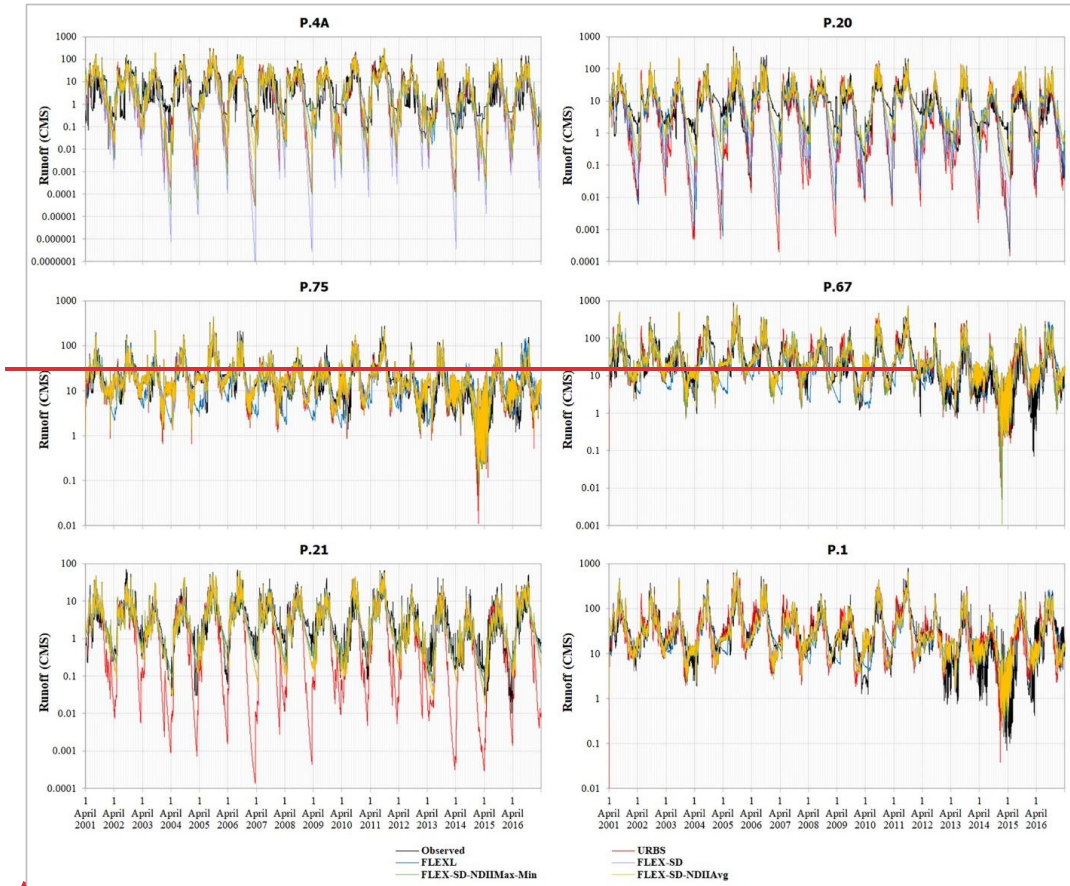
Formatted: Complex Script

Formatted: Thai Distributed

Formatted: Font: 10 pt, Co

Formatted: Thai Distributed
Hanging: 1.75 cm, Tab stop

Formatted: Font: 10 pt, Co
Roman, 10 pt, (Complex) Ar
(United Kingdom)



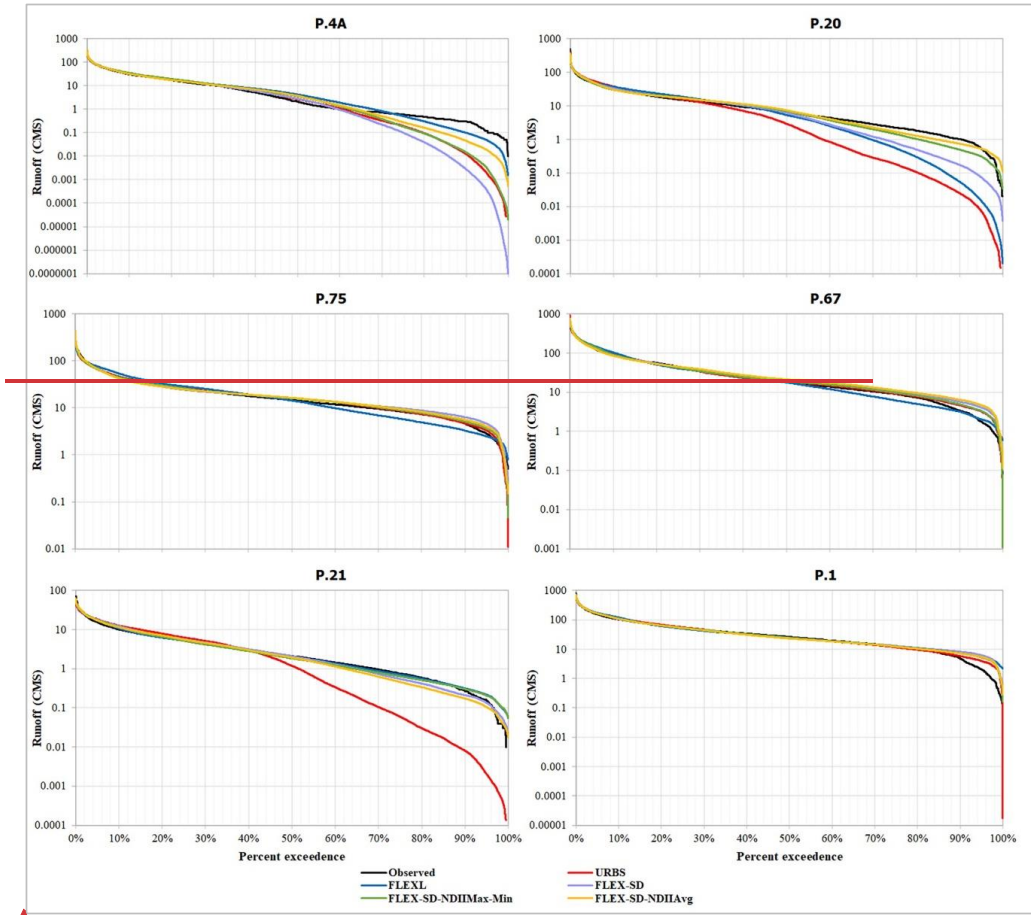
140 **Figure A2: Hydrograph of simulated and observed runoff at all stations produced by all models calibration and validation at each station**

Formatted: Font: 10 pt, Co

Formatted: Thai Distributed

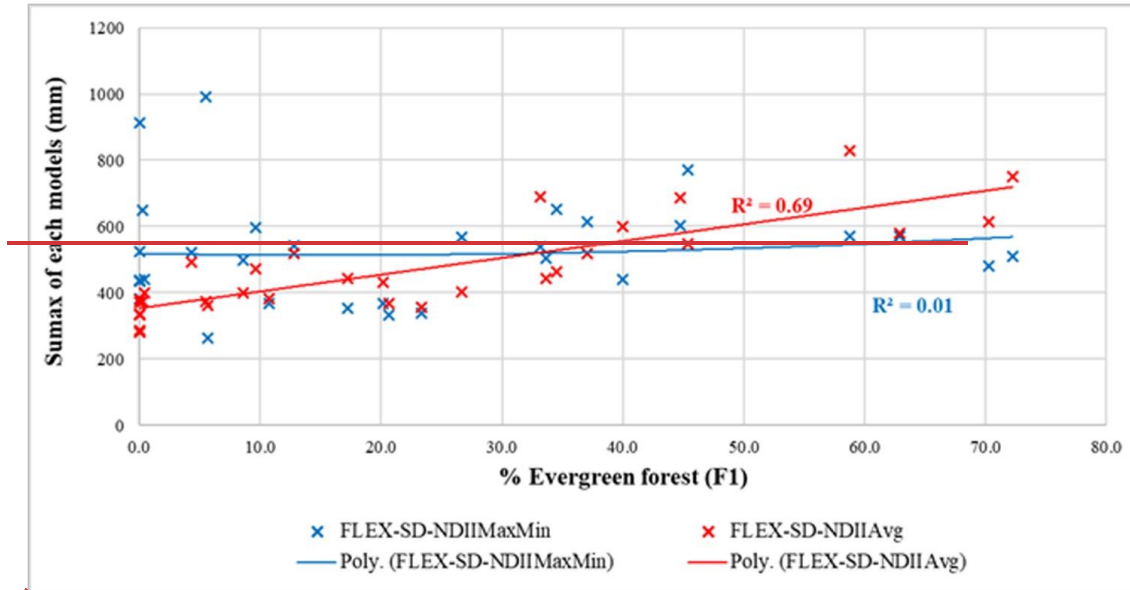
Formatted: Thai Distributed
Hanging: 1.75 cm, Tab stop

Formatted: Font: 10 pt, Co
Roman, 10 pt, (Complex) Ar
(United Kingdom)



145 **Figure A3: Duration curves of simulated and observed runoff at all stations produced by all models calibration and validation at each station**

Formatted: Font: 10 pt, Co



150

Figure A4: Relationships between percent of evergreen forest and Sumax in 31 sub-catchments calibrated and validated by FLEX-SD-NDIIAvg and FLEX-SD-NDIIMaxMins

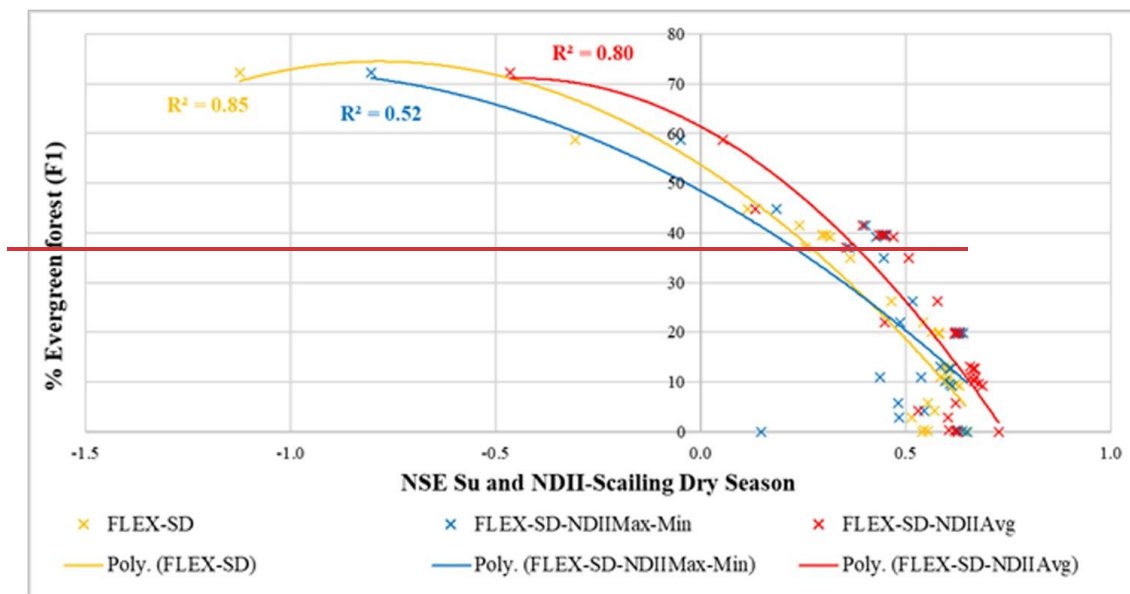


Figure A5: Relationships between percent of evergreen forest and NSE values from the relationships between the average scaling NDII values and simulated root zone moisture storage (Su) in 31 sub-basins calibrated and validated by FLEX SD, FLEX SD-NDIIAvg and FLEX SD-NDIIMax-Min.

155

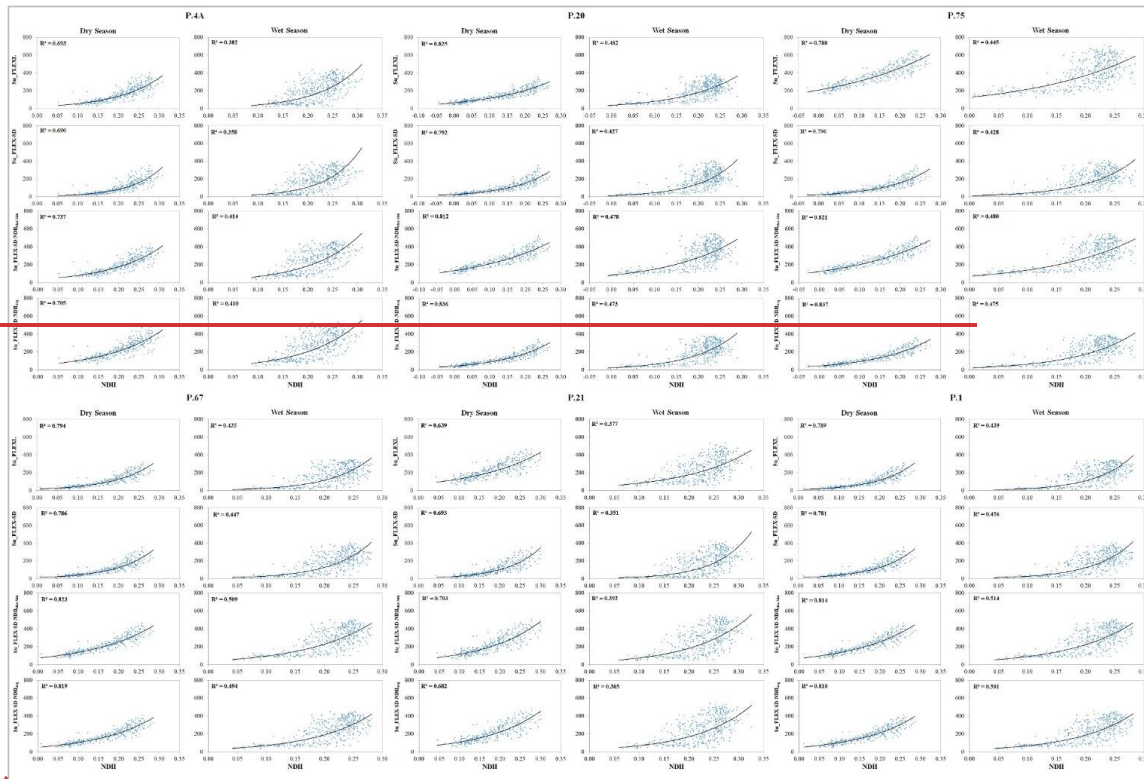
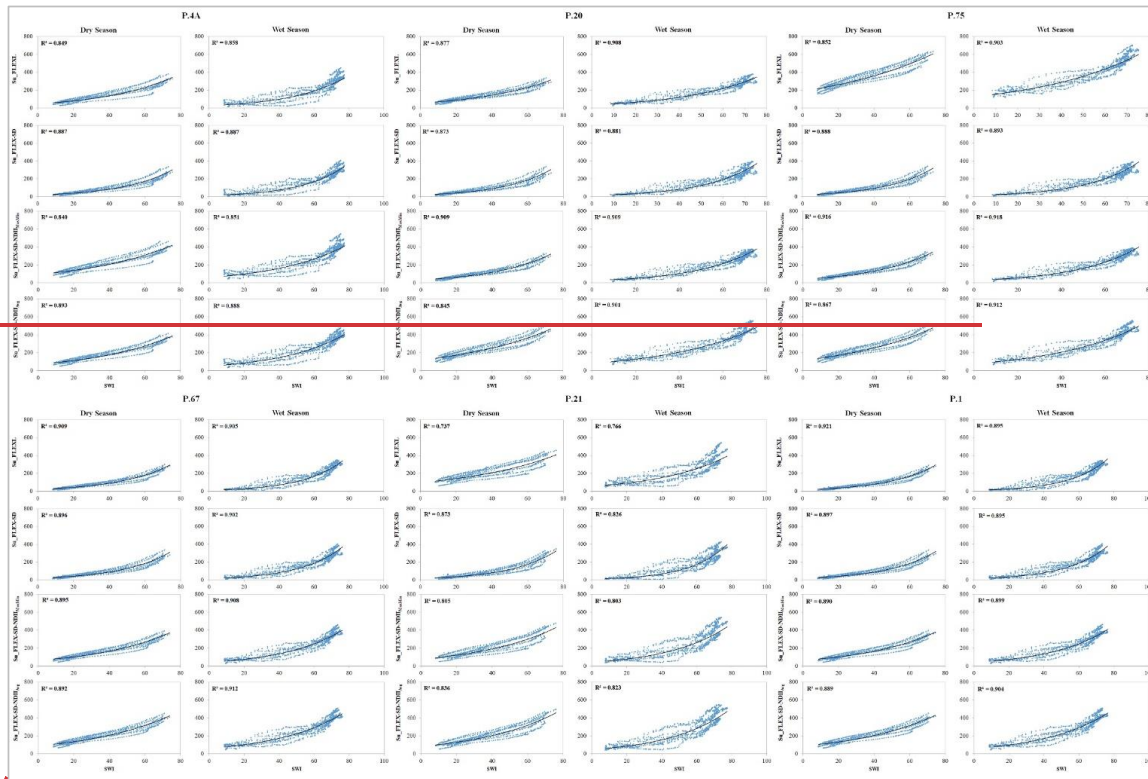
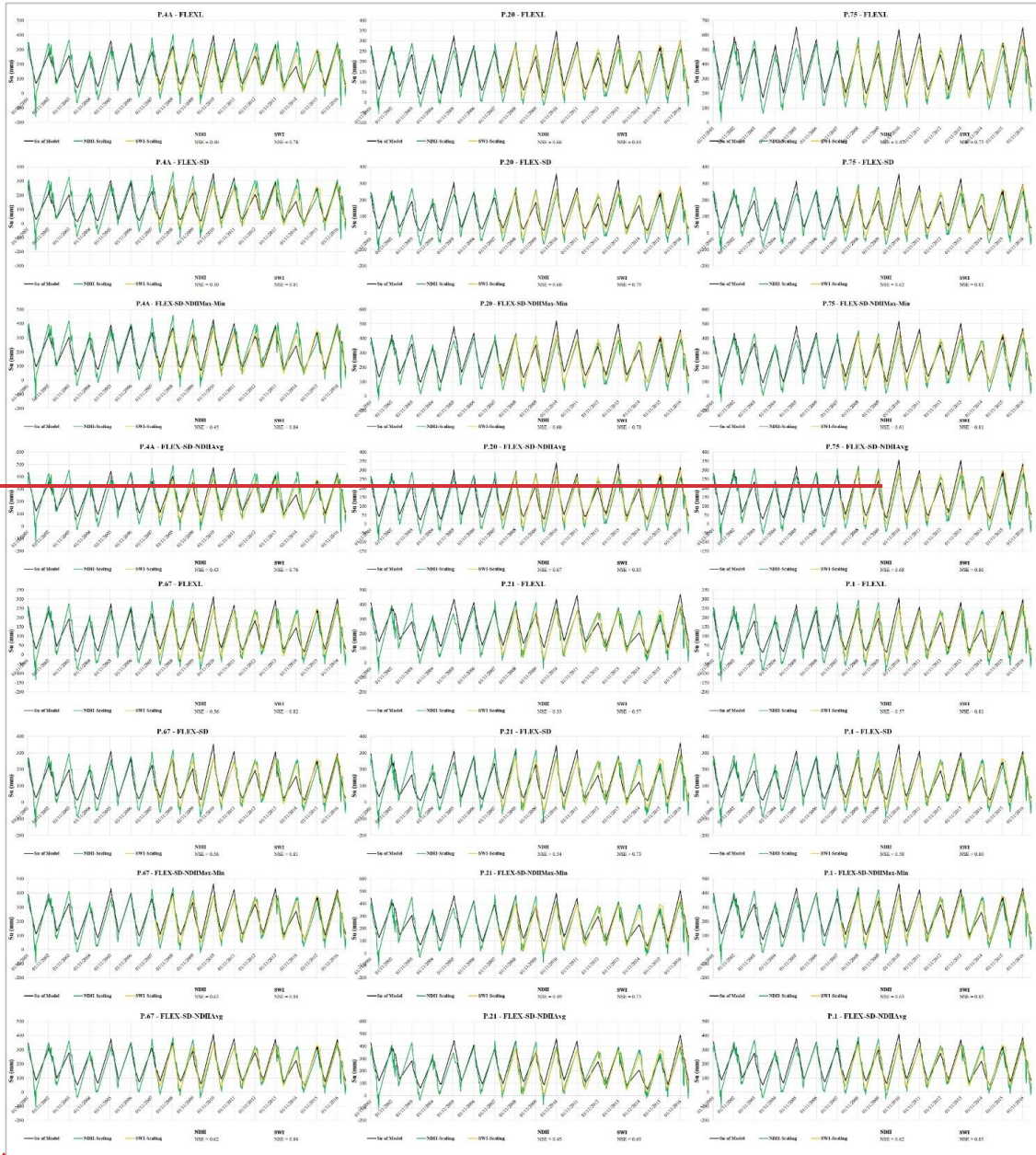


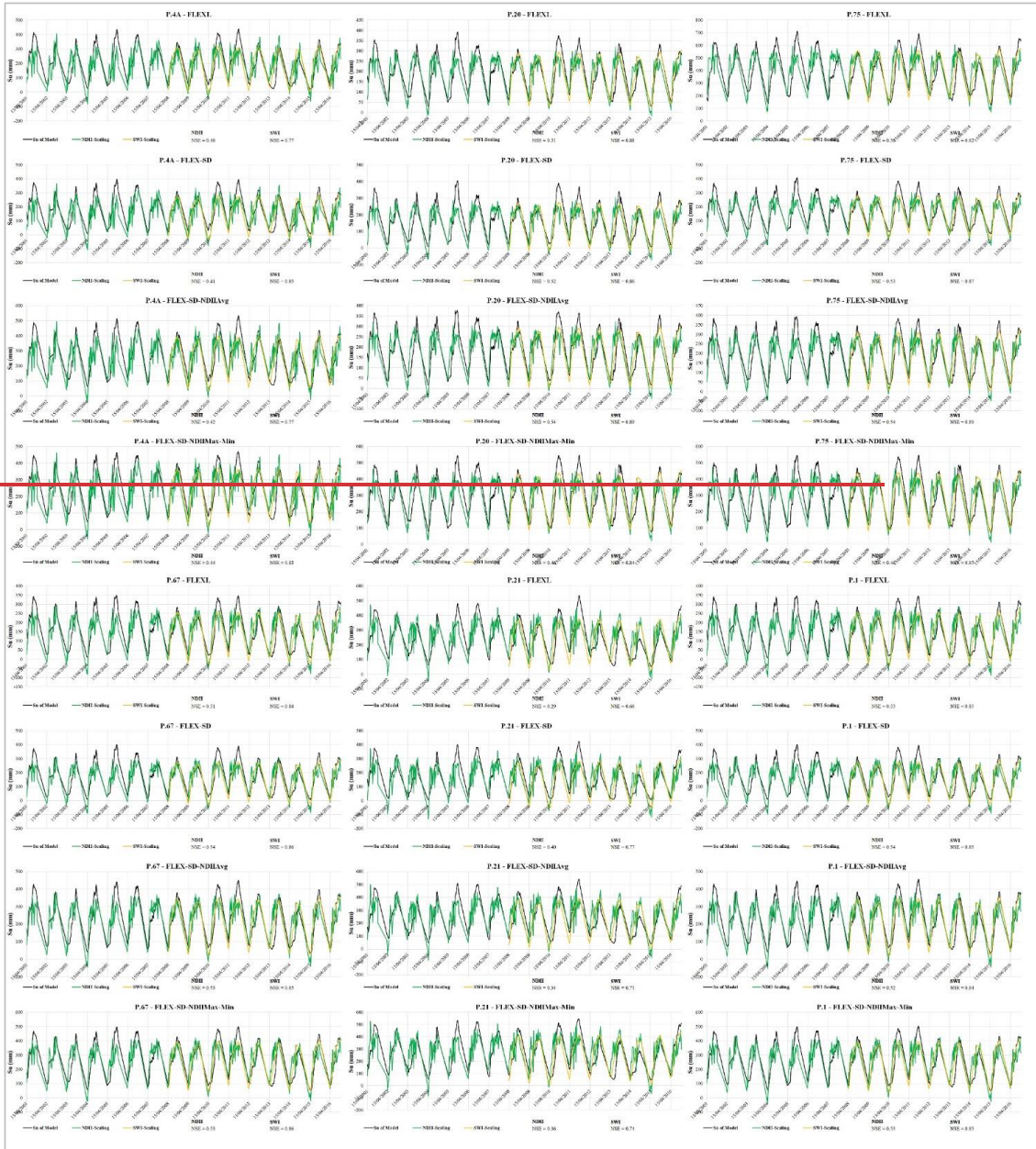
Figure A6: Scatter plots between the average NDII and the average root zone moisture storage (Su) calculated with all models for six runoff stations



165 **Figure A7: Scatter plots between the daily SWI and the daily root zone moisture storage (Sui) calculated with all models for six runoff stations**



~~Figure A8: Time series plots of the average NDII (scaling), average SWI (scaling) and the average root zone moisture storage (S_r) calculated with all models for six sub-basins controlled by runoff stations (dry season)~~



~~Figure A9: Time series plots of the average NDII (scaling), average SWI (scaling) and the average root zone moisture storage (S_r) calculated with all models for six sub-basins controlled by runoff stations (wet season).~~

Formatted: Font: 10 pt, Co
Roman, 10 pt, (Complex) Ar
(United Kingdom)